

Bond and Development of Straight Reinforcing Bars in Tension

Reported by ACI Committee 408

David Darwin*
Chair

Adolfo B. Matamoros*
Secretary

John H. Allen	Anthony L. Felder†	John F. McDermott
Atorod Azizinamini	Robert J. Frosch†	Denis Mitchell
Gyorgy L. Balazs	Bilal S. Hamad*	Stavroula J. Pantazopoulou
JoAnn Browning*†	Neil M. Hawkins	Max L. Porter
James V. Cox	Roberto T. Leon*	Julio A. Ramirez
Richard A. DeVries*	LeRoy A. Lutz†	John F. Silva
Rolf Eligehausen	Steven L. McCabe	Jun Zuo*
Fernando E. Fagundo		

*Members of the subcommittee who prepared this report.

†Members of the editorial subcommittee.

The performance of reinforced concrete structures depends on adequate bond strength between concrete and reinforcing steel. This report describes bond and development of straight reinforcing bars under tensile load. Bond behavior and the factors affecting bond are discussed, including concrete cover and bar spacing, bar size, transverse reinforcement, bar geometry, concrete properties, steel stress and yield strength, bar surface condition, bar casting position, development and splice length, distance between spliced bars, and concrete consolidation. Descriptive equations and design provisions for development and splice strength are presented and compared using a large database of test results. The contents of the database are summarized, and a protocol for bond tests is presented.

ACI Committee Reports, Guides, Standard Practices, and Commentaries are intended for guidance in planning, designing, executing, and inspecting construction. This document is intended for the use of individuals who are competent to evaluate the significance and limitations of its content and recommendations and who will accept responsibility for the application of the material it contains. The American Concrete Institute disclaims any and all responsibility for the stated principles. The Institute shall not be liable for any loss or damage arising therefrom.

Reference to this document shall not be made in contract documents. If items found in this document are desired by the Architect/Engineer to be a part of the contract documents, they shall be restated in mandatory language for incorporation by the Architect/Engineer.

It is the responsibility of the user of this document to establish health and safety practices appropriate to the specific circumstances involved with its use. ACI does not make any representations with regard to health and safety issues and the use of this document. The user must determine the applicability of all regulatory limitations before applying the document and must comply with all applicable laws and regulations, including but not limited to, United States Occupational Safety and Health Administration (OSHA) health and safety standards.

Test data and reliability analyses demonstrate that, for compressive strengths up to at least 16,000 psi (110 MPa), the contribution of concrete strength to bond is best represented by the compressive strength to the 1/4 power, while the contribution of concrete to the added bond strength provided by transverse reinforcement is best represented by compressive strength to a power between 3/4 and 1.0. The lower value is used in proposed design equations. These values are in contrast with the square root of compressive strength, which normally is used in both descriptive and design expressions. Provisions for bond in ACI 318-02 are shown to be unconservative in some instances; specifically, the 0.8 bar size factor for smaller bars should not be used and a ϕ -factor for bond is needed to provide a consistent level of reliability against bond failure. Descriptive equations and design procedures developed by Committee 408 that provide improved levels of reliability, safety, and economy are presented. The ACI Committee 408 design procedures do not require the use of the 1.3 factor for Class B splices that is required by ACI 318.

Keywords: anchorage; **bond**; concrete; **deformed reinforcement**; **development length**; reinforced concrete; reinforcement; relative rib area; **splice**; stirrup; tie.

CONTENTS

Preface, p. 408R-2

Chapter 1—Bond behavior, p. 408R-3

- 1.1—Bond forces—background
- 1.2—Test specimens
- 1.3—Details of bond response
- 1.4—Notation

ACI 408R-03 became effective September 24, 2003.

Copyright © 2003, American Concrete Institute.

All rights reserved including rights of reproduction and use in any form or by any means, including the making of copies by any photo process, or by electronic or mechanical device, printed, written, or oral, or recording for sound or visual reproduction or for use in any knowledge or retrieval system or device, unless permission in writing is obtained from the copyright proprietors.

Chapter 2—Factors affecting bond, p. 408R-9

- 2.1—Structural characteristics
- 2.2—Bar properties
- 2.3—Concrete properties
- 2.4—Summary

Chapter 3—Descriptive equations, p. 408R-25

- 3.1—Orangun, Jirsa, and Breen
- 3.2—Darwin et al.
- 3.3—Zuo and Darwin
- 3.4—Esfahani and Rangan
- 3.5—ACI Committee 408
- 3.6—Comparisons

Chapter 4—Design provisions, p. 408R-29

- 4.1—ACI 318
- 4.2—ACI 408.3
- 4.3—Recommendations by ACI Committee 408
- 4.4—CEB-FIP Model Code
- 4.5—Structural reliability and comparison of design expressions

Chapter 5—Database, p. 408R-38

- 5.1—Bar stresses
- 5.2—Database

Chapter 6—Test protocol, p. 408R-39

- 6.1—Reported properties of reinforcement
- 6.2—Concrete properties
- 6.3—Specimen properties
- 6.4—Details of test
- 6.5—Analysis method
- 6.6—Relative rib area

Chapter 7—References, p. 408R-41

- 7.1—Referenced standards and reports
- 7.2—Cited references

Appendix A—SI equations, p. 408R-47**PREFACE**

The bond between reinforcing bars and concrete has been acknowledged as a key to the proper performance of reinforced concrete structures for well over 100 years (Hyatt 1877). Much research has been performed during the intervening years, providing an ever-improving understanding of this aspect of reinforced concrete behavior. ACI Committee 408 issued its first report on the subject in 1966. The report emphasized key aspects of bond that are now well understood by the design community but that, at the time, represented conceptually new ways of looking at bond strength. The report emphasized the importance of splitting cracks in governing bond strength and the fact that bond forces did not vary monotonically and could even change direction in regions subjected to constant or smoothly varying moment. Committee 408 followed up in 1979 with suggested provisions for development, splice, and hook design (ACI 408.1R-79), in 1992 with a state-of-the-art report on bond under cyclic loads (ACI 408.2R-92), and in 2001 with design

provisions for splice and development design for high relative rib area bars (bars with improved bond characteristics) (ACI 408.3-01). This report represents the next in that line, emphasizing bond behavior and design of straight reinforcing bars that are placed in tension.

For many years, bond strength was represented in terms of the shear stress at the interface between the reinforcing bar and the concrete, effectively treating bond as a material property. It is now clear that bond, anchorage, development, and splice strength are structural properties, dependent not only on the materials but also on the geometry of the reinforcing bar and the structural member itself. The knowledge base on bond remains primarily empirical, as do the descriptive equations and design provisions. An understanding of the empirical behavior, however, is critical to the eventual development of rational analysis and design techniques.

Test results for bond specimens invariably exhibit large scatter. This scatter increases as the test results from different laboratories are compared. Research since 1990 indicates that much of the scatter is the result of differences in concrete material properties, such as fracture energy and reinforcing bar geometry, factors not normally considered in design. This report provides a summary of the current state of knowledge of the factors affecting the tensile bond strength of straight reinforcing bars, as well as realistic descriptions of development and splice strength as a function of these factors. The report covers bond under the loading conditions that are addressed in Chapter 12 of ACI 318; dynamic, blast, and seismic loading are not covered.

Chapter 1 provides an overview of bond behavior, including bond forces, test specimens, and details of bond response. **Chapter 2** covers the factors that affect bond, discussing the impact of structural characteristics as well as bar and concrete properties. The chapter provides insight not only into aspects that are normally considered in structural design, but into a broad range of factors that control anchorage, development, and splice strength in reinforced concrete members. **Chapter 3** presents a number of widely cited descriptive equations for development and splice strength, including expressions recently developed by ACI Committee 408. The expressions are compared for accuracy using the test results in the ACI Committee 408 database. **Chapter 4** summarizes the design provisions in ACI 318, ACI 408.3, the 1990 CEB-FIP Model Code, as well as design procedures recently developed by Committee 408. The design procedures are compared for accuracy, reliability, safety, and economy using the ACI Committee 408 database. The observations presented in **Chapters 3** and **4** demonstrate that $f_c'^{1/4}$ provides a realistic representation of the contribution of concrete strength to bond for values up to at least 16,000 psi (110 MPa), while $f_c'^{3/4}$ does the same for the effect of concrete strength on the increase in bond strength provided by transverse reinforcement. This is in contrast to $\sqrt{f_c'}$, which is used in most design provisions. The comparisons in Chapter 4 also demonstrate the need to modify the design provisions in ACI 318 by removing the bar size g factor of 0.8 for small bars and addressing the negative impact on bond reliability of changing the load factors while maintaining

the strength reduction factor for tension in the transition from ACI 318-99 to ACI 318-02. Design procedures recommended by ACI Committee 408 that provide both additional safety and economy are presented. Chapter 5 describes the ACI Committee 408 database, while Chapter 6 presents a recommended protocol for bond tests. The expressions within the body of the report are presented in inch-pound units. Expressions in SI units are presented in Appendix A.

A few words are appropriate with respect to terminology. The term *bond force* represents the force that tends to move a reinforcing bar parallel to its length with respect to the surrounding concrete. *Bond strength* represents the maximum bond force that may be sustained by a bar. The terms *development strength* and *splice strength* are, respectively, the bond strengths of bars that are not spliced with other bars and of bars that are spliced. The terms *anchored length*, *bonded length*, and *embedded length* are used interchangeably to represent the length of a bar over which bond force acts; in most cases, this is the distance between the point of maximum force in the bar and the end of the bar. Bonded length may refer to the length of a lap splice. *Developed length* and *development length* are used interchangeably to represent the bonded length of a bar that is not spliced with another bar, while *spliced length* and *splice length* are used to represent the bonded length of bars that are lapped spliced. When used in design, development length and splice length are understood to mean the “length of embedded reinforcement required to develop the design strength of reinforcement at a critical section,” as defined in ACI 318.

CHAPTER 1—BOND BEHAVIOR

In reinforced concrete construction, efficient and reliable force transfer between reinforcement and concrete is required for optimal design. The transfer of forces from the reinforcement to the surrounding concrete occurs for a deformed bar (Fig. 1.1) by:

- Chemical adhesion between the bar and the concrete;
- Frictional forces arising from the roughness of the interface, forces transverse to the bar surface, and relative slip between the bar and the surrounding concrete; and
- Mechanical anchorage or bearing of the ribs against the concrete surface.

After initial slip of the bar, most of the force is transferred by bearing. Friction, however, especially between the concrete and the bar deformations (ribs) plays a significant role in force transfer, as demonstrated by epoxy coatings, which lower the coefficient of friction and result in lower bond capacities. Friction also plays an important role for plain bars (that is, with no deformations), with slip-induced friction resulting from transverse stresses at the bar surface caused by small variations in bar shape and minor, though significant, surface roughness. Plain bars with suitably low allowable bond stresses were used for many years for reinforced concrete in North America and are still used in some regions of the world.

When a deformed bar moves with respect to the surrounding concrete, surface adhesion is lost, while bearing

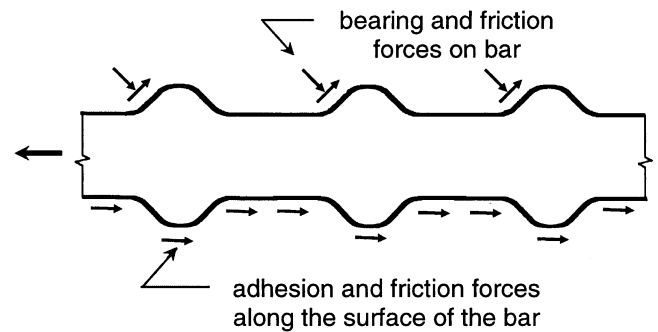


Fig. 1.1—Bond force transfer mechanisms.

forces on the ribs and friction forces on the ribs and barrel of the bar are mobilized. The compressive bearing forces on the ribs increase the value of the friction forces. As slip increases, friction on the barrel of the reinforcing bar is reduced, leaving the forces at the contact faces between the ribs and the surrounding concrete as the principal mechanism of force transfer. The forces on the bar surface are balanced by compressive and shear stresses on the concrete contact surfaces, which are resolved into tensile stresses that can result in cracking in planes that are both perpendicular and parallel to the reinforcement, as shown in Fig. 1.2(a) and 1.2(b). The cracks shown in Fig. 1.2(a), known as Goto (1971) cracks, can result in the formation of a conical failure surface for bars that project from concrete and are placed in tension. They otherwise play only a minor role in the anchorage and development of reinforcement. The transverse cracks shown in Fig. 1.2(b) form if the concrete cover or the spacing between bars is sufficiently small, leading to splitting cracks, as shown in Fig. 1.2(c). If the concrete cover, bar spacing, or transverse reinforcement is sufficient to prevent or delay a splitting failure, the system will fail by shearing along a surface at the top of the ribs around the bars, resulting in a “pullout” failure, as shown in Fig. 1.2(d). It is common, for both splitting and pullout failures, to observe crushed concrete in a region adjacent to the bearing surfaces of some of the deformations. If anchorage to the concrete is adequate, the stress in the reinforcement may become high enough to yield and even strain harden the bar. Tests have demonstrated that bond failures can occur at bar stresses up to the tensile strength of the steel.

From these simple qualitative descriptions, it is possible to say that bond resistance is governed by:

- The mechanical properties of the concrete (associated with tensile and bearing strength);
- The volume of the concrete around the bars (related to concrete cover and bar spacing parameters);
- The presence of confinement in the form of transverse reinforcement, which can delay and control crack propagation;
- The surface condition of the bar; and
- The geometry of the bar (deformation height, spacing, width, and face angle).

A useful parameter describing bar geometry is the so-called relative rib area R_r , illustrated in Fig. 1.3, which is the ratio of the bearing area of the bar deformations to the

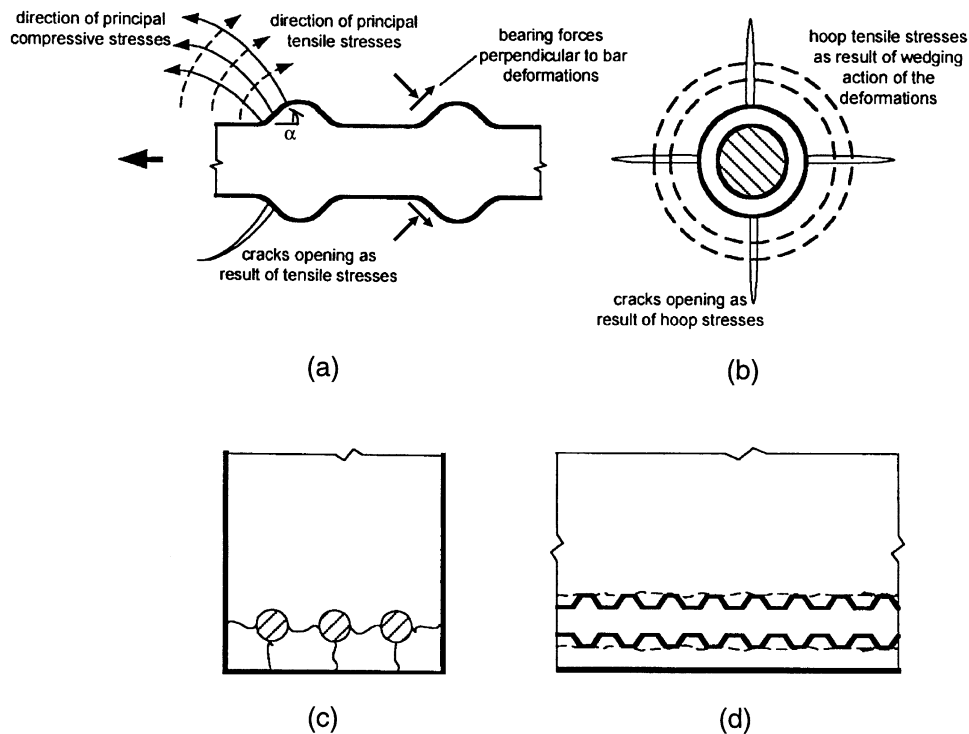


Fig. 1.2—Cracking and damage mechanisms in bond: (a) side view of a deformed bar with deformation face angle α showing formation of Goto (1971) cracks; (b) end view showing formation of splitting cracks parallel to the bar; (c) end view of a member showing splitting cracks between bars and through the concrete cover; and (d) side view of member showing shear crack and/or local concrete crushing due to bar pullout.

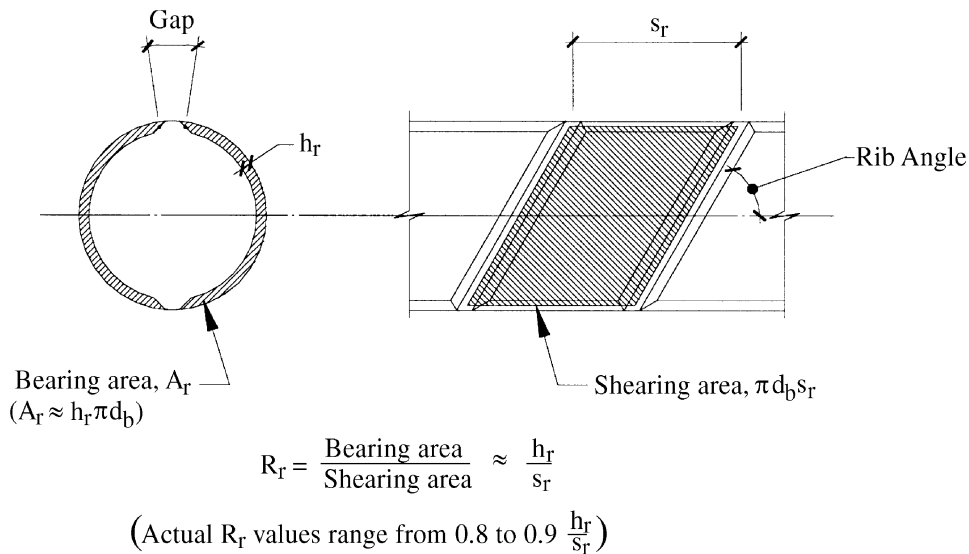


Fig. 1.3—Definition of R_r (ACI 408.3R).

shearing area between the deformations (in U.S. practice, this is taken as the ratio of the bearing area of the ribs to the product of the nominal bar perimeter and the average spacing of the ribs). Relative rib area is discussed at greater length in [Section 2.2.2](#).

1.1—Bond forces—background

To understand the design procedures used for selecting development and splice lengths of reinforcement, it is instructive to review the nature of bond forces and stresses in

a reinforced concrete flexural member. Historically, the difference in tensile force ΔT between two sections located at flexural cracks along a member ([Fig. 1.4](#)) was calculated as

$$\Delta T = T_1 - T_2 = \frac{M_1}{jd_1} - \frac{M_2}{jd_2} \quad (1-1)$$

where T_i ($T_2 > T_1$), M_i ($M_2 > M_1$), and jd_i are the tensile force, moment, and internal moment arm at section i ($i = 1, 2$). For

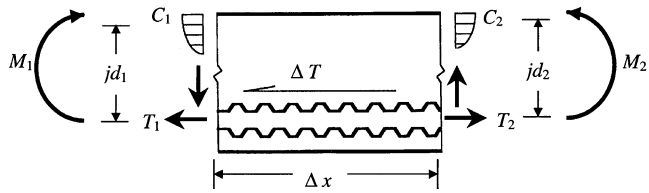


Fig. 1.4—Variation in bar force due to changes in moment in a beam.

an infinitesimally small distance between Sections 1 and 2, Eq. (1-1) becomes

$$dT = \frac{dM}{jd} \quad (1-2)$$

If the bond force per unit length U is defined as the change in tensile force per unit length, then

$$U = \frac{dT}{dl} = \frac{1}{jd} \frac{dM}{dl} \quad (1-3a)$$

$$U = \frac{1}{jd} V \quad (1-3b)$$

where V is the shear on the section.

Equation (1-3b) indicates that, away from concentrated loads, bond forces vary as a function of the applied shear along the length of reinforced concrete flexural members, and for many years, the bond force used in design U was based on this expression. Over time, however, it became apparent that the change in force in reinforcing bars dT does not vary strictly with the change in moment per unit length, as suggested in Eq. (1-3a), but simply with the force in the bar T , which varies from a relatively high value at cracks to a low value between cracks, where the concrete shares the tensile force with the reinforcing steel. Using the definition $U = dT/dl$, bond forces vary significantly along the length of a member, even varying in direction, as shown in Fig. 1.5. The real distribution of bond forces along the length of a bar, therefore, cannot be predicted because it depends on the locations of the flexural cracks and the amount of tensile load carried by the concrete—neither of which can be calculated. Given these facts and because a principal goal of design is to ensure that the bar is adequately anchored so that failure will manifest itself in some way other than in bond, it is both convenient and realistic for design purposes to treat bond forces as if they were uniform over the anchored, developed, or spliced length of the reinforcement.

Until adoption of the 1971 ACI Building Code (ACI 318-71), bond design was based on bond stress u , which is equal to bond force per unit length U divided by the sum of the perimeters of the bars developed at a section Σ_o .

$$u = \frac{U}{\Sigma_o} = \frac{\Delta T}{\Delta l \Sigma_o} = \frac{\Delta f_s A_b}{\Delta l \Sigma_o} = \frac{\Delta f_s d_b}{4 \Delta l} \quad (1-4)$$

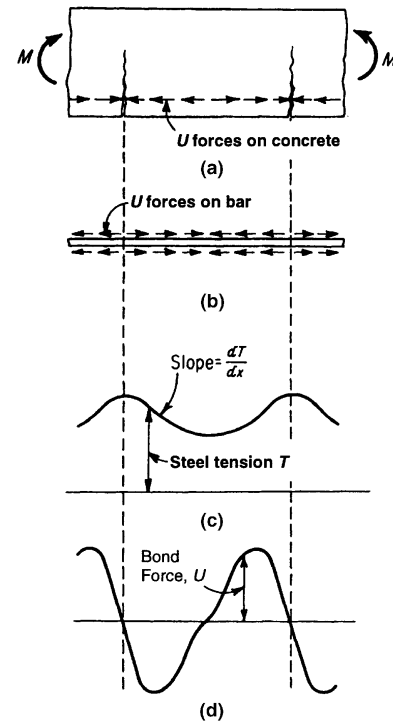


Fig. 1.5—Variation of steel and bond forces in reinforced concrete member subjected to pure bending: (a) cracked concrete segment; (b) bond stresses acting on reinforcing bar; (c) variation of tensile force in steel; and (d) variation of bond force along bar (adapted from Nilson et al. [2004]).

where A_b = area of bars; d_b = diameter of bars; and Δf_s = change in steel stress over length Δl .

For design purposes, the change in stress Δf_s equals the yield stress of the steel f_y and Δl equals the development length l_d . In ACI 318-63, the maximum bond stress was set at *

$$u = 9.5 \frac{\sqrt{f'_c}}{d_b} \leq 800 \text{ psi} \quad (1-5)$$

Substituting Eq. (1-5) into Eq. (1-4), solving for $\Delta l = l_d$, and multiplying the resultant value by 1.2 to account for the reduced bond strength of closely spaced bars (due to the interaction of splitting cracks) gives the development length

$$l_d = 0.04 A_b \frac{f_y}{\sqrt{f'_c}} \quad (1-6)$$

Equation (1-6) was used for design, beginning with ACI 318-71, until a design approach that more closely matched observed behavior was adopted in ACI 318-95.

While convenient, equations for development length [like Eq. (1-6) and some of those presented in Chapter 4] have led many designers to believe that the real force that must be developed is equal to the product of the area and yield

*SI conversions of equations that contain terms that depend on units of measure are presented in Appendix A.

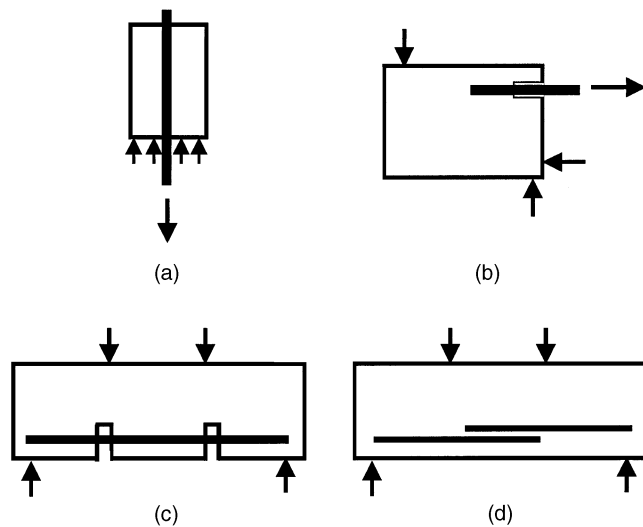


Fig. 1.6—Schematic of: (a) pullout specimen; (b) beam-end specimen; (c) beam anchorage specimen; and (d) splice specimen.

strength of a bar. In fact, the basis for the expressions for development length l_d lies in Eq. (1-3) and (1-4), which are based on the change in bar force ΔT , the result of externally applied load. The force in the bar $A_b f_y$ used in the Eq. (1-6) is the designer-selected value for ΔT . If, for example, a bar in a flexural member has a higher yield strength than specified (the usual case), a longer development length will be needed to ensure that a ductile bending failure will occur before a brittle bond failure.

1.2—Test specimens

A variety of test specimen configurations have been used to study bond between reinforcing bars and concrete. The four most common configurations are shown in Fig. 1.6. The details of the specimen affect not only the measured bond strength, but also the nature of the bond response.

The pullout specimen (Fig. 1.6(a)) is widely used because of its ease of fabrication and the simplicity of the test. The specimen often incorporates transverse reinforcement to limit splitting when the bar is placed in tension. This specimen is the least realistic of the four shown in Fig. 1.6 because the stress fields within the specimen match few cases in actual construction. As the bar is placed in tension, the concrete is placed in compression. Further, compressive struts form between the support points for the concrete and the surface of the reinforcing bar, placing the bar surface in compression. This stress state differs markedly from most reinforced concrete members, in which both the bar and the surrounding concrete are in tension, and the bearing surfaces of the bar ribs are subjected to a compressive force due to relative movement of the bar with respect to the concrete, not due to the basic load application. In cases where bar surface properties (such as epoxy coatings) or bar surface strength (such as for fiber-reinforced polymer reinforcement) are important, the compression developed at the bar surface in the pullout test reduces the applicability of the test results to structural design. Thus, the use of pullout test results as the

sole basis for determining development length is inappropriate and not recommended by Committee 408.

The specimens shown in Fig. 1.6(b) through (d) provide more realistic measures of bond strength in actual structures. The modified cantilever beam, or beam-end specimen, shown in Fig. 1.6(b), provides a relatively simple test that generally duplicates the stress state obtained in reinforced concrete members; the reinforcing steel and the surrounding concrete are simultaneously placed in tension. To achieve the desired stress state, the compressive force must be located away from the reinforcing bar by a distance approximately equal to the embedded or bonded length of the bar within the concrete. To prevent a conical failure surface from forming, a small length of bar near the surface is usually unbonded. A specimen like that shown in Fig. 1.6(b), proportioned to satisfy the spacing requirements between the bar and the compressive force and reinforced to ensure bond rather than flexural or shear failure, is specified in ASTM A 944. The shear reinforcement is placed in the specimen so as not to intercept longitudinal splitting cracks that occur at bond failure. Transverse reinforcement can be added in cases where its effect is of interest (Darwin and Graham 1993a,b). The bond strengths obtained with the test specimen closely match those obtained in other specimens designed to represent full-scale reinforced concrete members.

Beam anchorage and splice specimens shown in Fig. 1.6(c) and (d), respectively, represent larger-scale specimens designed to directly measure development and splice strengths in full-size members. The anchorage specimen simulates a member with a flexural crack and a known bonded length. Based on concern that increased normal stresses at the bar surface, caused by the reactions, may increase bond strength, some anchorage specimens have been designed so that the reactions are displaced laterally from the centerline of the beam. The splice specimen, normally fabricated with the splice in a constant moment region, is easier to fabricate and produces similar bond strengths to those obtained with the anchorage specimen. Because of both its relative simplicity of fabrication and realistic stress-state in the vicinity of the bars, the splice specimen has provided the bulk of the data used to establish the current design provisions for development length, as well as splice length, in ACI 318 (starting with ACI 318-95).

Other specimens have also been used to study bond strength. These include the wall specimen, to determine the “top-bar” effect, and the tension specimen, consisting of a bar surrounded by concrete, with tension applied to both ends of the bar, which project from the concrete. Variations on the beam-end specimen have also been used in which the compressive force is placed relatively close to the bar, resulting in higher bond strengths due to the compressive strut reaching the bar surface. These specimens generally lack the realism obtained with the specimens shown in Fig. 1.6(b) through (d).

1.3—Details of bond response

Bond force-slip and bond stress-slip curves can be used to better understand the nature of bond response. In their

simplest and most widely used form, the curves are based on known bar forces, such as obtained in the beam-end and beam anchorage specimens (Fig. 1.6(b) and (c)). Bar forces are compared with the external slip of the reinforcing bar, measured with respect to the concrete at either the loaded or unloaded end of the bar. Examples of bar force-loaded end and unloaded end slip curves are shown in Fig. 1.7(a) and (b), respectively. The loaded end bond force-slip curve shows a lower initial stiffness than the unloaded end curve. The difference represents the lengthening of the reinforcing bar between the two points of slip measurement.

More detailed information, at a smaller scale along the length of a bar, can be obtained by placing strain gages on the bar as a method to determine changes in bar force ΔT , which can be converted to bond force per unit length, $U \approx \Delta T / \Delta l$, and bar stress, $u = U / \Sigma_o$. In the most detailed studies, the strain gages are installed by splitting the bar in half, forming a small channel along the centerline, installing the strain gages and wires in the channel, and welding the bar back together. As an acceptable alternative, strain gages and wires are placed in longitudinal grooves cut at the location of longitudinal ribs. These types of installation minimize disturbances at the interface between the bar and the concrete.

A bond stress versus slip curve for a bar loaded monotonically and failing by pullout is shown in Fig. 1.8 (Eligehausen, Popov, and Bertero 1983). Bond force and bond stress-slip curves, like bond strength, are structural properties that depend on both the geometry of the bar and the details of the concrete member, including the cover, transverse reinforcement, and state of stress in the concrete surrounding the reinforcement. As shown in Fig. 1.7 and 1.8, bond force and bond stress-slip curves are initially very steep because of adhesion.

Because of concrete shrinkage, which is restrained by the reinforcing bar, small internal cracks exist immediately adjacent to the reinforcing bar. These cracks can act as stress raisers and points of crack initiation at the bar ribs at relatively low loads. Because cracks tend to form in front of the ribs, small splitting cracks may begin to propagate from the ribs, as shown in Fig. 1.2(a). If the reinforcing bar is placed in tension from a free surface, such as a beam-end specimen, it is possible for the crack to propagate to the surface, separating a roughly conical region of concrete from the rest of the specimen.

As loading continues, longitudinal splitting cracks form, as shown in Fig. 1.2(b) and (c), leading to a softening in the bond force-slip curve. In regions where these splitting cracks open and where confinement by transverse reinforcement is limited, the bar may slip with little local damage to the concrete at the contact surface with the bar ribs. In regions of greater confinement, higher rates of loading, or both, the concrete in front of the reinforcing bar ribs may crush as the bar moves, forming effective ribs with a reduced face angle (less than α in Fig. 1.2(a)). For higher values of confinement, all of the concrete between the ribs may crush or a shear crack may form along the periphery of the bar, or both, resulting in a pullout failure (Fig. 1.2(d)). Depending on the details of the member and the loading, bond failure may entail a combination of the failure modes. Transverse reinforcement, however, rarely yields during a bond failure

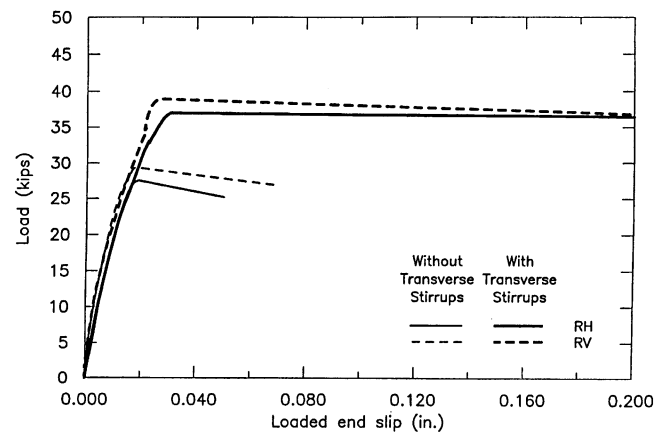


Fig. 1.7(a)—Average load-loaded end slip curves for No. 8 (No. 25) ASTM A 615 reinforcing bars in an ASTM A 944 beam-end specimen. RH and RV represent bars with longitudinal ribs oriented horizontally and vertically, respectively (Darwin and Graham 1993a). (Note: 1 in. = 25.4 mm; 1 kip = 4.45 kN)

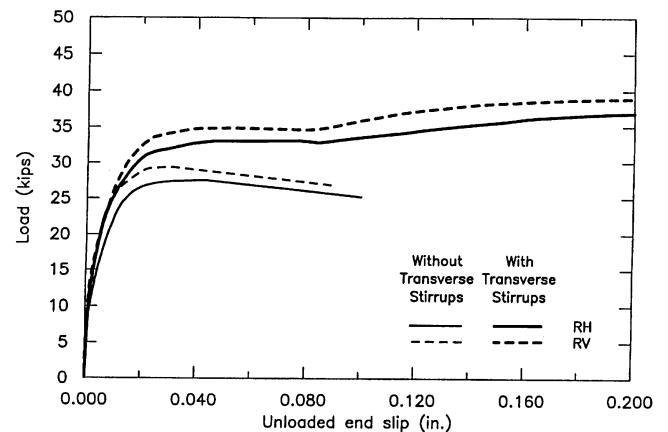


Fig. 1.7(b)—Average load-unloaded end slip curves for No. 8 (No. 25) ASTM A 615 reinforcing bars in an ASTM A 944 beam-end specimen. RH and RV represent bars with longitudinal ribs oriented horizontally and vertically, respectively (Darwin and Graham 1993a). (Note: 1 in. = 25.4 mm; 1 kip = 4.45 kN)

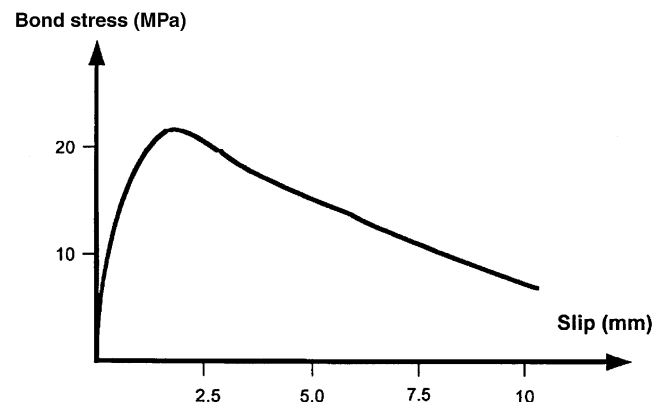


Fig. 1.8—Bond stress-slip curve for bar loaded monotonically and failing by pullout (Eligehausen, Popov, and Bertero 1983). (Note: 1 MPa = 145 psi; 1 mm = 0.0394 in.)

(Maeda, Otani, and Aoyama 1991; Sakurada, Morohashi, and Tanaka 1993; Azizinamini, Chisala, and Ghosh 1995).

Pullout failure (Fig. 1.2(d)) occurs primarily in cases of high confinement and low bonded lengths. In most structural applications, however, splitting failure (Fig. 1.2(b) and (c)) is more common (Clark 1950; Menzel 1952; Chinn, Ferguson, and Thompson 1955; Ferguson and Thompson 1962; Losberg and Olsson 1979; Soretz and Holzenbein 1979; Johnston and Zia 1982; Treece and Jirsa 1989; Choi et al. 1991). For this reason, data used for design are normally limited to members with a minimum development (or splice) length to bar diameter ratio of 15 or 16 and specified maximum values of confinement provided by the concrete and the transverse reinforcement (the latter will be discussed at greater length in Chapter 3). When extended to higher values of confinement, design expressions based on splitting give unrealistically high bond strengths (ACI 318; Orangun, Jirsa, and Breen 1977; Darwin et al. 1996a).

The role played by splitting cracks in bond failure emphasizes the importance of the tensile properties of concrete in controlling bond strength. As will be discussed in Section 2.3.3, the tensile properties involve more than strength, and include fracture energy; that is, the capacity of the concrete to dissipate energy as a crack opens.

1.4—Notation

A_b	= area of bar being developed or spliced	f_{ct}	= average splitting tensile strength of concrete, based on split cylinder test
	= area of largest bar being developed or spliced (CEB-FIP 1990)	f_s	= stress in reinforcing bar
A_{tr}	= area of each stirrup or tie crossing the potential plane of splitting adjacent to the reinforcement being developed, spliced, or anchored	f_y	= yield strength of steel being developed or spliced
b_w	= width of the web of a beam	f_{yt}	= yield strength of transverse reinforcement
c	= spacing or cover dimension	G_f	= fracture energy
	= $c_{min} + d_b/2$	h_r	= average height of deformations on reinforcing bar
c_b	= bottom concrete cover for reinforcing bar being developed or spliced	jd_i	= internal moment arm at section i
c_{max}	= maximum (c_b, c_s)	K	= constant used in CEB-FIP design expression for development length
c_{med}	= median ($c_{so}, c_b, c_{si} + d_b/2$) [that is, middle value], (Esfahani and Rangan 1998a,b)	K_1	= constant used to calculate T_s
c_{min}	= minimum cover used in expressions for the bond strength of bars not confined by transverse reinforcement	K_{tr}	= transverse reinforcement index
	= minimum ($c_{so}, c_b, c_{si} + d_b/2$) (Esfahani and Rangan 1998a,b)		= $\frac{A_{tr}f_{yt}}{1500sn}, \left(\frac{A_{tr}f_{yt}}{10.34sn}\right)^*$ (ACI 318)
c_{min}	= smaller of minimum concrete cover or 1/2 of the clear spacing between bars		= $35.3 t_r t_d A_{tr} / sn$ (ACI T2-98)
	= minimum (c_b, c_s)		= $C_R(0.72d_b + 0.28)\frac{A_{tr}}{sn}, \left(C_R(0.0283d_b + 0.28)\frac{A_{tr}}{sn}\right)^*$ (ACI 408.3)
c_s	= minimum [$c_{so}, c_{si} + 0.25$ in. (6.35 mm)]		= $(0.52t_r t_d A_{tr} / sn)f_c'^{1/2}, [(6.26t_d A_{tr} / sn)f_c'^{1/2}]^*$ (see Section 4.3)
c_{si}	= 1/2 of the bar clear spacing	l_d	= development or splice length
c_{so}	= side concrete cover for reinforcing bar	$l_{d,min}$	= minimum development length
C_R	= $44 + 330(R_r - 0.10)$ (ACI 408.3)	$l_{s,min}$	= minimum splice length
d_b	= diameter of bar	M	= constant used in expressions for the bond strength of bars not confined by transverse reinforcement
E_c	= modulus of elasticity of concrete		= $\cosh(0.00092l_d \sqrt{rf_c' / d_b}),$ [$\cosh(0.0022l_d \sqrt{rf_c' / d_b})$]* (Esfahani and Rangan 1998a,b)
f_c	= stress in concrete	M	= ratio of the average yield strength to the design yield strength of the developed bar (CEB-FIP)
f_c'	= concrete compressive strength based on 6 x 12 in. (150 x 300 mm) cylinders	M_i	= internal moment at section i
	= specified compressive strength of concrete	n	= number of bars being developed or spliced
		N	= the number of transverse stirrups, or ties, within the development or splice length
		p	= nominal perimeter of bar
		p	= power of f_c'
		r	= constant used in expressions for the bond strength of bars not confined by transverse reinforcement; a function of R_r
			= 3 for conventional reinforcement ($R_r \approx 0.07$) (Esfahani and Rangan 1998a,b)
		R_r	= relative rib area of the reinforcement
		s	= spacing of transverse reinforcement
		s_r	= average spacing of deformations on reinforcing bar
		t_d	= term representing the effect of bar size on T_s
			= $0.72d_b + 0.28, (0.028d_b + 0.28)^*$ (Darwin et al. 1996a,b)
			= $0.78d_b + 0.22, (0.03d_b + 0.22)^*$ (Zuo and Darwin 1998, 2000) (see Section 4.3)
		t_r	= term representing the effect of relative rib area on T_s
			= $9.6R_r + 0.28$ (Darwin et al. 1996a,b; Zuo and Darwin 1998, 2000) (see Section 4.3)
		T_b	= total bond force of a developed or spliced bar
			= $T_c + T_s$

*SI expressions.

T_c	= concrete contribution to total bond force, the bond force that would be developed without transverse reinforcement
T_i	= tensile force at section i
T_s	= steel contribution to total bond force, the additional bond strength provided by the transverse steel
u	= bond stress
u_b	= bond strength of a bar confined by transverse reinforcement
	= $u_c + u_s$
u_c	= average bond strength at failure of a bar not confined by transverse reinforcement
u_s	= bond strength of a bar attributed to the confinement provided by the transverse reinforcement
U	= bond force per unit length
V	= shear on a section
α	= rib face angle
a	= reinforcement location factor
a_b	= factor used to increase the development length of a bar for lap splices (CEB-FIP 1990)
	= coating factor
b	= angle between transverse rib and longitudinal axis of the bar
b	= reliability index
Δf_s	= change in steel stress over length Δl
ΔT	= change in the bar force as a result of an externally applied load
ϵ_c	= strain in concrete in uniaxial compression
ϵ_o	= concrete strain at maximum concrete stress under uniaxial compression
g	= reinforcement size factor
l	= lightweight aggregate concrete factor
f	= capacity-reduction factor
f_b	= capacity-reduction factor for bond
f_d	= effective f -factor for bond
	= f_b/f_{tension}
f_{tension}	= capacity-reduction factor for section in tension
ΣA_r	= total area of ribs around bar perimeter measured on the longitudinal section of each rib using the trapezoidal method to approximate the area under the curve
ΣA_{tr}	= area of transverse reinforcement along l_d
Σgaps	= sum of the gaps between ends of transverse deformations on reinforcing bar
Σ_o	= perimeters of the bars anchored at a section
w	= $0.1 \frac{c_{\max}}{c_{\min}} + 0.9 \leq 1.25$ (ACI 408.3) (see Section 4.3)

CHAPTER 2—FACTORS AFFECTING BOND

Many factors affect the bond between reinforcing bars and concrete. The major factors are discussed in this chapter. Background research, bond behavior, and relationships between bond strength and geometric and material properties are presented under three major subject headings: structural characteristics, bar properties, and concrete properties. The structural characteristics addressed include concrete cover and bar spacing, the bonded length of the bar, the degree of transverse reinforcement, the bar casting position, and the

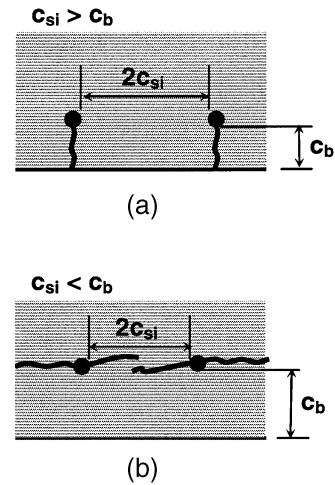


Fig. 2.1—Bond cracks: (a) $c_{si} > c_b$; and (b) $c_{si} < c_b$.

use of noncontact lap splices. The bar properties covered include bar size and geometry, steel stress and yield strength, and bar surface condition, while the concrete properties include compressive strength, tensile strength and fracture energy, aggregate type and quantity, concrete slump and workability, and the effects of admixtures, fiber reinforcement, and degree of consolidation.

2.1—Structural characteristics

2.1.1 Concrete cover and bar spacing—Bond force-slip curves become steeper and bond strength increases as cover and bar spacing increase. The mode of failure also depends on cover and bar spacing (Untrauer 1965; Tepfers 1973; Orangun, Jirsa, and Breen 1977; Eligehausen 1979; Darwin et al. 1996a). For large cover and bar spacing, it is possible to obtain a pullout failure, such as shown in Fig. 1.2(d). For smaller cover and bar spacing, a splitting tensile failure occurs (Fig. 1.2(c)), resulting in lower bond strength. The latter failure mode is the type expected to govern for most structural members. Splitting failures can occur between the bars, between the bars and the free surface, or both. Pullout-like failures can occur with some splitting if the member has significant transverse reinforcement to confine the anchored steel.

With bond failures involving splitting of the concrete for bars that are not confined by transverse reinforcement, the peak load is governed by the tensile response of the concrete, which depends on both tensile capacity and energy dissipation capacity, normally described as fracture energy G_f . As described in Section 2.3.1, concrete exhibiting higher fracture energies provide improved bond capacities, even if the concrete has similar tensile strengths.

When splitting failures occur, the nature of the splitting failure depends, in general, on whether the concrete cover c_b is smaller than either the concrete side cover c_{so} or 1/2 of the bar clear spacing c_{si} . (In this case, the symbol for bottom cover c_b is used, but the discussion applies equally to bottom, top, and side cover.) When c_b is smaller than c_{so} and c_{si} , the splitting crack occurs through the cover to the free surface (Fig. 2.1(a)). When c_{so} or c_{si} is smaller than c_b , the splitting crack forms through the side cover or between the reinforcing bars (Fig. 2.1(b)), respectively.

In ACI 318, the effective value of c_{si} for development length calculations is equal to the actual value of c_{si} . In the Canadian requirements for reinforced concrete design (CSA Standard A23.3-94), however, a greater value $[2/3 \text{ of the center-to-center spacing of the bars being developed minus } 1/2 \text{ of the bar diameter} = (2/3)(2c_{si} + d_b) - (1/2)d_b = (4/3)c_{si} + (1/6)d_b]$ is used. In an analysis of bars not confined by transverse reinforcement, Zuo and Darwin (1998) found that the best match with tests is obtained: 1) using $1.6c_{si}$ as the effective value of c_{si} when using a multiple of c_{si} ; and 2) using $c_{si} + 0.25 \text{ in. } (c_{si} + 6.4 \text{ mm})$ as the effective value of c_{si} when a constant value is added to c_{si} . Of the two procedures, $1.6c_{si}$ provides the better predictions. The fact that the effective value of c_{si} is greater than the actual value is most likely “due to the longer effective crack lengths that occur when concrete splits between bars” (Darwin et al. 1996a) (Fig. 2.1(b)), which make the bars behave as if they have an increased separation.

Although $1.6c_{si}$ gives the best match for development and splice strengths for bars not confined by transverse reinforcement, the value tends to overestimate the effective crack length between bars confined by transverse reinforcement (Zuo and Darwin 1998). In the latter case, $c_{si} + 0.25 \text{ in. } (c_{si} + 6.4 \text{ mm})$, provides a better match with tests. This observation suggests that there is a small but significant difference in the effect of cracks between bars on bond strength in the presence of confining reinforcement. In the presence of transverse reinforcement, the effective crack length between bars is still greater than the clear distance between the bars, but not as great as for similar members without confining transverse reinforcement.

Orangun, Jirsa, and Breen (1975) and Darwin et al. (1992, 1996a) observed that, although the minimum value of c_b , c_{so} , and c_{si} has the principal effect on bond strength, the relative value of c_{so} or c_{si} to c_b is also important. For bars not confined by transverse reinforcement, Darwin et al. (1996a) found that, compared to cases in which the minimum value of c_{so} or c_{si} equals c_b , the bond strength of bars for which the minimum value c_{so} or c_{si} does not equal c_b increases by the ratio

$$\left(0.1 \frac{c_{\max}}{c_{\min}} + 0.9\right) \leq 1.25 \quad (2-1)$$

where

- c_{\max} = maximum (c_b , c_s);
- c_{\min} = minimum (c_b , c_s);
- c_b = bottom cover;
- c_s = minimum [c_{so} , $c_{si} + 0.25 \text{ in. } (6.4 \text{ mm})$];
- c_{so} = side cover; and
- c_{si} = 1/2 of the bar clear spacing.

In addition to cover thickness, the nature of the cover plays a role in bond strength. With emphasis on methods of construction for reinforced concrete bridge decks, Donahey and Darwin (1983, 1985) evaluated the bond strength of bars with 3 in. (76 mm) of monolithic cover and bars with laminar cover, consisting of 3/4 in. (19 mm) monolithic cover topped with a 2-1/4 in. (57 mm) high-density concrete overlay. The bars with the 3 in. (76 mm) laminar cover achieved about the

same bond strengths (average = 97%) as achieved by bars with the same thickness of monolithic cover, even though greater bond strengths would have been expected based on the compressive strength of the overlay concrete, which ranged between 110 and 155% of the compressive strength of the base concrete.

2.1.2 Development and splice length—Increasing the development or splice length of a reinforcing bar will increase its bond capacity. The nature of bond failure, however, results in an increase in strength that is not proportional to the increase in bonded length. The explanation starts with the observations that bond forces are not uniform (Fig. 1.5) and that bond failures tend to be incremental, starting in the region of the highest bond force per unit length. In the case of anchored bars, longitudinal splitting of the concrete initiates at a free surface or transverse flexural crack where the bar is most highly stressed. For spliced bars, splitting starts at the ends of the splice, moving towards the center. For normal-strength concrete, splitting may also be accompanied by crushing of the concrete in front of the ribs as the bar moves (or slips) with respect to the concrete. For higher-strength concrete and for normal-strength concrete in which the bars are epoxy coated, the degree of crushing in front of the ribs is significantly decreased. For splice specimens studied after failure, it is common to see no crushed concrete at ribs near the tensioned end of a spliced bar, with the crushed concrete located at the end of the bar, indicating that failure occurred by a slow wedging action followed by rapid final slip of the bar at failure. Because of the mode of bond failure, the nonloaded end of a developed or spliced bar is less effective than the loaded end in transferring bond forces, explaining the nonproportional relationship between development or splice length and bond strength.

Although the relationship between the bond force and the bonded length is not proportional, it is nearly linear, as illustrated in Fig. 2.2 for No. 4 to 14 (No. 13 to 43) bars. Figure 2.2 indicates that bars will have measurable bond strengths even at low embedded lengths. This occurs because, in the tests, there is always at least one set of ribs that forces the concrete to split before failure. When failure occurs, a significant crack area is opened in the member due to splitting (Brown, Darwin, and McCabe 1993; Darwin et al. 1994; Tholen and Darwin 1996). As the bonded length of the bar increases, the crack surface at failure also increases in a linear but not proportional manner with respect to the bonded length. Thus, the total energy needed to form the crack and, in turn, the total bond force required to fail the member, increase at a rate that is less than the increase in bonded length. Therefore, the common design practice (ACI 318) of establishing a proportional relationship between bond force and development or splice length is conservative for short bonded lengths, but becomes progressively less conservative, and eventually unconservative, as the bonded length and stress in the developed or spliced bar increase.

2.1.3 Transverse reinforcement—Transverse reinforcement confines developed and spliced bars by limiting the progression of splitting cracks and, thus, increasing the bond force required to cause failure (Tepfers 1973; Orangun, Jirsa

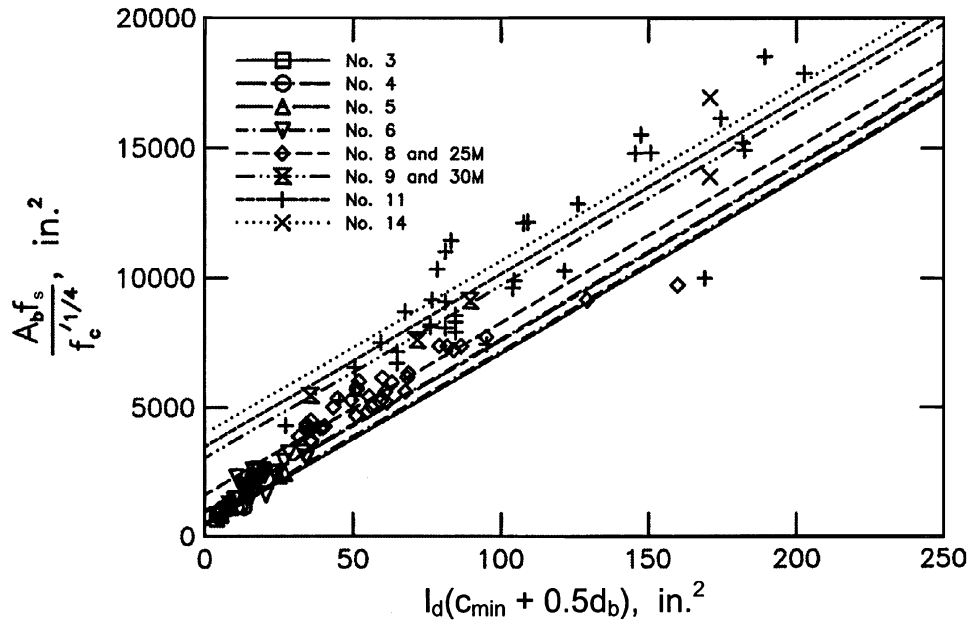


Fig. 2.2—Bond strength $A_b f_s$ normalized with respect to $f_c^{1/4}$ versus the product of the development or splice length l_d and the smaller of the minimum concrete cover to the center of the bar or 1/2 of the center-to-center bar spacing ($c_{min} + 0.5d_b$) (Darwin et al. 1996b). (Note: 1 in.² = 645 mm²)

and Breen 1977; Darwin and Graham 1993a,b). An increase in transverse reinforcement results in an increase in bond force, eventually converting a splitting failure to a pullout failure. Additional transverse reinforcement, above that needed to cause the transition from a splitting to a pullout failure, becomes progressively less effective, eventually providing no increase in bond strength (Orangun, Jirsa, and Breen 1977).

The total bond force of a developed or spliced bar T_b can be represented as the sum of a concrete contribution T_c , representing the bond force that would be developed without the transverse reinforcement, plus a steel contribution T_s , representing the additional bond strength provided by the transverse steel

$$T_b = T_c + T_s \quad (2-2)$$

The value of the concrete contribution is affected somewhat by the presence of the transverse steel, as discussed in Section 2.1.1, because the effective crack length between bars is reduced as bar slip continues in the process of mobilizing the additional bond strength provided by the transverse reinforcement (Zuo and Darwin 1998, 2000). The effect of transverse reinforcement on T_c is small but measurable.

The value of the steel contribution T_s is a function of the area of reinforcing steel that crosses potential crack planes, the strength of the concrete, and both the size and deformation properties of the developed or spliced reinforcement. It can be represented in the form (Zuo and Darwin 1998, 2000)

$$T_s = K_1 t_r t_d \frac{N A_{tr}}{n} f_c'^p \quad (2-3)$$

where

- K_1 = a constant;
- t_r = a factor that depends on the relative rib area R_r of the reinforcement;
- t_d = a factor that depends on the diameter d_b of the developed or spliced bar;
- N = the number of transverse stirrups, or ties, within the development or splice length;
- A_{tr} = area of each stirrup or tie crossing the potential plane of splitting adjacent to the reinforcement being developed or spliced;
- n = number of bars being developed or spliced along the plane of splitting;
- f_c' = concrete compressive strength based on 6 x 12 in. (150 x 300 mm) cylinders; and
- p = power of f_c' between 0.75 and 1.00 (see Section 3.3 for values of K_1 and p).

In the case shown in Fig. 2.3, illustrating a two-leg stirrup confining three spliced reinforcing bars in the same plane, A_{tr} = two times the area of the stirrup A_t and $n = 3$ if c_{so} or the effective value of c_{si} is less than c_b . $A_{tr} = A_t$ and $n = 1$ if c_{so} and the effective value of c_{si} are greater than c_b .

The values of t_r and t_d can be represented as linear functions of R_r and d_b , respectively (Zuo and Darwin 1998, 2000).

$$t_r = 9.6R_r + 0.28 \quad (2-4)$$

$$t_d = 0.78d_b + 0.22 \quad (2-5)$$

with d_b in inches and $R_r \leq 0.14$.

The relationships given in Eq. (2-4) and (2-5) suggest that an increase in the wedging action of the bars, resulting from

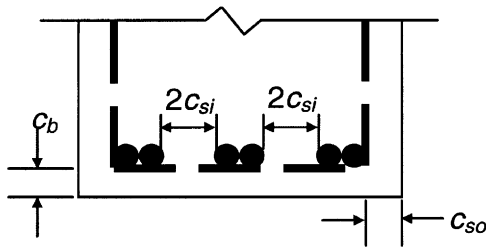


Fig. 2.3—Beam cross sections showing definition of c_b , c_{si} , and c_{so} .

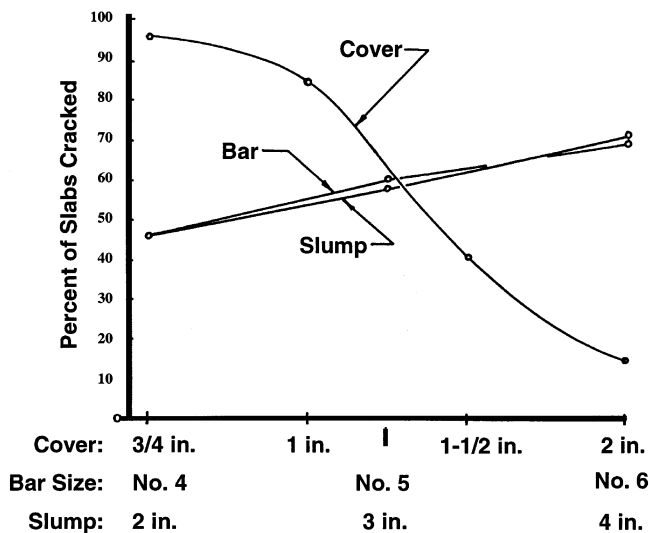


Fig. 2.4—Settlement cracking as a function of bar size, slump, and cover (Dakhil et al. 1975). (Note: 1 in. = 25.4 mm)

both an increase in R_r (a relative measure of rib size and spacing) and an increase in bar size d_b (an absolute measure of rib size), will increase the stress in the stirrups, resulting in an increase in confining force. The relationship between confinement and the degree of wedging action is in concert with the observation that stirrups rarely yield (Maeda, Otani, and Aoyama 1991; Sakurada, Morohashi, and Tanaka 1993; Azizinamini, Chisala, and Ghosh 1995), allowing an increase in lateral displacement caused by wedging to be translated into an increase in confining force. As a result, the yield strength of the transverse reinforcement f_{yt} does not play a role in the steel contribution to bond force, T_s . The effect of concrete strength on T_s is discussed further in [Section 2.3.1](#).

2.1.4 Bar casting position—As early as 1913, Abrams observed that bar position during concrete placement plays an important role in the bond strength between concrete and reinforcing steel. Top-cast bars have lower bond strengths than bars cast lower in a member (Clark 1946, 1949; Collier 1947; Larnach 1952; Menzel 1952; Menzel and Woods 1952; Ferguson and Thompson 1962, 1965; CUR 1963; Untrauer 1965; Welch and Patten 1965; Untrauer and Warren 1977; Thompson et al. 1975; Jirsa and Breen 1981; Luke et al. 1981; Zekany et al. 1981; Donahey and Darwin 1983, 1985; Altowaiji, Darwin, and Donahey 1984, 1986; Brettmann, Darwin, and Donahey 1984, 1986; Jeanty,

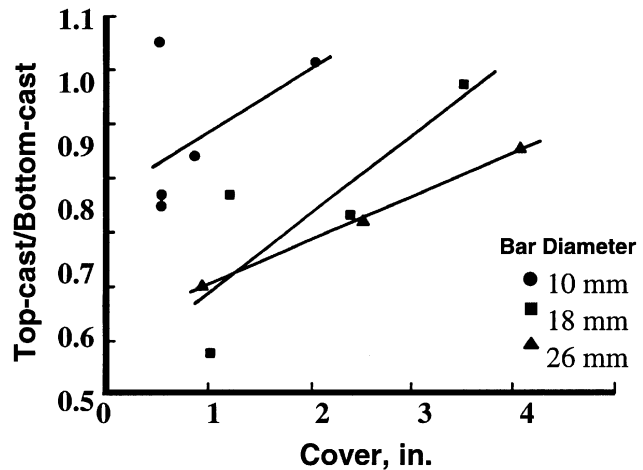


Fig. 2.5—Ratio of top-cast to bottom-cast bar bond strength versus cover (CUR 1963). (Note: 1 in. = 25.4 mm)

Mitchell, and Mirza 1988). This behavior is recognized in ACI 318 and the AASHTO Bridge Specifications (1996). Top-reinforcement, horizontal reinforcement with more than 12 in. (300 mm) of fresh concrete cast in the member below the development length or splice, requires a 30% increase in development length (ACI 318). Most research, however, indicates that while an increased depth of concrete below a bar reduces bond strength, the effect of shallow top cover is of greater significance. The impact of shallow top cover on the top-cast bar effect is emphasized by the fact that the strength reduction becomes progressively greater as cover is decreased.

The lower bond strength of top-cast bars may be explained as follows: the greater the depth of concrete below a bar, the greater will be the settlement and accumulation of bleed water at the bar, because there is more concrete beneath the bar to settle and bleed. The effects of settlement and bleeding on the concrete around a bar are aggravated by increased concrete slump and decreased cover above the bar. Dakhil, Cady, and Carrier (1975) found that longitudinal settlement cracking increased above top-cast bars with increased slump and bar size and especially with decreased top cover (Fig. 2.4).

Menzel (1952) observed settlement cracks over 1 in. (25 mm) diameter top-cast bars with a 2 in. (50 mm) cover for specimens placed with 6 in. (150 mm) slump concrete that was consolidated by hand. Cracks were not observed in lower slump concrete that was vibrated internally. Menzel (1952) also observed that the bond strength of top-cast reinforcement decreases as specimen depth increases. He observed the greatest reduction for high-slump concrete consolidated by hand rodding and the least for low-slump concrete consolidated with vibration.

The importance of cover on the reduction in bond strength for top-cast bars is demonstrated by tests in the Netherlands (CUR 1963). As shown in [Fig. 2.5](#), the ratio of top-cast bar to bottom-cast bar bond strength decreased significantly as cover decreased.

Ferguson and Thompson (1965) conducted beam tests to compare the ratio of top-cast to bottom-cast bar bond

strength. The bond strength of top-cast bars decreased with increasing slump and decreasing top cover.

Zekany et al. (1981) conducted splice tests in 16 in. (406 mm) deep beams with both top- and bottom-cast bars. Splice strength decreased for both top- and bottom-cast bars with increasing slump, but the decrease was consistently greater for the top-cast bars.

In a study of casting position, Luke et al. (1981) clearly demonstrated that as the depth of concrete below a bar increases, the bond strength decreases (Fig. 2.6). They observed the greatest incremental decrease in strength for top-cast bars. As will be discussed in more detail in [Section 2.3.5](#), they also observed that bond strength decreased with increasing slump, but that the decrease was most pronounced for top-cast bars. For bars cast below the specimen mid-depth, slump appeared to have little effect.

Brettmann, Darwin, and Donahey (1984, 1986) also found that as the amount of concrete below a bar increases, bond strength decreases. The measured decrease was least for low-slump concrete and greatest for high-slump concrete obtained without the use of a high-range, water-reducing admixture. Bond strength decreased for bars with as little as 8 in. (200 mm) of concrete below the bar, bars that would not be defined as top reinforcement under the provisions of ACI 318. In similar tests run by Zilveti et al. (1985), a “top-bar effect” was obtained for top-cast bars with as little 6 in. (150 mm) of concrete below the bars. Brettmann, Darwin, and Donahey (1984, 1986) found that bond strength was similar for bars placed 8 and 15 in. (200 and 380 mm) above the bottom of the forms. Bond strength was lowest for bars placed 36 in. (915 mm) above the bottom of the forms, with the largest reductions obtained for high slump, nonvibrated specimens, as shown in Fig. 2.7. In all cases (even for bars with only 8 in. [200 mm] of concrete below the bars), the decrease in bond strength between bottom-cast and top-cast bars was greater than between top-cast bars with 8 and 36 in. (203 and 914 mm) of concrete below the bars. These results indicate that the choice of 12 in. (300 mm) of concrete below a bar for the 30% increase in development length for top reinforcement is arbitrary. Based on concrete depth alone, there seems to be a gradual decrease in bond strength with no sharp drop-off.

2.1.5 Noncontact lap splices—A noncontact lap splice (also called a spaced splice) provides continuity of reinforcement by overlapping the ends of the steel bars without the bars touching each other. According to ACI 318, “bars spliced by noncontact lap splices in flexural members shall not be spaced transversely farther apart than one-fifth the required lap splice length, nor 6 in. (150 mm).” This provision was first incorporated in ACI 318-71. The commentary to ACI 318 argues that if individual bars in noncontact lap splices are too widely spaced, an unreinforced section is created, and that forcing a potential crack to follow a zigzag line (5 to 1 slope) is considered to be a minimum precaution. The commentary points out that the 6 in. (150 mm) maximum spacing is added because most research available on lap splices of deformed bars was conducted with reinforcement within this spacing.

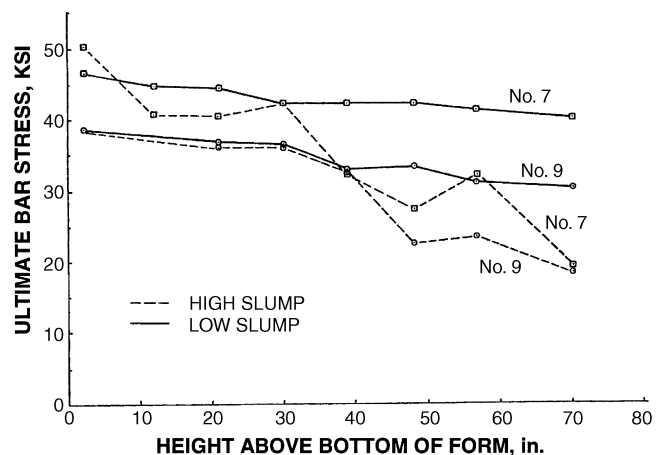


Fig. 2.6—Bond strength as a function of bar location within a wall specimen. High slump = 8-1/2 in. (215 mm). Low slump = 3 in. (75 mm) (Luke et al. 1981). (Note: 1 ksi = 6.89 MPa; 1 in. = 25.4 mm)

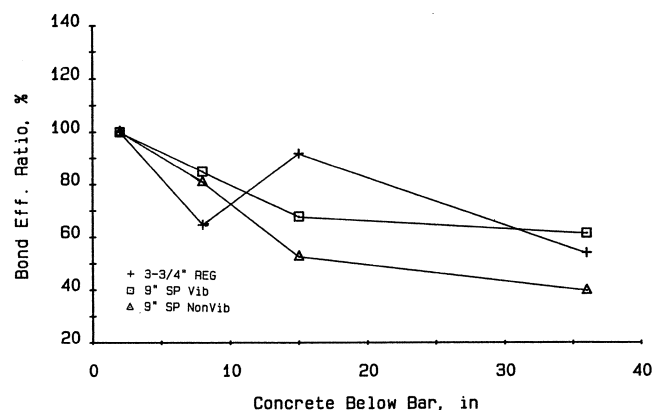


Fig. 2.7—Bond efficiency ratio versus concrete depth below the bar for lower temperature concrete (53 °F [12 °C]). REG = concrete without a superplasticizer; and SP = superplasticized concrete (Brettmann, Darwin, and Donahey 1986) (Note: 1 in. = 25.4 mm)

In earlier codes, a minimum clear spacing was actually required. ACI 318-47 specified that the minimum clear spacing between spliced bars must not be less than $1.5d_b$ for round bars or $1\frac{1}{3}$ times the maximum size of aggregate, and at least 1 in. (25 mm) in any case. ACI 318-51 retained these requirements, except that the $1.5d_b$ requirement was changed to $1.0d_b$. Engineering practice before 1950 usually required that an allowance be made for a reduction in bonded area for tied lap splices to account for the fact that concrete does not completely surround spliced bars that are in contact. This was provided by lengthening the splice. It was only in 1963 that the ACI Building Code (ACI 318-63) allowed both spaced and contact lap splices.

In a lap splice, the force in one bar is transferred to the concrete which, in turn, transfers it to the adjacent bar. This transfer of forces from one bar to another in a noncontact splice can be seen from the crack pattern, as shown in [Fig. 2.8](#) (MacGregor 1997).

Walker (1951) reported on a series of pullout and beam tests to compare the performance of spaced and tied lap

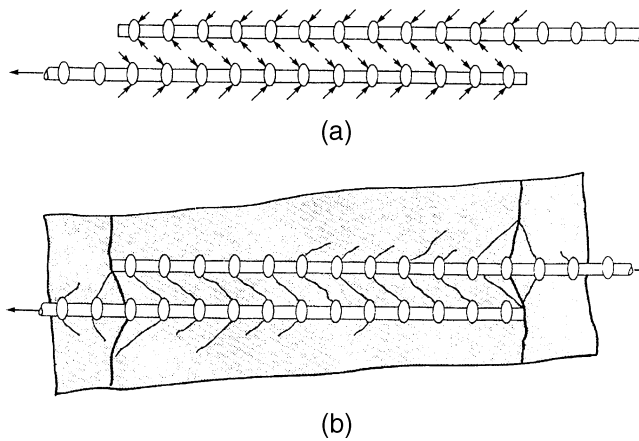


Fig. 2.8—Noncontact tension lapped splices: (a) forces on bars at splice; and (b) internal cracks at splice (MacGregor 1997).

splices. Two levels of concrete strength and three types of deformed reinforcing bars were studied. In all tests where the spliced bars were spaced, the clear spacing was $1.5d_b$. Beam tests showed no significant difference between the two splicing methods (zero spacing and $1.5d_b$ spacing), but at loads close to ultimate, there was some indication that spaced spliced bars might be slightly preferable, showing less center beam deflection and end slip at a given load level. In the pullout tests, there was no weakening of bond at the tied splice. Considering all of the data, however, Walker concluded that within the scope of his study there was no significant loss of bond when deformed bars were tied together at the splice.

Chamberlin (1952) investigated the effect of spacing of spliced bars in tension pull-out specimens. The tests were designed to provide data on the effect of spacing of lapped bars on bond and also on the effect of length of overlap in relation to effectiveness of stress transfer from one bar to another at a splice. Confinement was provided by spiral wire to prevent splitting. Based on test results, Chamberlin concluded deformed bars developed better average bond stress in adjacent tied splices (zero spacing) than in spaced splices, but that the differences in bond strength for clear spacings of one-bar diameter and three-bar diameters were not significant.

Chinn, Ferguson, and Thompson (1955) reported on research investigating the effects of many variables on the bond capacity of spliced reinforcement including the clear spacing between spliced bars, with values of 0 (contact splice), 0.75, 1.0, 1.25, and 1.88 in. (20, 25, 32, and 48 mm). Forty beam specimens were tested. Each beam contained either one or two splices, placed in a constant moment region at the center of the beam. They concluded that their tests confirmed the earlier tests by Walker (1951) and Chamberlin (1952), showing little difference in strength between contact and spaced lap splices.

Chamberlin (1958) studied the effect of spacing of lapped bars on bond strength and the effect of length of lap on the load-carrying capacity of small beams. Twenty-one beams were tested with no restraint against splitting. All beams were 6 x 6 in. (150 x 150 mm) in cross section and 36 in.

(915 mm) in length, simply supported under symmetrical two-point loading. The clear spacing between lapped bars was either 1/2 or 1 in. (12 or 25 mm). Chamberlin concluded that there was little difference in strength between adjacent and spaced splices.

Sagan, Gergely, and White (1991) studied the behavior of noncontact lap splices subjected to monotonic and repeated inelastic loading. Forty-seven full-scale flat-plate specimens were tested. Each specimen contained two splices. Variables included splice-bar spacing, concrete compressive strength, bar size, the amount and distribution of transverse reinforcement, and the lap length. The specimens were loaded slowly in direct tension. If a specimen survived the first loading to yield, it was unloaded slowly and then reloaded to yield; this process was repeated until failure. Sagan, Gergely, and White observed that:

1. A noncontact lap splice can be modeled as a plane truss, with load transferred between the two spliced bars through compressive struts in the concrete; the tension elements are provided by the transverse reinforcement and surrounding concrete;

2. An in-plane splitting crack forms between the bars of spaced bar splices. The crack results from bond-induced bursting stresses and Poisson strains generated by the compression stress field. Diagonal surface cracking of the concrete between the spliced bars becomes more prominent as the bar spacing increases. Even the large cracks that formed at the ends of the splice were diagonal;

3. The splice strength of the monotonically loaded specimens increased when transverse reinforcement was provided. Also, the number of inelastic load cycles sustained by a tension splice depends on the amount of confinement provided by transverse reinforcement; and

4. The strength of a splice is independent of the splice-bar spacing up to at least six times the bar diameter for monotonic loading. Under repeated loading up to the yield strength of the splice bars, the maximum load (equal to the yield load) is also independent of bar spacing, up to eight times the bar diameter for both No. 6 and No. 8 (No. 19 and No. 25 mm) bars.

To check the validity of the ACI 318 provisions for noncontact splices, Hamad and Mansour (1996) tested 17 slabs in positive bending. Reinforcement on the tension side consisted of three reinforcing bars spliced at the center of the span. No transverse reinforcement was provided in the splice region. The clear spacing between lapped bars varied between 0 and 50% of the splice length for slabs reinforced with 0.55 and 0.63 in. (14 and 16 mm^{*}) bars, and between 0 and 40% of the splice length for 0.80 in. (20 mm) bars. For eight specimens, the clear transverse spacing between the spliced bars was at least 20% of the splice length specified by ACI 318. The splice lengths were limited to 11.8 in. (300 mm) for slabs reinforced with 0.55 and 0.63 in. (14 and 16 mm) bars, and 13.8 in. (350 mm) for 0.8 in. (20 mm) bars. They observed that the noncontact splices developed greater

*The bars used in these tests were sized in millimeters.

bond strength than the contact splices, up to an optimum clear spacing of about $5d_b$. They concluded that the ACI limit on the transverse spacing of noncontact tensile lap splices to 20% of the lap length is conservative and that a limit of 30% could be used.

2.2—Bar properties

2.2.1 Bar size—The relationship between bar size and bond strength is not always appreciated. The reason is that, while (1) a longer development or splice length is required as bar size increases, and (2) for a given development or splice length, larger bars achieve higher total bond forces than smaller bars for the same degree of confinement.

Addressing the second point first, for a given bonded length, larger bars require larger forces to cause either a splitting or pullout failure, as illustrated in Fig. 2.2, for bars not confined by transverse reinforcement. The result is that the total force developed at bond failure is not only an increasing function of concrete cover, bar spacing, and bonded length, but also of bar area (Orangun, Jirsa, and Breen 1977; Darwin et al. 1992, 1996a). The bond force at failure, however, increases more slowly than the bar area, which means that a longer embedment length is needed for a larger bar to fully develop a given bar stress (the first point). When evaluated in terms of bond stress (Eq. (1-4) and (1-5)), smaller bars appear to have even a greater advantage; thus, conventional wisdom suggests that it is desirable to use a larger number of small bars rather than a smaller number of large bars; this is true until bar spacings are reduced to the point that bond strength is decreased (Ferguson 1977; Rehm and Eligehausen 1979).

The size of a developed bar also plays an important role in the contribution of confining transverse reinforcement to bond strength. As larger bars slip, higher strains and, thus, higher stresses, are mobilized in the transverse reinforcement, providing better confinement. As a result, the added bond strength provided by transverse reinforcement increases as the size of the developed or spliced bars increases, as shown in Fig. 2.9, which compares the relative effect of transverse reinforcement on bond strength M , normalized to the effect of the relative rib area t_r , versus bar diameter, for No. 5, No. 8, and No. 11 (No. 16, No. 25, and No. 36) bars with a wide range of relative rib area R_r . The term M is the ratio of the additional bond force provided by the transverse steel T_s , normalized with respect to $f_c'^{3/4}$ (see Section 2.3.2), to the area of transverse steel confining the bar.

2.2.2 Bar geometry—Historically, there have been widely conflicting views of the effect of bar geometry on bond strength. Some studies indicate that deformation patterns have a strong influence on bond strength. Other studies show that deformation pattern has little influence, and it is not uncommon for bars with different patterns to produce nearly identical development and splice strengths. Over time, however, the effects of bar geometry on bond behavior have become increasingly clear, as will be described in this section.

The earliest study on bond resistance of plain and deformed reinforcing bars was done by Abrams (1913) using pullout and beam specimens. The test results showed that

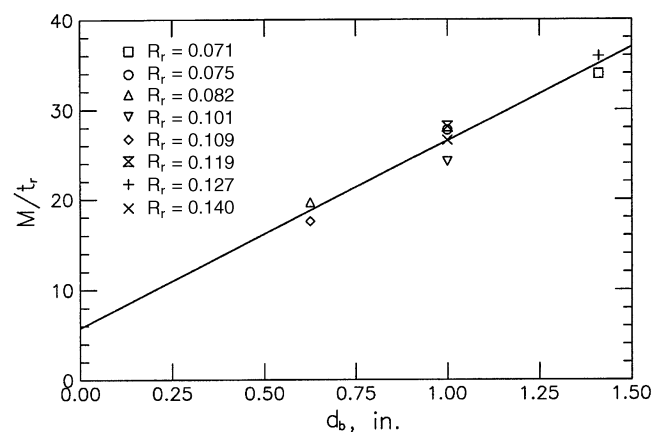


Fig. 2.9—Relative contribution of transverse reinforcement M , normalized with respect to the relative rib area ($t_r = 9.6R_r + 0.28$) versus bar diameter (Zuo and Darwin 1998). (Note: 1 in. = 25.4 mm)

deformed bars produced higher bond resistance than plain (smooth) bars. Abrams found that in pullout tests of plain bars, bond resistance reached its maximum value at a loaded end slip of about 0.01 in. (0.25 mm). For deformed bars, the load-slip performance was the same as for plain bars up to the slip corresponding to the maximum bond resistance of the plain bars. As slip continued, the ribs on deformed bars increased the bond resistance by bearing directly on the adjacent concrete. Abrams observed that the ratio of the bearing area of the projections (projected area measured perpendicular to the bar axis) to the entire surface area of the bar in the same length could be used as a criterion for evaluating the bond resistance of deformed bars. To improve bond resistance, he recommended that this ratio not be less than 0.2, resulting in closer spacings of the projections than were used in commercial deformed bars at the time.

Over 30 years later, Clark (1946, 1949) investigated 17 commercial deformation patterns using pullout and beam tests. The bond performance for each pattern was evaluated based on the bond stress developed at predetermined values of slip. Based on Clark's investigations, standard deformation requirements were introduced for the first time in the Tentative Specification ASTM A 305-47T, later appearing as ASTM A 305-49. The requirements included a maximum average spacing of deformations equal to 70% of the nominal diameter of the bar and a minimum height of deformations equal to 4% of the nominal diameter for bars with a nominal diameter of 1/2 in. (13 mm) or smaller, 4.5% of the nominal diameter for bars with a nominal diameter of 5/8 in. (16 mm), and 5% for larger bars. These requirements remain unchanged in the current ASTM specifications for reinforcing bars (ASTM A 615; ASTM A 706; ASTM A 767; ASTM A 955; ASTM A 996).

In his study, Clark (1946, 1949) found that bond performance improved for bars with lower ratios of shearing area (bar perimeter times center-to-center distance between ribs) to bearing area (projected rib area normal to the bar axis) and recommended that the ratio of shearing area to bearing area be limited to a maximum of 10 and, if possible, 5 or 6. In

current practice, this criterion is described in terms of the inverse ratio, that is, the ratio of the bearing area to the shearing area, which is known alternately as the rib area, related rib area, or relative rib area (DIN 488; Soretz and Holzenbein 1979; ACI 408.3). Relative rib area R_r is the term used in U.S. practice (ASTM A 775, ASTM A 934, ASTM A 944, ACI 408.3).

$$R_r = \quad (2-6)$$

$$\frac{\text{projected rib area normal to bar axis}}{\text{nominal bar perimeter} \times \text{center-to-center rib spacing}}$$

Clark's recommendations then become a minimum value of R_r equal to 0.1, with desirable values of 0.2 or 0.17, which are not so different from Abrams' (1913) recommendations. These later recommendations, however, were not incorporated in the ASTM requirements, so that the typical values of relative rib area for bars currently used in the U.S. range between 0.057 and 0.087 (Choi et al. 1990).

Rehm (1961) reported that one of two failure modes, splitting or pullout, can occur when a reinforcing bar slips with respect to the concrete. If the ratio of rib spacing to rib height was greater than 10 and the rib face angle (the angle between the face of the rib and the longitudinal axis of the bar, α in Fig. 1.2(a)) is greater than 40 degrees, he observed that the concrete in front of the rib crushes, forming wedges and then inducing tensile stress perpendicular to the bar axis. This results in transverse cracking and splitting of surrounding concrete. If the ribs had a spacing to height ratio less than 7, with a rib face angle greater than 40 degrees, he observed that the concrete in front of ribs gradually crushes, causing a pullout failure.

Lutz, Gergely, and Winter (1966), and Lutz and Gergely (1967) found that for a deformed bar with a rib face angle greater than 40 degrees, slip occurs by progressively crushing concrete in front of the ribs, producing a region of crushed concrete with a face angle of 30 to 40 degrees, which acts as a wedge. Lutz, Gergely, and Winter also showed that no crushing of concrete occurs if the rib face angle is less than 30 degrees. These observations were supported by Skorobogatov and Edwards (1979). Based on tests using bars with face angles of 48.5 and 57.8 degrees, Skorobogatov and Edwards showed that these differences in face angle do not affect bond strength because the high face angle is flattened by crushed concrete in front of the ribs.

Losberg and Olsson (1979) tested three commercial deformation patterns used in Sweden and some machined bars with different values of rib spacing and rib height. They found that the bond forces produced by the three patterns were obviously different in pullout tests in which a pullout failure governed. If splitting failure governed, however, as in beam-end and ring pullout tests, there was little difference in the bond forces obtained using the three patterns. Losberg and Olsson concluded that pullout tests are not suitable to study bond performance because the state of stress in a pullout test resulting from the additional confinement

provided to the concrete does not represent the state of stress in actual structures where splitting failure typically governs. Their test results also showed that the splitting force is not sensitive to rib spacing and that ribs oriented perpendicular to the longitudinal axis of the bar give slightly higher splitting force than inclined ribs.

Soretz and Holzenbein (1979) studied the effect of rib height and spacing, rib inclination, and the cross-sectional shape of ribs on bond. Three bars were machined with different rib heights and spacings but with the same rib bearing area per unit length. In pullout tests, Soretz and Holzenbein found that, for the three patterns, the bond forces showed no significant differences up to 0.04 in. (1 mm) of slip. Once the slip was greater than 0.04 in. (1 mm), however, the bond force for the bar with the lowest rib height was about 20% smaller than that of the other two patterns. They recommended a combination of a minimum rib height of 0.03 bar diameters and a rib spacing of 0.3 bar diameters as the optimum geometry for deformed bars to limit splitting and to increase bond strength.

Darwin and Graham (1993a,b) studied the effect of deformation pattern on bond strength using beam-end specimens. The principal parameters in the study were rib height, rib spacing, relative rib area, and degree of confinement from concrete cover and transverse reinforcement. Both specially machined and conventional 1 in. (25 mm) diameter bars were used in the study. The machined bars had three different rib heights, 0.050, 0.075, and 0.100 in. (1.27, 1.91, and 2.54 mm), with center-to-center rib spacings ranging from 0.263 to 2.2 in. (6.68 to 55.9 mm), producing relative rib areas of 0.20, 0.10, and 0.05. Darwin and Graham concluded that bond strength is independent of deformation pattern if the bar is under relatively low confinement (small concrete cover and no transverse reinforcement) and bond strength is governed by a splitting failure in the concrete. If additional confinement is provided by transverse reinforcement, however, bond strength increases with an increase in relative rib area. They found that the bond force-slip response of bars is related to the relative rib area of the bars, but independent of the specific combination of rib height and spacing. The initial stiffness of the load-slip curve increases with an increase in relative rib area. Darwin and Graham also observed that, when tested in beam-end specimens, bars with the longitudinal ribs oriented in a plane parallel to the splitting cracks provide higher bond strength than bars with the longitudinal ribs oriented in a plane perpendicular to the splitting cracks.

Cairns and Jones (1995) investigated 14 different bar geometries using lapped bar test specimens. The lapped bars were confined by stirrups. The relative rib area R_r of the tested bars ranged from 0.031 to 0.090. The inclination of the transverse ribs with respect to the longitudinal axis of the bar varied from 40 to 90 degrees and the rib face angle varied from 28 to 51 degrees. Bars were placed in two ways, either alignment A0 (with the plane of two longitudinal ribs parallel to the concrete splitting face) or alignment A90 (with the plane of longitudinal ribs perpendicular to the concrete splitting face). Cairns and Jones reported that there

were no significant effects of rib inclination and rib face angle on bond strength, but that, as observed by Darwin and Graham (1993a,b), the alignment of longitudinal ribs influenced bond strength: the bond force for alignment A0 was higher than for alignment A90. They also found that relative rib area plays an important role in bond strength. The test results indicated that doubling relative rib area could reduce development and splice length by 20%.

Darwin et al. (1996b), Tan et al. (1996), and Zuo and Darwin (1998, 2000) used splice and beam-end specimens to study the effect of relative rib area on bond strength. The tests in these studies involved commercially produced high R_r reinforcing bars with relative rib areas ranging from 0.101 to 0.141 and conventional bars with relative rib areas ranging from 0.068 to 0.087. The tests included top and bottom-cast bars plus specimens to study the effect of relative rib area on the splice strength of epoxy-coated bars. The test results indicated that the splice strength of uncoated bars is not affected by the deformation pattern if the bars are not confined by transverse reinforcement. For bars confined by transverse reinforcement, splice strength increases with increasing bar diameter and relative rib area. As shown in Fig. 2.9 and Eq. (2-5) for d_b and Eq. (2-4) for R_r , the contribution of transverse reinforcement to bond strength T_s increases linearly with increases in d_b and R_r .

For epoxy-coated bars under all conditions of confinement, bond strength increases with relative rib area (Darwin et al. 1996b; Tan et al. 1996; Zuo and Darwin 1998). For bars with $R_r \geq 0.10$ and concrete with $f'_c \leq 10,000$ psi (69 MPa), development or splice length should be increased by 20%, in contrast to the 50% increase in length needed for conventional reinforcement. For $f'_c > 10,000$ psi (69 MPa), a 50% increase in development or splice length appears warranted, even for high R_r bars (Zuo and Darwin 1998).

2.2.3 Steel stress and yield strength—For a number of years, concern existed that bars that yielded before bond failure produced average bond stresses significantly lower than higher strength steel in similar test specimens that did not yield (Orangun, Jirsa, and Breen 1975). As a result, test specimens were often deliberately configured to ensure that the bars did not yield prior to bond failure.

As it turns out, the bond strengths of bars that yield average only about 2% less when not confined by transverse reinforcement and about 10% greater when confined by transverse reinforcement than similar bars with the same bonded lengths made of higher strength steel that does not yield (Darwin et al. 1996a; Zuo and Darwin 1998, 2000).

2.2.4 Bar surface condition—The surface of a reinforcing bar plays an important role in bond because of its effect on the friction between reinforcing steel and concrete and the ability of ribs to transfer force between the two materials. Bar surface condition involves the cleanliness of reinforcement, the presence of rust on the bar surface, and the application of epoxy coatings to protect the reinforcement from corrosion.

2.2.4.1 Bar cleanliness—To prevent a reduction in the bond strength, ACI 318 requires that reinforcement must be free of mud, oil, and other nonmetallic coatings that decrease bond strength. Based on the work of Kemp, Brezny, and

Unterspan (1968), steel reinforcement with rust, mill scale, or a combination of the two is considered satisfactory provided that the minimum dimensions, including the height of the deformations, and the weight of a hand-wire-brushed test specimen, comply with the applicable ASTM specifications.

2.2.4.2 Epoxy-coated bars—Epoxy coatings are used to improve the corrosion resistance of reinforcing bars. Under the provisions of ASTM A 775 and ASTM A 934, at least 90% of coating thickness measurements must be between 7 and 12 mils (175 and 300 μm). Bars are rejected if more than 5% of the coating thickness measurements are below 5 mils (125 μm). Epoxy coatings tend to reduce bond strength.

In the earliest study on the bond of epoxy-coated bars, Mathey and Clifton (1976) investigated the effect of coating thickness on bond strength using pullout tests. For bars with epoxy coatings between 1 to 11 mils (25 to 280 μm) in thickness, bond strength was about 6% lower than for uncoated bars. For bars with a coating thickness of 25 mils (635 μm), however, the peak bond force was between 34 and 60% of the strength of uncoated bars.

Johnston and Zia (1982) studied the effect of epoxy coating on bond strength using slab and beam-end specimens. Coating thickness was between 6.7 and 11.1 mils (170 to 282 μm). The bars were confined by transverse reinforcement. The slab specimens with coated bars had slightly larger deflections and wider cracks than those with uncoated bars. Compared with uncoated bars, the bond strength of coated bars was about 4% lower for the slab specimens and 15% lower for the beam-end specimens. Johnston and Zia recommended an increase of 15% in the development length when coated bars are used in place of uncoated bars.

Treece and Jirsa (1989) tested 21 beam-splice specimens without transverse reinforcement in the splice region. Twelve of the specimens contained epoxy-coated bars with coating thicknesses between 4.5 and 14 mils (114 to 356 μm). Seventeen specimens contained top-cast bars; four contained bottom-cast bars. Concrete strength ranged from 3860 to 12,600 psi (27 to 87 MPa). An average reduction in bond strength of 34% compared to uncoated bars was observed in the tests. The deformation patterns used in the study were discontinued shortly after the tests due to difficulties in obtaining a uniform coating thickness. The work by Treece and Jirsa is the basis of the development length modification factors for epoxy-coated bars in ACI 318 and the AASHTO bridge specifications. In ACI 318, development length is multiplied by a factor of 1.5 for epoxy-coated bars with a cover of less than $3d_b$ or clear spacing between bars less than $6d_b$ and a factor of 1.2 for other cases, with a maximum of 1.7 for the product of top-bar factor and epoxy-coating factors. In the AASHTO bridge specifications (1996), the three factors are 1.5, 1.15, and 1.7, respectively. The 1.2 (ACI) and 1.15 (AASHTO) factors were selected based on the work of Johnston and Zia (1982).

DeVries, Moehle, and Hester (1991) and Hadje-Ghaffari et al. (1992, 1994) found the maximum of 1.7 for the product of the top factor and epoxy-coating factor to be too conservative and recommended a value of 1.5.

Choi et al. (1990, 1991) studied the roles of coating thickness, bar size, and deformation pattern on the bond strength of epoxy-coated bars. They observed that coating thickness has little effect on the reduction in bond strength due to epoxy coating for No. 6 (No. 19) and larger bars. For No. 5 (No. 16) and smaller bars, however, the bond strength ratio of coated to uncoated bars (the C/U ratio) decreases with increasing coating thickness. Their tests also showed that, in general, the C/U ratio decreases as bar size increases, and epoxy coating is less detrimental to the bond strength of bars with higher relative rib areas. The average bond strength ratio for epoxy-coated bars to uncoated bars, C/U, was observed to be 0.82 for 15 splice specimens. Cleary and Ramirez (1993) obtained similar results for bars in slabs.

In a small study (12 splice specimens), Hamad and Jirsa (1993) observed that an increase in confinement provided by transverse reinforcement reduced the negative impact of epoxy coating on bond strength. Subsequent studies representing more than 140 splice specimens (Hester et al. 1993; Darwin et al. 1996b; Tan et al. 1996; Zuo and Darwin 1998), however, demonstrated no measurable effect of transverse reinforcement on the C/U ratio.

Idun and Darwin (1999) found that epoxy coating is less detrimental to bond strength for high relative rib area bars, matching the results of Choi et al. (1991). Idun and Darwin also measured the coefficient of friction of both uncoated and coated reinforcing steel, obtaining values of 0.56 and 0.49, respectively. These values are similar to values of 0.53 and 0.49 for uncoated and coated steel plates, respectively (Cairns and Abdullah 1994). Using the results of the coefficient of friction tests and a theoretical relation between C/U ratio and rib face angle developed by Hodge-Ghaffari, Darwin, and McCabe (1991), Idun and Darwin observed that epoxy coating should cause the least reduction (theoretically no reduction) in bond strength for rib face angles greater than 43 degrees, a finding supported by their experimental results. Rib face angles steeper than 40 degrees, however, are hard to produce in practice.

Tan et al. (1996) and Zuo and Darwin (1998) found, for concrete with $f'_c \leq 10,000$ psi (69 MPa), that an increase in the relative rib area improves the splice strength of epoxy-coated bars relative to uncoated bars, whether or not the splices are confined by transverse reinforcement. The presence of transverse reinforcement does not affect the relative splice strength. The relative splice strengths of coated high R_r bars in concrete with $f'_c > 10,000$ psi (69 MPa) were increased less than for the same bars in lower strength concrete. For normalweight concrete, they recommended the use of a development length modification factor of 1.2 for epoxy-coated high relative rib area bars ($R_r \geq 0.10$) in concrete with $f'_c \leq 10,000$ psi (69 MPa) and 1.5 for conventional bars for all concrete strengths and for high R_r bars in concrete with $f'_c > 10,000$ psi (69 MPa). These factors apply for all values of cover and bar spacings.

2.3—Concrete properties

A number of concrete properties affect bond strength. While compressive strength and the use of lightweight

concrete are normally considered in design, other properties, such as tensile strength and fracture energy, aggregate type and quantity, the use of admixtures, concrete slump, and fiber reinforcement, also play a role. Each of these will be discussed in this section.

2.3.1 Compressive strength—Traditionally, in most descriptive (Tepfers 1973; Orangun, Jirsa, and Breen 1977; Darwin et al. 1992; Esfahani and Rangan 1998a,b) and design (ACI 318; AASHTO; CEB-FIP) expressions, the effect of concrete properties on bond strength is represented using the square root of the compressive strength $\sqrt{f'_c}$. This representation has proven to be adequate as long as concrete strengths remain below about 8000 psi (55 MPa). For higher-strength concrete, however, the average bond strength at failure, normalized with respect to $\sqrt{f'_c}$, decreases with an increase in compressive strength (Azizinamini et al. 1993; Azizinamini, Chisala, and Ghosh 1995; and Zuo and Darwin 1998, 2000; Hamad and Itani 1998). Azizinamini et al. (1993) and Azizinamini, Chisala, and Ghosh (1999) observed that the rate of decrease becomes more pronounced as splice length increases. They noted that the bearing capacity of concrete (related to f'_c) increases more rapidly than tensile strength (related to $\sqrt{f'_c}$) as compressive strength increases. For high-strength concrete, the higher bearing capacity prevents crushing of the concrete in front of the bar ribs (as occurs for normal-strength concrete), which reduces local slip. They concluded that because of the reduced slip, fewer ribs transfer load between the steel and the concrete, which increases the local tensile stresses and initiates a splitting failure in the concrete before achieving a uniform distribution of the bond force. Esfahani and Rangan (1996) observed that, when no confining transverse reinforcement is used, as concrete strength increases, the degree of crushing decreases, with no concrete crushing observed for $f'_c \geq 11,000$ psi (75 MPa). In contrast to the other studies, they found that the average bond stress at failure, normalized with respect to $\sqrt{f'_c}$, is higher for higher-strength concrete than for normal-strength concrete.

The use of $\sqrt{f'_c}$ has not been universal. Zsutty (1985) found that $f_c'^{1/3}$ provided an improved match with data, compared to $\sqrt{f'_c}$. Darwin et al. (1996a) combined their own test results with a large international database and observed that a best fit with existing data was obtained using $f_c'^{1/4}$ to represent the effect of concrete compressive strength on development and splice strength. That work was continued by Zuo and Darwin (1998, 2000), who added significantly to the number of tests with high-strength concrete and incorporated additional tests into the database. Zuo and Darwin also observed that $f_c'^{1/4}$ provides the best representation for the effect of compressive strength on the concrete contribution to bond strength T_c . The ability of $f_c'^{1/4}$ to represent the effect of concrete strength on the concrete contribution T_c is demonstrated in Fig. 2.10, which is based on comparisons with 171 test specimens with bottom-cast bars not confined by transverse reinforcement. Two best-fit lines are shown, comparing test-prediction ratios versus f'_c based on two optimized descriptive expressions for bond strength, one using $f_c'^{1/2}$ and the other using $f_c'^{1/4}$. The best-fit line based on $f_c'^{1/2}$ has a negative slope,

decreasing as f'_c increases, while the best-fit line based on $f'_c{}^{1/4}$ has nearly a horizontal slope, indicating that the 1/4 power provides an unbiased representation of the effect of concrete strength on bond strength. As will be demonstrated in Section 3.6, the advantage of the 1/4 power over the 1/2 power does not depend on the specific expressions used for this comparison.

For bars confined by transverse reinforcement, Zuo and Darwin (1998, 2000) found that $f'_c{}^{1/4}$ significantly underestimates the effect of concrete strength on the additional bond strength provided by transverse reinforcement T_s . They observed that $f'_c{}^{3/4}$ provides a good representation of the influence of compressive strength on bond strength. Figure 2.11 shows best-fit lines of test-prediction ratios based on $f'_c{}^p$, with $p = 1/4, 1/2, 3/4$, and 1, versus f'_c . Of the four values, $f'_c{}^{3/4}$ provides a nearly horizontal best-fit line. Using f'_c ($p = 1$) overestimates the effect of concrete strength on T_s , while using $f'_c{}^{1/2}$ underpredicts the effect of concrete strength on T_s . The small positive slope for the $f'_c{}^{3/4}$ line indicates that a power slightly greater than 3/4 would provide a slightly better match with the data.

The observation that $f'_c{}^{1/2}$ does not accurately represent the effect of concrete strength on bond means that many earlier interpretations of the effects of parameters other than compressive strength on bond strength need to be re-examined. This reexamination is necessary because test results have often been normalized with respect to $f'_c{}^{1/2}$ to compare results for different concrete strengths. For example, changes in concrete properties, such as caused by the addition of a high-range water-reducing admixture or the use of silica fume as a cement replacement, often result in changes in compressive strength. When bond strengths are normalized with respect to $f'_c{}^{1/2}$, the effect of concrete strength is exaggerated, resulting in an overestimation of bond strength for higher strength concretes. A reexamination of earlier test results often indicates much less of an effect and, in some cases, no effect on bond strength due to changes in mixture proportions.

2.3.2 Aggregate type and quantity—For bars not confined by transverse reinforcement, Zuo and Darwin (1998, 2000) observed that a higher-strength coarse aggregate (basalt) increased T_c by up to 13% compared with a weaker coarse aggregate (limestone). This observation was explained based on studies using the same materials (Kozul and Darwin 1997; Barham and Darwin 1999) that showed that concrete containing the basalt had only slightly higher flexural strengths, but significantly higher fracture energies (more than two times higher) than concrete of similar compressive strength containing limestone for compressive strengths between 2900 and 14,000 psi (20 and 96 MPa). The higher fracture energy provided by the basalt resulted in increased resistance to crack propagation, which delays splitting failure and increases bond strength. Zuo and Darwin observed no effect of coarse aggregate quantity on T_c .

For bars confined by transverse reinforcement, increases in both the strength and the quantity of coarse aggregate have been observed to increase the contribution of transverse reinforcement to bond strength (Darwin et al. 1996b; Zuo and Darwin 1998), with differences in T_s as high as 45%.

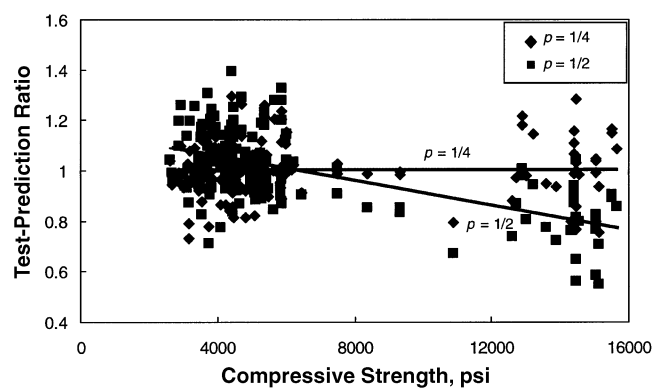


Fig. 2.10—Variation of test-prediction ratio versus compressive strength for developed/spliced bars not confined by transverse reinforcement. The contribution of concrete to bond strength is characterized as $f'_c{}^p$, with $p = 1/4$ and $1/2$. (Note: 1 psi = 0.00689 MPa)

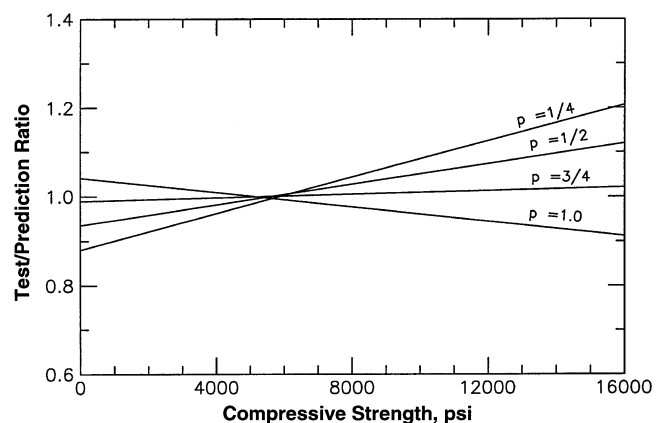


Fig. 2.11—Best-fit lines for test-prediction ratios versus compressive strength for developed/spliced bars confined by transverse reinforcement. $f'_c{}^p$ is used to represent the influence of compressive strength on the additional bond strength provided by transverse reinforcement T_s . (Note: 1 psi = 0.00689 MPa)

The effects of aggregate strength and quantity on T_s explain some of the wide scatter observed for test results obtained in different studies, where the scatter in values of T_s far exceeds the scatter observed for T_c .

2.3.3 Tensile strength and fracture energy—The observed effects of aggregate strength and quantity and of concrete compressive strength on bond strength strongly indicate that the tensile properties of concrete play a significant role in determining bond strength. The concrete contribution T_c increases approximately with $f'_c{}^{1/4}$. This contrasts with the relationship between compressive strength and tensile strength, where it is generally agreed that tensile strength increases approximately with $f'_c{}^{1/2}$. [In some studies dealing with high-strength concrete, a power higher than 1/2 has been observed to relate f'_c to tensile strength (Ahmad and Shah 1985; Kozul and Darwin 1997)].

If tensile strength alone were the key governing factor in bond strength, $f'_c{}^{1/2}$ should provide a good representation of the relationship between compressive strength and bond strength, and aggregate strength should have little effect on

T_c . The actual relationships appear to be directly related to the fracture energy of concrete. As observed earlier, higher-strength aggregates produce concrete with both higher fracture energy and higher bond strengths. For both high and low-strength aggregates, however, fracture energy increases very little, and, in fact, may decrease as compressive strength increases (Niwa and Tangtermsirikul 1997; Kozul and Darwin 1997; Barham and Darwin 1999; Darwin et al. 2001). Overall, as concrete compressive strength increases, bond strength increases at a progressively slower rate, while the failure mode becomes more brittle. Higher fracture energy, such as may be provided by high-strength fibers, should increase the bond strength of reinforcement (see Section 2.3.7).

2.3.4 Lightweight concrete—Due to the lower strength of the aggregate, lightweight concrete should be expected to have lower tensile strength, fracture energy, and local bearing capacity than normalweight concrete with the same compressive strength. As a result, the bond strength of bars cast in lightweight concrete, with or without transverse reinforcement, is lower than that of bars cast in normalweight concrete.

Previous reports by Committee 408 (1966, 1970) have emphasized the paucity of experimental data on the bond strength of reinforced concrete elements made with lightweight aggregate concrete. ACI 318 includes a factor for development length of 1.3 to reflect the lower tensile strength of lightweight-aggregate concrete, when compared with normalweight concrete with the same compressive strength, and allows that factor to be taken as $6.7 \sqrt{f'_c} / f_{ct} \geq 1.0$ if the average splitting strength f_{ct} of the lightweight-aggregate concrete is specified. Although design provisions, in general, require longer development lengths for lightweight-aggregate concrete (CEB-FIP 1999), test results from previous research are contradictory, in part, because of the different characteristics associated with different aggregates and mixture designs.

The majority of published experimental results found in the literature are from different configurations of pullout tests. Early research by Lyse (1934), Petersen (1948), and Shideler (1957) concluded that the bond strength of reinforcing steel in lightweight-aggregate concrete was comparable to that of normalweight concrete. Lyse conducted pullout tests of 3/4 in. (19 mm) bars embedded in 6 x 12 in. (150 x 300 mm) cylinders. The mixture designs used by Lyse included natural sand for fine aggregate and gravel or slag for coarse aggregate. Among his conclusions, Lyse stated that “the compressive, bond, flexural, and diagonal tension strengths of the concrete were very nearly the same for slag and for gravel aggregates.” Petersen tested beams made with expanded shale and expanded slag and concluded that the bond strength of reinforcement in lightweight-aggregate concrete was comparable to that of reinforcement in normalweight concrete. The tests by Petersen used No. 8 (25 mm) bars with embedment lengths of 10, 20, and 30 in. (250, 510, and 760 mm). Shideler (1957) conducted pullout tests on 9 in. (230 mm) cube specimens with six different types of aggregates. No. 6 (19 mm) bars were embedded in specimens with compressive strengths of 3000 and 4500 psi (21 and 31 MPa), and No. 9 (29 mm) bars were used in 9000 psi

(62 MPa) specimens. Although the bond strength of normalweight concrete specimens was slightly higher than that of lightweight concrete specimens, Shideler stated that the difference was not significant.

Similar behavior has been observed in more recent studies. Based on a series of pullout tests, Martin (1982) concluded that there was no significant difference between the bond strength in normalweight and lightweight-aggregate concrete. Berge (1981) obtained similar results from pullout tests; although in a limited testing program involving beams, he observed lower bond strengths in specimens made with lightweight-aggregate concrete. The observed difference in bond strength was approximately 10%.

Clarke and Birjandi (1993) used a specimen developed by the British Cement Association (Chana 1990) and tested four lightweight aggregates with various densities available in the United Kingdom: Lytag (sintered pulverized fuel ash), Leca (expanded clay), Pellite (pelletized expanded blast furnace slag), and Fibo (expanded clay). In addition to the type of aggregate, the study investigated the effect of casting position. The fine aggregate in all mixtures was natural sand. Test results indicated that, with the exception of the lightest aggregate (Fibo), all specimens had higher bond strengths than those of specimens made with normalweight aggregate. This behavior was partially attributed by the authors to the fact that natural sand, as opposed to lightweight aggregate, was used as fine aggregate.

In contrast to the studies just described, there are several studies that indicate significant differences between bond strengths in lightweight- and normalweight-aggregate concrete. In pullout tests, Baldwin (1965) obtained bond strengths for lightweight concrete that were only 65% of those obtained for normalweight concrete. These results contradicted the prevailing assumption at the time that bond strength in lightweight-aggregate concrete was similar to that of normalweight concrete (ACI Committee 408 1966).

Robins and Standish (1982) conducted a series of pullout tests to investigate the effect of lateral stresses on the bond strength of plain and deformed bars in specimens made with lightweight-aggregate (Lytag) concrete. As the lateral pressure applied to the specimens increased, the mode of failure changed from splitting to pullout. Bond strength increased with confining pressure for both normalweight and lightweight concrete. For specimens that failed by splitting, bond strength was 10 to 15% higher for normalweight concrete than for lightweight concrete. When the lateral pressure was large enough to prevent a splitting failure, however, the difference in bond strength was much higher, on the order of 45%.

Mor (1992) tested No. 6 (19 mm) bars embedded in 3 x 3 x 20 in. (76 x 76 x 508 mm) pullout specimens to investigate the effect of condensed silica fume on the bond strength of normalweight and lightweight-aggregate concrete. His specimens had compressive strengths of about 10,000 psi (70 MPa). In specimens without silica fume, the maximum bond stress for specimens made with lightweight concrete was 88% of that of specimens made with normalweight concrete. For concrete with 13 to 15% condensed silica fume, the ratio was 82%. The specimens made with lightweight concrete devel-

oped splitting failures at 75 to 80% of the slip of specimens made with normalweight concrete. The use of silica fume had little effect on bond strength, with an increase of 2% for normalweight concrete and a decrease of 5% for lightweight concrete.

Overall, the data indicate that the use of lightweight concrete can result in bond strengths that range from nearly equal to 65% of the values obtained with normalweight concrete.

2.3.5 Concrete slump and workability admixtures—The workability of concrete, generally measured by slump, affects the bond strength between concrete and reinforcing steel (Darwin 1987). After concrete is cast, it continues to settle and bleed. Settlement leaves a void below rigidly held bars. Bleed water collects below bars, whether rigidly held in place or not. The higher the concrete slump, the greater the tendency to settle and bleed. Water reducers and high-range water-reducing admixtures extend the time during which settlement and bleeding occur.

Properly consolidated, low-slump concrete usually provides the best bond with reinforcing steel. For normal-strength concrete, high slump, used primarily where it is desirable to use little or no consolidation effort, results in decreased bond. The bond strength of top-cast bars (bars near the upper surface of a concrete placement) appears to be especially sensitive to slump. Top-cast bars may or may not be top reinforcement, defined as “horizontal reinforcement so placed that more than 12 in. (300 mm) of fresh concrete is cast in the member below the reinforcement” (ACI 318).

Menzel (1952) studied the effect of slump on bond strength for top-cast bars. He observed a marked reduction in bond strength as the height of top-cast bars was increased from 2-1/8 to 33-1/8 in. (54 to 841 mm) when using 5 to 6 in. (127 to 152 mm) slump, hand-rodde concrete. The rate of decrease in bond strength with the increasing height of the top bars was greatly reduced by decreasing the concrete slump to a range of 2 to 3 in. (51 to 76 mm).

Zekany et al. (1981) studied the effect of concrete slump on top-cast and bottom-cast splices. They found that the bond strength of both top-cast and bottom-cast bars decreased with increasing slump. The effect was most pronounced for the top-cast bars. Luke et al. (1981) studied the influence of casting position on development and splice strength using 72 in. (1.83 m) deep wall specimens (Fig. 2.6). As shown in Fig. 2.6, the bond of top-cast reinforcement was reduced significantly when high (8-1/2 in. [215 mm]) slump concrete was used, as compared to when low (3 in. [75 mm]) slump concrete was used. The bond strength of these bars decreased 40 to 50% due to the increase in slump alone.

Donahey and Darwin (1983, 1985) studied the bond strength of top-cast bars in bridge decks. The bars had different amounts and types of cover. These included two monolithic covers, 3/4 and 3 in. (19 and 75 mm), and a laminar cover consisting of a 3/4 in. (19 mm) monolithic concrete topped with a 2-1/4 in. (57 mm) high-density concrete overlay. Eight inches (203 mm) of concrete was used below the reinforcement. Increasing slump resulted in decreased bond strength.

High-slump concrete can be obtained in a number of ways. It can be obtained by the addition of water, in which case the strength of the concrete is reduced. It can be obtained by the addition of water and cement, in which case the strength of the concrete remains approximately constant. Or, it can be obtained by the addition of a high-range water-reducer or superplasticizer, in which case the strength is usually increased.

Brettmann, Darwin, and Donahey (1984, 1986) used beam-end specimens, with three depths and concretes varying in slump from 1-3/4 to 9 in. (44 to 229 mm). The key variables were degree of consolidation, concrete slump with and without high-range water-reducing admixture, concrete temperature, and bar position. Based on their work, Brettmann, Darwin, and Donahey (1986) concluded that, if cast at a relatively high temperature (resulting in a short setting time), properly vibrated (ACI 309R) high-slump superplasticized concrete and its low-slump nonsuperplasticized base concrete (the concrete before the superplasticizer is added) provide approximately the same bond strength. The equal bond strength is due largely to the increased concrete strength obtained with the high-range water-reducing admixture. Brettmann, Darwin, and Donahey, however, observed that for concrete with the same strength, high-slump concrete made with a high-range water-reducer has lower bond strength than low-slump concrete; the observed differences varied widely, but averaged about 10%. Brettmann, Darwin, and Donahey also observed that if high-slump, superplasticized concrete is cast at a low temperature (resulting in a longer setting time), or if high-slump, high cement content, nonsuperplasticized concrete is used, bond strength decreases regardless of concrete strength.

Musser et al. (1985) and Zilveti et al. (1985) also studied the effect of high-slump, superplasticized concrete on bond strength. Specimens were consolidated using an internal vibrator. Musser et al. considered the anchorage of deformed bars in wall specimens. Bond strength was measured using a straight pull-out procedure. Zilveti et al. used beam-end specimens. Musser et al. found little effect of superplasticizers on bond strength. Zilveti et al. concluded that the addition of a high-range water-reducing admixture simply to improve workability has no effect on bond strength. When corrected for increased concrete strength, however, the bond strength obtained with high-slump, superplasticized concrete was lower than the bond strength obtained with low-slump concrete. Also, like Brettmann, Darwin, and Donahey, Zilveti et al. observed that high slump is more detrimental to bond strength when the temperature of the concrete is initially low. The lower temperature provides a longer period during which the concrete remains plastic and, thus, a longer period during which settlement and bleeding occur.

Hamad and Itani (1998) studied the effects of silica fume, high-range water-reducing admixture dosage, and bar position on splice strength in high-strength concrete. Due to the range of mixture proportion variables in the study, the splice strength of individual specimens varied significantly. When normalized with respect to the $f'_c{}^{1/4}$, doubling the high-range water-reducing admixture dosage from 0.5 to 1 gal./yd³ (2 to

4 L/m³) resulted in a 32% decrease in splice strength for one pair of bottom-cast bars as the slump increased from 1-1/2 to 8-1/4 in. (40 to 210 mm). For two other pairs of bottom-cast bars, splice strength dropped by 10% as concrete slump increased from 5-1/2 to 7 in. (140 to 180 mm) and by 3% as slump increased from 4-1/2 to 8-1/2 in. (115 to 215 mm) for the same increase in high-range water-reducing admixture dosage. For three pairs of top-cast bars, splice strength decreased by 3% or less for increases in slump (6-1/4 to 7 in. [160 to 180 mm], 1-1/2 to 8-1/2 in. [40 to 210 mm], and 5 to 8-1/2 in. [125 to 215 mm]) with an increase in high-range water-reducing admixture dosage.

Overall, an increase in slump and the use of workability-enhancing admixtures tends to have a negative effect on bond strength. The longer that concrete has time to settle and bleed, the lower the bond strength. This effect is especially important for top bars.

2.3.6 Mineral admixtures—Most studies of the effect of mineral admixtures on bond strength have been limited to the effects of silica fume, the principal mineral admixture used in high-strength concrete. Because of significantly increased compressive strength for many of the concretes containing silica fume, comparisons have usually been based on bond strengths that are normalized with respect to $f'_c{}^{1/2}$. Because this value overestimates the effect of compressive strength, the conclusion has often been made that silica fume has a negative effect on bond strength. If the test results are normalized with respect to $f'_c{}^{1/4}$, however, the apparent negative impact of silica fume on bond is significantly decreased. The comparisons that follow are based on results normalized with respect to $f'_c{}^{1/4}$.

Gjorv, Monteiro, and Mehta (1990) observed that silica fume increases the bond strength between concrete and reinforcing steel, as measured using the ASTM C 234* pullout test (ASTM 1991). For concrete strengths between 3000 and 12,000 psi (21 and 83 MPa) and silica fume replacements of 0, 8, and 16% by weight (mass) of cement, they concluded that (as expected) bond strength increases with compressive strength and that top-cast bars develop lower bond strength than bottom-cast bars due to the accumulation of bleed water and air below the bars. Increasing the silica fume content resulted in an increase in pullout strength. They felt that the major effects of silica fume involve reduction in bleed water and strengthening of the cement paste in the transition zone adjacent to the reinforcing bars.

Hwang, Lee, and Lee (1994) evaluated the effect of silica fume using eight splice specimens. The specimens were tested in pairs in which one specimen included a 10% replacement of portland cement by an equal weight (mass) of silica fume. In this case, bond strength decreased by an average of 7-1/2% with the addition of silica fume. Test results obtained by DeVries, Moehle, and Hester (1991) and Olsen (1990a,b) show little or no negative effects of silica fume on bond strength. In fact, Olsen's tests show a 10%

increase in splice strength for concrete containing silica fume and a 17% increase for concrete containing fly ash.

Hamad and Itani (1998) carried out 16 splice tests that included both top- and bottom-cast bars. The test strengths showed reductions in bond strength averaging 5% for silica fume replacements of portland cement between 5 and 20%.

2.3.7 Fiber reinforcement—For centuries, fibers have been added to concrete and mortar to improve the inherently low tensile strength of these materials. Fibers such as straw or horsehair were used originally. Asbestos was used starting at the beginning of the twentieth century, and today, ACI 544.1R lists many different types of fiber that can be used to enhance the toughness of concrete and mortar.

ACI Committee 544 divides modern fiber-reinforced concrete (FRC) into four categories based on the type of fiber used: steel fiber-reinforced concrete (SFRC), glass fiber-reinforced concrete (GFRF), synthetic fiber-reinforced concrete (SNFRC), and natural fiber-reinforced concrete (NFRC).

Within each category, many types and lengths of fiber are available to achieve different material properties. For example: steel fibers may or may not have hooked ends; many chemical compositions of glass fibers exist; synthetic fibers may be manufactured with carbon, acrylic, polyester or other materials; and natural fibers can be obtained from many sources such as coconut or jute. In addition, the use of a new category of FRC using fibers recycled from industrial wastes from the manufacture of carpet, plastics, and other processes is gaining acceptance.

One reason to add fibers is to increase the tensile strength of concrete. The increase, however, is small. For example, Wafa and Ashour (1992) report a 10 to 20% increase in modulus of rupture for FRC over plain concrete for concrete with nominal compressive strength of 14,000 psi (100 MPa). Even with these increases, the tensile strength remains significantly less than the compressive strength.

A more important goal of adding fibers is to increase the post-cracking resistance of the concrete, which allows FRC to be used in applications where crack control is important. Fibers bridge across cracks and allow some tensile stress to be transferred. At failure, the fibers pull out of the concrete, increasing the energy required to open and propagate the cracks.

The provisions in ACI 318 for the development of deformed bars are based on bond strengths that are governed by a splitting failure of the concrete around the bar. Factors that affect the splitting resistance of the concrete, such as concrete tensile strength, transverse reinforcement, and amount of cover, are considered in design. Theoretically, the use of FRC should improve resistance to splitting cracks and reduce required development lengths.

A study of the test results described in the balance of this section indicates that fibers, especially steel fibers, behave as both transverse and longitudinal reinforcement, the former having the major effect on bond strength. The fiber volume fractions used in these tests are generally high compared with values used for conventional transverse reinforcing bars.

Davies (1981) explored the bond strength of steel reinforcing bars in polypropylene fiber-reinforced concrete. In his study, pullout specimens with No. 4 or No. 6 (No. 13 or

*This test method has been withdrawn by ASTM International.

No. 19) Grade 60 (420 MPa) reinforcement and nominal concrete compressive strengths between 4000 and 6000 psi (28 and 41 MPa) were used. In addition, the percent of fiber by volume and length of individual fibers were variables. In general, the addition of longer fibers (3-1/2 in. [90 mm]) resulted in higher average bond strengths. The increase in bond strength, however, was not greater than the increase in $\sqrt{f'_c}$ resulting from the increase in fiber volume. Increases in the volume of shorter fibers (2-1/4 in. [57 mm]) reduced average bond strengths in some cases.

Ezeldin and Balaguru (1989) studied the effects of steel fibers on the bond strength of deformed bars in normal and high-strength concrete. Fiber content ranged up to 0.75% by volume. Using pullout specimens in which the concrete was placed in tension under load, they observed that using a fiber content of 0.25% resulted in a decrease in bond strength compared with concrete without fibers. The addition of fiber contents of 0.5 and 0.75%, however, resulted in increases in bond strength of up to 18%. Improvements in bond strength were greater for No. 5 and No. 6 bars than for No. 3 bars. Increases in fiber content and fiber length resulted in improved ductility following the peak load.

Soroushian, Mirza, and Alhozaimy (1994) tested the bond strength of a $4d_b$ embedded length of bar centered in a $15d_b$ long pullout specimen. They observed that local bond strength increased by about one-third for a 0.5% volume addition of steel fibers. Further increases in fiber volume, up to 1.5%, provided only an additional 5% increase in bond strength. The fibers reduced slip at the peak bond stress, while fiber aspect ratio and type had little effect on bond.

Harajli, Hout, and Jalkh (1995) measured the local bond stress-slip behavior for bars embedded in pullout specimens. They evaluated the effect of bar diameter (No. 6 and No. 8 [No. 19 and No. 25] bars), mode of failure (pullout, splitting), and type, volume fraction, and aspect ratio of the fibers. They observed that fiber contents up to 2% by volume resulted in an increase in bond strengths of about 20%. As in other studies, fibers significantly increased the bond force after the peak load. Polypropylene fibers provided about 1/3 of the increase in bond resistance provided by hooked steel fibers after the peak load had been reached. As would be expected, fibers had little effect on the strength or behavior of specimens that failed by pullout rather than splitting.

In a study of the bond strength of deformed bars in slurry infiltrated fiber-reinforced concrete (SIFCON), Hamza and Naaman (1996) obtained a 150% increase in bond strength for a 5% volume content of steel fibers. Bond forces equal to 50% of the peak bond force were maintained at slips equal to 10 times the maximum slip obtained for plain concrete specimens. The initial bond stiffness obtained for SIFCON was 2.5 times the value measured for plain concrete.

Harajli and Salloukh (1997) evaluated the effects of fibers on the splice strength of reinforcing bars using 15 beams, each with a lap splice at midspan. The beams were loaded in positive bending with a constant moment in the splice region. The results of the tests demonstrated that steel fibers (up to 2% by volume) increased member strength by up to 55%. The increase included the effects of the fibers both on

bond and on the contribution of the concrete to the local flexural capacity of the section. The presence of fibers increased the number of cracks formed around the splices, delayed splitting cracks, and improved the ductility of members undergoing a bond failure. Polypropylene fibers improved performance in the post splitting range, but had less effect on bond strength. At 0.6% by volume, polypropylene fibers provided between 0 and a 25% increase in the failure load.

Hota and Naaman (1997) compared the bond strengths of deformed bars in plain concrete, FRC, and SIFCON using pullout specimens. The bonded length was 4 in. (100 mm). Concrete containing a 2% volume fraction of steel fibers produced a peak bond strength about twice that produced by plain concrete, while SIFCON, containing a 9% steel fiber volume fraction, produced a bond strength equal to three times that obtained with the plain concrete specimens.

Because most of the bond tests involving FRC have been pullout tests, rather than splice or development tests, and because fibers affect the failure load for splice or development specimens by altering the contribution of the concrete to the flexural strength of a section, as well as to bond, significantly more work is needed before data is available to properly judge the effect of fibers on bond strength.

2.3.8 Consolidation—Adequate consolidation is a key factor in quality concrete construction. The role of consolidation is usually described in terms of removing voids that may have been entrapped during handling and placement. In terms of bond, adequate consolidation, usually obtained with high frequency internal vibration, plays the additional role of reducing the effects of settlement and bleeding, which result in the accumulation of bleed water and low density, weak concrete just below horizontal reinforcement. By disturbing the concrete, vibration helps restore local uniformity. Both the removal of entrapped air and the restoration of local uniformity play an important role in improving bond strength. The balance of this section discusses the effects of initial vibration, delayed vibration, construction-induced vibration, and revibration.

2.3.8.1 Vibration—Davis, Brown, and Kelly (1938) studied the effects of delayed vibration and sustained jiggling* on bond strength. Using 4 in. (100 mm) slump concrete, vibration was applied from 0 to 9 h after concrete placement in pullout specimens consisting of deformed bars held vertically in cylindrical specimens. Delayed vibration, up to 9 h, improved bond strength compared with initial vibration. Increases in bond strength of up to 62% were recorded. This improved bond strength has been used as evidence of the positive effect of revibration (Tuthill and Davis 1938; Tuthill 1977). Because the specimens were not initially vibrated, however, the improved bond strength must be attributed to delayed vibration not revibration. Using similar specimens for sustained jiggling tests, Davis, Brown, and Kelly obtained increases in bond strength as the period of jiggling increased from 1/2 to 2 h, after which there was no significant change up to a maximum of 6 h.

*Jiggling involves raising opposite sides of a form and allowing the form to drop so as to sharply strike the floor.

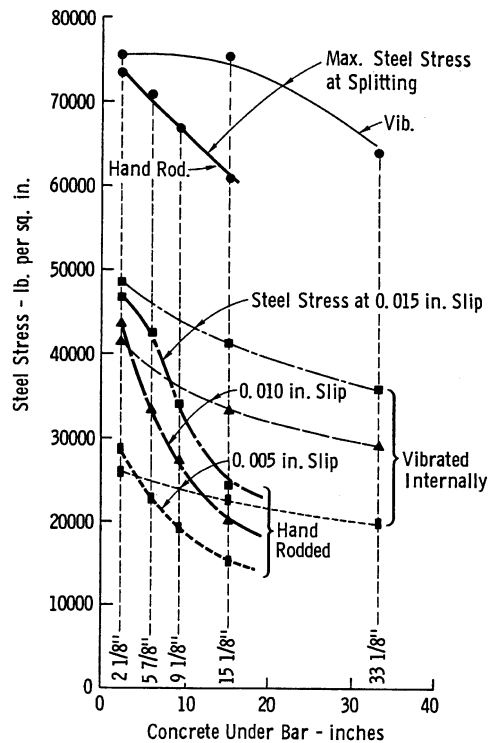


Fig. 2.12—Steel stress in beam-end specimens for vibrated and hand-rodde concrete (Menzel 1952). (Note: 1 in. = 25.4 mm; 1 psi = 0.00689 MPa)

Robin, Olsen, and Kinnane (1942) compared bond strengths of horizontally cast bars consolidated with external vibration and hand rodding. External vibration of 3 to 4 in. (75 to 100 mm) slump concrete produced lower strengths than hand rodding for bars 1-1/2 or 3 in. (38 or 75 mm) from the bottom of the forms, but higher bond strengths than hand rodding for bars 6 or 7-1/2 in. (150 or 190 mm) from the bottom of the forms.

Using 2 in. (50 mm) slump concrete and both top-cast and bottom-cast deformed bars, Menzel (1952) found that internal vibration significantly increased bond strength compared with hand rodding (Fig. 2.12). The relative improvement in bond strength with vibration increased as the distance of the bar above the base of the specimen increased.

Donahey and Darwin (1983, 1985) considered the effects of the density of vibration on bond strength. They compared procedures using high-density vibration (in which the vibrator radii of influence overlapped) and low-density vibration (in which the radii of influence did not overlap). They found that high-density internal vibration improves bond strength. Brettmann, Darwin, and Donahey (1984, 1986) observed that vibration is especially important when high-slump concrete is used, whether the high slump is produced with the addition of water and cement or with the addition of a high-range water-reducing admixture. Brettmann, Darwin, and Donahey used internal vibration and followed standard practices for vibration (ACI 309R). For 9 in. (230 mm) slump concrete obtained without a high-range water-reducing admixture (Group 2 in Fig. 2.13), bond strengths averaged 14% lower for nonvibrated specimens than for vibrated specimens. For bottom-cast bars, the average

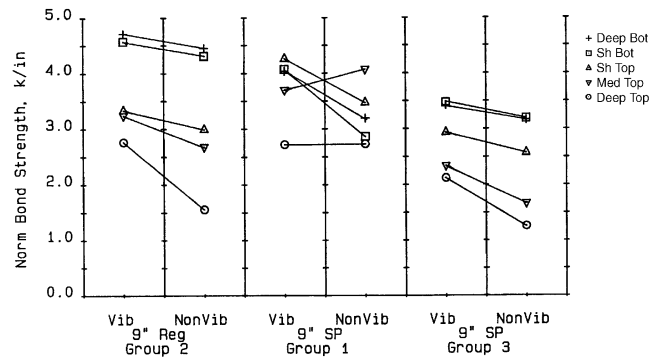


Fig. 2.13—Comparison of average normalized bond strengths for vibrated and nonvibrated high-slump concretes in beam-end specimens. REG = concrete without a high-range water-reducing admixture; and SP = superplasticized concrete. The bond strengths normalized by multiplying by $(4000/f'_c)^{1/2}$ (Brettmann, Darwin, and Donahey 1986). (Note: 1 in. = 25.4 mm; 1 kip/in. = 175 kN/m)

decrease was only 6% for nonvibrated specimens, largely due to the consolidation provided by the concrete above the bars. For top-cast bars, bond strength decreased 23% when the concrete was not vibrated. For 9 in. (230 mm) slump (Groups 1 and 3 in Fig. 2.13) superplasticized concrete, nonvibrated specimens also exhibited lower bond strength. There were two exceptions involving top-cast bars in high-temperature (84 °F [29 °C]) (Group 1) concrete, which received additional consolidation due to finishing operations. For the high-temperature concrete (Group 1), nonvibrated bottom-cast bars had 25% lower bond strength than vibrated bars. For lower-temperature (54 °F [12 °C]) concrete (Group 3), the lack of vibration caused a decrease in bond strength that ranged from 8% for bottom-cast bars to 41% for top-cast bars in deep specimens.

2.3.8.2 Construction-related vibrations—Both field and laboratory studies have considered the effects of external construction-related vibrations. The concern has been that these vibrations, which occur while the concrete is setting, damage the bond between the reinforcement and the concrete.

Furr and Fouad (1981) studied the effects of maintaining traffic on existing lanes of a bridge while the bridge was being widened. In both field and laboratory investigations, they found that it was possible to have some reduction in bond strength. This reduction, however, was limited to areas close to longitudinal construction joints, where relative movement between the concrete and the steel was greatest.

Hulshizer and Desai (1984) evaluated the effects of "simulated blast loading" on bond strength using pullout specimens subjected to vibrations ranging from 50 to 150 Hz while the concrete set. They found that pullout strength increased slightly due to the vibrations.

Harsh and Darwin (1984, 1986) studied the effects of simulated traffic-induced vibrations on bond strength in bridge deck repairs. They found that, if low-slump concrete is used, bond strength actually increases. For slumps in excess of 4 in. (100 mm), however, traffic-induced vibrations result in a reduction in bond strength, in some cases by over 10%. Overall, traffic-induced vibrations do not appear to be

detrimental to bond strength in bridge deck repairs if low-slump concrete is used.

2.3.8.3 Revibration—When properly executed, internal vibration improves the quality of bond between concrete and steel. Much less is known about the effects of revibration, the process in which a vibrator is reapplied to concrete at some time after initial vibration.

Vollick (1958) found that internal revibration increases concrete compressive strength from 7 to 19%, depending on the concrete mixture. He did not study the effect of revibration on bond strength. Larnach (1952) studied the effects of external revibration on both bond and compressive strength, finding that external revibration reduced the bond strength of horizontally cast plain bars by 6 to 33%, depending on the time after initial consolidation. He obtained reductions in compressive strength of about 15%.

Menzel (1952) studied the effects of internal revibration on the bond strength of deformed bars with 2 to 3 in. (50 to 75 mm) slump concrete. He found that revibration after 1 h had no adverse effect on bottom-cast bars, but reduced the bond strength of top-cast bars by 28 to 60%.

Altowaiji, Darwin, and Donahey (1986) studied the effects of internal revibration on bond strength for concretes with initial slumps between 2-3/4 and 7-1/2 in. (70 and 190 mm). Forty-five and 90 minute intervals were used between initial vibration and revibration. They found that revibration improves the bond strength of top-cast bars and bars placed in high-slump concrete by 5 to 20%. Revibration, however, can reduce the bond strength of bars cast in well-consolidated, low-slump concrete by 10 to 20%. Revibration is almost universally detrimental to the bond strength of bottom-cast bars.

The bars benefiting most from revibration, top-cast bars placed in high-slump concrete, are the bars that are affected most by settlement and bleeding. Revibration helps to reconsolidate the concrete adjacent to the bars, reducing voids caused by settlement and bleeding and, thus, improving bond. From a practical standpoint, structures in which revibration has its greatest advantage (structures placed with high-slump concrete) are the least likely to receive proper consolidation at any stage.

The detrimental effects of revibration to bottom-cast bars are probably due to the fact that settlement and bleeding help to consolidate the concrete around these bars, while revibration only serves to disrupt the concrete. Thus, full-depth revibration appears to be a poor construction practice. When used, revibration should be limited to the upper portions of a placement, no deeper than about 6 in. (150 mm) below the concrete surface. This limitation allows the effects of settlement and bleeding to be counteracted around top-cast reinforcement without damaging the bond of deeper bars. The use of a vibrator to tie together two lifts of concrete is a common application of revibration under these guidelines.

2.4—Summary

Many factors affect the bond of reinforcing bars to concrete. As was discussed in this chapter, bond force increases with increasing concrete cover and bar spacing, development and splice length, and the use of confining

transverse reinforcement. Top-cast bars have a lower bond strength than bottom-cast bars, while for realistic bar spacing, noncontact lap splices provide a higher strength than contact lap splices. For a given length of bar, the bond force mobilized by both concrete and transverse reinforcement increases as the bar diameter increases. The bond strength of bars confined by transverse reinforcement increases with an increase in the relative rib area. The bond strength of developed and spliced bars is little affected if the stress in the bar exceeds the yield strength. Epoxy coatings reduce the bond strength of bars, but for all conditions of confinement, the higher the relative rib area of the bar, the lower the reduction. Bond strength increases with increasing concrete compressive strength for bars not confined by transverse reinforcement approximately with the 1/4 power (rather than the 1/2 power, as often assumed) of the compressive strength. The additional bond strength provided by transverse reinforcement increases approximately with the 3/4 power of the compressive strength. An increase in aggregate strength and quantity results in an increase in bond strength. This increase appears to be tied to the effect of aggregate properties on tensile strength and, even more importantly, the fracture energy of the concrete. Lightweight aggregate concrete develops lower bond strength than normalweight concrete with the same compressive strength. An increase in concrete slump and the use of workability-enhancing admixtures, in general, have a negative impact on bond strength. The longer the period that concrete has to settle and bleed, the lower the bond strength. This effect is especially important for top-cast bars. The use of silica fume has been observed to increase bond strength in some cases and decrease bond strength in others for a given compressive strength. Fiber reinforcement, especially steel fibers, tends to act as transverse reinforcement, providing increased bond strength to reinforcing steel. Improved consolidation of concrete results in improved bond strength.

CHAPTER 3—DESCRIPTIVE EQUATIONS

An accurate theory-based analysis procedure for development and splice strength has yet to be formulated. As a result, expressions for bond strength have been developed based on comparisons with test results. The expressions presented in this chapter capture the key aspects of bond behavior and produce reasonably accurate predictions of bond strength. The chapter concludes with a comparison of the expressions using the test results for bottom-cast bars in ACI Committee 408 Database 10-2001 (refer to [Chapter 5](#)), a comparison that illustrates the relative merits of each and demonstrates the advisability of representing the effect of concrete strength on bond by a factor other than $\sqrt{f'_c}$.

3.1—Orangun, Jirsa, and Breen

Using statistical techniques, Orangun, Jirsa, and Breen (1975, 1977) developed expressions to describe the bond strength of bars without and with confining transverse reinforcement. For bars not confined by transverse reinforcement, a regression analysis based on 62 beams, including four with side-cast bars, one with top-cast bars, and 57 with bottom-

cast bars, produced an expression for the average bond stress at failure.

$$\frac{u_c}{\sqrt{f'_c}} = 1.22 + 3.23 \frac{c_{\min}}{d_b} + 53 \frac{d_b}{l_d} \quad (3-1)$$

where c_{\min} = smaller of minimum concrete cover or 1/2 of the clear spacing between bars; l_d = development or splice length; and d_b = bar diameter. In their analysis, the coefficients in Eq. (3-1) were rounded as follows

$$\frac{u_c}{\sqrt{f'_c}} = 1.2 + 3 \frac{c_{\min}}{d_b} + 50 \frac{d_b}{l_d} \quad (3-2)$$

The bond strength of a bar confined by transverse reinforcement was represented by

$$\frac{u_b}{\sqrt{f'_c}} = \frac{u_c + u_s}{\sqrt{f'_c}} = 1.2 + 3 \frac{c_{\min}}{d_b} + \frac{50d_b}{l_d} + \frac{A_{tr}f_{yt}}{500snd_b} \quad (3-3)$$

where A_{tr} = area of transverse reinforcement normal to the plane of splitting through the anchored bars; f_{yt} = yield strength of transverse reinforcement; s = spacing of transverse reinforcement; and n = number of bars developed or spliced at the same location.

In terms of total bond force, Eq. (3-3) may be written as

$$\frac{T_b}{\sqrt{f'_c}} = \frac{T_c + T_s}{\sqrt{f'_c}} = \frac{A_b f_s}{\sqrt{f'_c}} = \quad (3-4)$$

$$3\pi l_d(c_{\min} + 0.4d_b) + 200A_b + \frac{\pi l_d A_{tr} f_{yt}}{500sn}$$

where A_b = area of developed or spliced bar.

Equations (3-3) and (3-4) are limited to cases in which splitting failure, rather than pullout, governs. This leads to a restriction in applying the expressions that

$$\frac{1}{d_b} \left(c_{\min} + 0.4d_b + \frac{A_{tr} f_{yt}}{1500sn} \right) \leq 2.5 \quad (3-5)$$

As shown in Section 4.1, Eq. (3-3) and (3-4) serve as the basis for the design expression for development length that first appeared in ACI 318-95.

3.2—Darwin et al.

Darwin et al. (1992) reanalyzed the data used by Orangun, Jirsa, and Breen (1975, 1977) to establish Eq. (3-1) and (3-2) for bars not confined by transverse reinforcement. Darwin et al. (1992) incorporated the effect of the relative value of c_{\max} and c_{\min} (refer to Section 2.1) to obtain

$$\frac{T_c}{\sqrt{f'_c}} = \frac{A_b f_s}{\sqrt{f'_c}} = \quad (3-6)$$

$$6.67l_d(c_{\min} + 0.5d_b) \left(0.08 \frac{c_{\max}}{c_{\min}} + 0.92 \right) + 300A_b$$

Darwin et al. (1996a) used a larger database, consisting of 133 splice and development specimens in which the bars were not confined by transverse reinforcement and 166 specimens in which the bars were confined by transverse reinforcement. All specimens contained bottom-cast bars. They observed that $f'_c{}^{1/4}$ provided a better representation of concrete strength on development and splice strength than the more traditional $f'_c{}^{1/2}$. They also incorporated the effect of relative rib area R_r , which they observed to have a significant effect on the bond strength of bars confined by transverse reinforcement. Based on their studies, the best-fit equation for the bond strength of bars not confined by transverse reinforcement was

$$\frac{T_c}{f'_c{}^{1/4}} = \frac{A_b f_s}{f'_c{}^{1/4}} = \quad (3-7)$$

$$[63l_d(c_{\min} + 0.5d_b) + 2130A_b] \left(0.1 \frac{c_{\max}}{c_{\min}} + 0.9 \right)$$

where $\left(0.1 \frac{c_{\max}}{c_{\min}} + 0.9 \right) \leq 1.25$.

The best-fit equation for bars confined by transverse reinforcement was

$$\frac{T_b}{f'_c{}^{1/4}} = \frac{T_c + T_s}{f'_c{}^{1/4}} = \frac{A_b f_s}{f'_c{}^{1/4}} = \quad (3-8)$$

$$[63l_d(c_{\min} + 0.5d_b) + 2130A_b] \left(0.1 \frac{c_{\max}}{c_{\min}} + 0.9 \right)$$

$$+ 2226t_r t_d \frac{NA_{tr}}{n} + 66$$

where c_{\max} and c_{\min} are defined following Eq. (2-1), N = number of transverse bars in the development or splice length, $t_r = 9.6R_r + 0.28$, and $t_d = 0.72d_b + 0.28$.

Like the expressions developed in Section 3.1, Eq. (3-7) and (3-8) are applicable to cases in which a splitting failure, rather than pullout, governs. The following restriction applies to the expressions.

$$\frac{1}{d_b} \left[(c_{\min} + 0.5d_b) \left(0.1 \frac{c_{\max}}{c_{\min}} + 0.90 \right) + \left(\frac{35.3t_r t_d A_{tr}}{sn} \right) \right] \leq 4.0 \quad (3-9)$$

3.3—Zuo and Darwin

Zuo and Darwin (1998, 2000) expanded the work of Darwin et al. (1996a) by increasing the database and adding substantially to the percentage of test specimens containing high-strength concrete ($f'_c > 8000$ psi [55 MPa]). The database included 171 specimens containing bars not confined by transverse reinforcement and 196 specimens containing bars confined by transverse reinforcement. All bars were bottom cast. Their analysis supported the earlier observations that $f'_c{}^{1/4}$ realistically represents the contribution of concrete strength to bond strength for bars not confined by transverse reinforcement. As discussed in Section 2.3.1, however, they observed that $f'_c{}^p$, with p between 3/4 and 1.0, best represents the effect of concrete strength on T_s , the contribution of confining transverse reinforcement to bond strength. They selected $p = 3/4$ for their descriptive equations. For bars not confined by transverse reinforcement, the best-fit equation describing development and splice strength is

$$\frac{T_c}{f'_c{}^{1/4}} = \frac{A_b f_s}{f'_c{}^{1/4}} = \quad (3-10)$$

$$[59.8l_d(c_{\min} + 0.5d_b) + 2350A_b] \left(0.1 \frac{c_{\max}}{c_{\min}} + 0.90 \right)$$

For bars confined by transverse reinforcement, the descriptive equation is

$$\frac{T_b}{f'_c{}^{1/4}} = \frac{T_c + T_s}{f'_c{}^{1/4}} = \frac{A_b f_s}{f'_c{}^{1/4}} = \quad (3-11)$$

$$[59.8l_d(c_{\min} + 0.5d_b) + 2350A_b] \left(0.1 \frac{c_{\max}}{c_{\min}} + 0.90 \right)$$

$$+ \left(31.14t_r t_d \frac{NA_{tr}}{n} + 4 \right) f'_c{}^{1/2}$$

where $t_r = 9.6R_r + 0.28$ and $t_d = 0.78d_b + 0.22$.

To limit applicability of Eq. (3-10) and (3-11) to cases in which a splitting failure governs

$$\frac{1}{d_b} \left[(c_{\min} + 0.5d_b) \left(0.1 \frac{c_{\max}}{c_{\min}} + 0.90 \right) + \left(\frac{0.52t_r t_d A_{tr}}{sn} \right) f'_c{}^{1/2} \right] \leq 4.0 \quad (3-12)$$

3.4—Esfahani and Rangan

Extending the local bond stress theory of Tepfers (1973) to splices, Esfahani and Rangan (1998a,b) developed expressions for the bond strength of bars not confined by transverse reinforcement.

For $f'_c < 7250$ psi (50 MPa),

$$\frac{T_c}{\sqrt{f'_c}} = \frac{A_b f_s}{\sqrt{f'_c}} = \quad (3-13)$$

$$32.45\pi l_d \frac{(c_{\min} + 0.5d_b) \left(1 + \frac{1}{M} \right)}{\left(\frac{c_{\min}}{d_b} + 3.6 \right) (1.85 + 0.024\sqrt{M})} \left(0.12 \frac{c_{\text{med}}}{c_{\min}} + 0.88 \right)$$

For $f'_c \geq 7250$ psi (50 MPa),

$$\frac{T_c}{\sqrt{f'_c}} = \frac{A_b f_s}{\sqrt{f'_c}} = \quad (3-14)$$

$$56.97\pi l_d \frac{(c_{\min} + 0.5d_b) \left(1 + \frac{1}{M} \right)}{\left(\frac{c_{\min}}{d_b} + 5.5 \right) (1.85 + 0.024\sqrt{M})} \left(0.12 \frac{c_{\text{med}}}{c_{\min}} + 0.88 \right)$$

where c_{\min} = minimum (c_{so} , c_b , $c_{si} + d_b/2$), c_{med} = median (c_{so} , c_b , $c_{si} + d_b/2$) [that is, middle value], and $M = \cosh(0.00092l_d \sqrt{r f'_c} / d_b)$. For conventional reinforcement ($R_r \approx 0.07$), $r = 3$. The hyperbolic cosine enters the relationship based on the assumed variation in bond stress along the developed or spliced length of a bar.

3.5—ACI Committee 408

Using ACI 408 Database 10-2001 (Section 5.2), the committee has updated Eq. (3-10) and (3-11) with only minor changes.

$$\frac{T_c}{f'_c{}^{1/4}} = \frac{A_b f_s}{f'_c{}^{1/4}} = \quad (3-15)$$

$$[59.9l_d(c_{\min} + 0.5d_b) + 2400A_b] \left(0.1 \frac{c_{\max}}{c_{\min}} + 0.90 \right)$$

$$\frac{T_b}{f'_c{}^{1/4}} = \frac{T_c + T_s}{f'_c{}^{1/4}} = \frac{A_b f_s}{f'_c{}^{1/4}} = \quad (3-16)$$

$$[59.9l_d(c_{\min} + 0.5d_b) + 2400A_b] \left(0.1 \frac{c_{\max}}{c_{\min}} + 0.90 \right)$$

$$+ \left(30.88t_r t_d \frac{NA_{tr}}{n} + 3 \right) f'_c{}^{1/2}$$

The restriction in Eq. (3-12) applies to Eq. (3-15) and (3-16).

3.6—Comparisons

The six descriptive equations for bars not confined by transverse reinforcement [Eq. (3-4), (3-6), (3-7), (3-10), ((3-13) or (3-14)), and (3-15)] and the four equations for bars confined by transverse reinforcement [Eq. (3-4), (3-8), (3-11),

Table 3.1—Test-prediction ratios for bars not confined by transverse reinforcement

	OJB* (Eq. (3-4))	DMIS† (Eq. (3-6))	DZTI‡ (Eq. (3-7))	Z & D§ (Eq. (3-10))	E & R (Eq. (3-13) Eq. (3-14))	ACI 408R (Eq. (3-15))
Maximum	1.55	1.383	1.342	1.304	2.790	1.288
Minimum	0.505	0.528	0.719	0.729	0.545	0.724
Average	1.030	1.014	1.020	1.010	0.938	1.00
Standard deviation	0.208	0.189	0.118	0.113	0.190	0.111
Coefficient of variation	0.202	0.187	0.116	0.111	0.202	0.111

*Orangun, Jirsa, and Breen (1977).

†Darwin et al. (1992).

‡Darwin et al. (1996b).

§Zuo and Darwin (2000).

||Esfahani and Rangan (1998a,b).

Table 3.2—Test-prediction ratios for bars confined by transverse reinforcement

	OJB* (Eq. (3-4))	DZTI† (Eq. (3-8))	Z & D‡ (Eq. (3-11))	ACI 408R (Eq. (3-16))
Maximum	1.902	1.479	1.309	1.333
Minimum	0.595	0.776	0.739	0.755
Average	1.074	1.052	0.989	1.002
Standard deviation	0.255	0.132	0.119	0.121
Coefficient of variation	0.238	0.125	0.121	0.120

*Orangun, Jirsa, and Breen (1977).

†Darwin et al. (1996b).

‡Zuo and Darwin (2000).

and (3-16)] are compared with the test results from ACI 408 Database 10-2001 in Table 3.1 and 3.2 and Fig. 3.1 and 3.2. The tables compare the test-prediction ratios and include the maximum, minimum, and average values. The tables also include the standard deviations and coefficients of variation of the ratios. The figures compare test-prediction ratios as a function of compressive strength—test-prediction ratio should not be highly sensitive to compressive strength.

Table 3.1 shows that for bars not confined by transverse reinforcement the average test-prediction ratio is within 3% of 1.0, with the exception of the predictions based on Esfahani and Rangan (1998a,b), which produce an average test-prediction ratio of 0.94. The comparisons for Esfahani and Rangan also exhibit the highest extremes between maximum and minimum test-prediction values. The lowest scatter is exhibited by the expressions obtained by Zuo and Darwin (2000) and Committee ACI 408, both of which produce a coefficient of variation of 0.111. The highest coefficients of variation, 0.202 and 0.207, are obtained using the expressions of Orangun, Jirsa, and Breen (1977) and Esfahani and Rangan, respectively. The Esfahani and Rangan expressions were not developed using tests with large values of l_d and appear to be more appropriate for predicting bond strength for shorter development and splice lengths. For example, if M [defined following Eq. (3-14)] is limited to 100 by excluding specimens with combinations of l_d and f'_c that

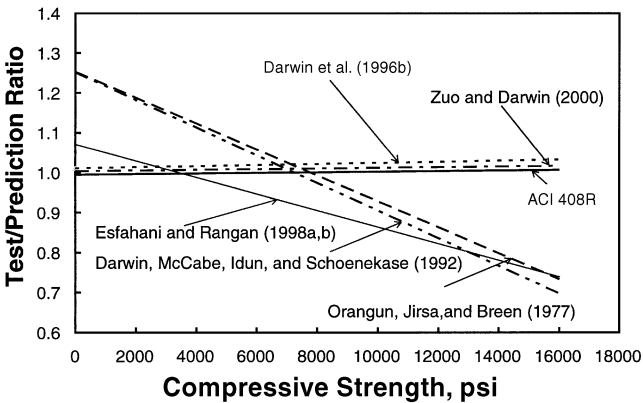


Fig. 3.1—Test-prediction ratios for six descriptive equations for bars not confined with transverse reinforcement. (Note: 1 psi = 0.00689 MPa)

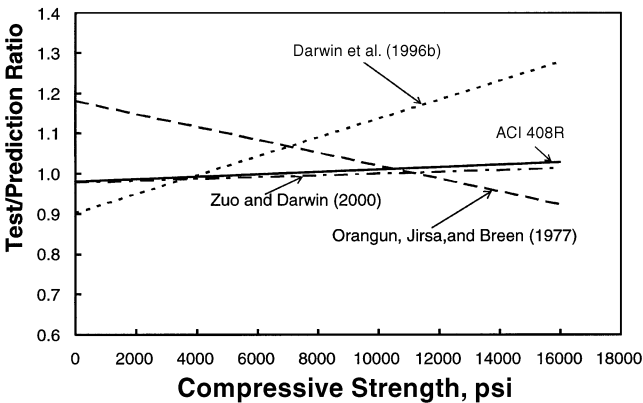


Fig. 3.2—Test-prediction ratios for descriptive equations with confinement provided by transverse reinforcement. (Note: 1 psi = 0.00689 MPa)

produce higher values, the mean changes only slightly (0.94), but the coefficient of variation drops to 0.14.

Figure 3.1 demonstrates why average test-prediction ratios and coefficients of variation do not always provide an adequate evaluation of descriptive expressions. The three expressions in which concrete strength is characterized based on the $\sqrt{f'_c}$, Orangun, Jirsa, and Breen (1977), Darwin et al. (1992), and Esfahani and Rangan (1998a,b) exhibit a significant decrease in test-prediction ratio with increasing

compressive strength. The Orangun, Jirsa, and Breen (1977) and Darwin et al. (1992) expressions were not developed using tests with the wide range of compressive strengths now available. In contrast, the three expressions based on f'_c ^{1/4} exhibit much less variation in test-prediction ratio and have only small increases in test-prediction ratio as compressive strength increases from 3000 to 16,000 psi (21 to 110 MPa). The figures reemphasize the observations made earlier about Fig. 2.10.

The test-prediction ratios for the four expressions for bars confined by transverse reinforcement are shown in Table 3.2. In this case, the average test-prediction ratios range from a high of 1.07 for the Orangun, Jirsa, and Breen (1977) to a low of 0.99 for Zuo and Darwin (2000). The best overall match is obtained by the ACI 408R expression, with an average test-prediction ratio of 1.00 and a coefficient of variation of 0.12. As shown in Fig. 3.2, the expressions developed by Zuo and Darwin and Committee 408 are largely unbiased with respect to compressive strength, whereas the other two expressions give biased results that depend upon compressive strength. Equation (3-4) by Orangun, Jirsa, and Breen (1977), which treats the contributions of both the concrete and the transverse reinforcement as functions of $\sqrt{f'_c}$, exhibits high test-prediction ratios for lower-strength concretes and low test-prediction ratios for high-strength concretes. In contrast, the expression developed by Darwin et al. (1996a) [Eq. (3-8)], in which the contributions of both the concrete and transverse reinforcement are functions of f'_c ^{1/4}, provides low test-prediction ratios for lower-strength concrete and progressively higher test-prediction ratios as concrete strength increases. Both Eq. (3-11) (Zuo and Darwin 2000) and Eq. (3-16) (ACI Committee 408), which characterize the contribution of the concrete as a function of f'_c ^{1/4} and the contribution of transverse reinforcement as a function of f'_c ^{3/4}, provide test-prediction ratios that are essentially independent of concrete compressive strength. The small increase in test-prediction ratio with increasing compressive strength shows that a power of f'_c between 3/4 and 1.0 for the transverse steel contribution would give a slightly better representation (Zuo and Darwin 2000).

CHAPTER 4—DESIGN PROVISIONS

Design provisions should be understandable, simple to apply, and result in an acceptably low probability of failure. This chapter presents the tension development and splice provisions adopted by ACI Committee 318, this committee, and the 1990 CEB-FIP Model Code. The provisions are compared for the relative accuracy, safety, and economy using ACI Committee 408 Database 10-2001. Specific aspects of the provisions of ACI 318, such as the bar size factor g , are evaluated along with the reliability provided by the ACI 318 and ACI 408R design procedures. Special attention is given to the impact of the new load factors and ϕ -factors adopted in ACI 318-02. Comparisons are then made of the development and splice lengths obtained using the design procedures of the two committees. The procedures developed by ACI Committee 408 provide improved reliability and economy compared with those in ACI 318-02,

especially for members with higher compressive strengths or transverse reinforcement and for all spliced bars.

4.1—ACI 318

The design provisions in ACI 318 for development and splice length of straight reinforcement in tension are based on the expressions developed by Orangun, Jirsa, and Breen (1975, 1977) described in Section 3.1. Solving Eq. (3-4) for the ratio of the development length l_d to the bar diameter d_b and replacing $(c_{\min} + 0.4 d_b)$ with $c = (c_{\min} + 0.5 d_b)$ gives

$$\frac{l_d}{d_b} = \frac{\frac{f_s}{\sqrt{f'_c}} - 200}{12 \left(\frac{c + K_{tr}}{d_b} \right)} \quad (4-1)$$

$$\text{where } K_{tr} = \frac{A_{tr} f_{yt}}{1500 s n}$$

In Eq. (4-1), l_d is the length of bar required to develop f_s , the stress in the reinforcement resulting from the loads applied to the structure. At nominal capacity, $f_s = f_y$, and Eq. (4-1) is simplified to give the expression used in ACI 318, by removing the 200 from the numerator and changing the constant multiplying the expression from 1/12 (= 0.0833...) to 3/40 (= 0.075).

$$\frac{l_d}{d_b} = \frac{3}{40} \frac{f_y}{\sqrt{f'_c} \left(\frac{c + K_{tr}}{d_b} \right)} \quad (4-2)$$

To limit the probability of a pullout failure, ACI 318 requires that

$$\frac{c + K_{tr}}{d_b} \leq 2.5 \quad (4-3)$$

Due largely to a lack of data on concretes with compressive strengths in excess of 10,000 psi (69 MPa) at the time that Eq. (3-4) was developed, the value of $\sqrt{f'_c}$ is limited to a maximum value of 100 psi (8.3 MPa).

The effects of bar location, epoxy coating, and lightweight concrete on bond are included by multiplying l_d by the factors a , b , and I , where

- a = reinforcement location factor (1.3 for reinforcement placed so that more than 12 in. (300 mm) of fresh concrete is cast below the development length or splice; 1.0 for other reinforcement);
- b = coating factor (1.5 for epoxy-coated reinforcement with cover less than $3d_b$ or clear spacing less than $6d_b$; 1.2 for other epoxy-coated reinforcement; 1.0 for uncoated reinforcement); with $ab \leq 1.7$; and
- I = lightweight-concrete factor (1.3 for lightweight concrete; 1.0 for normalweight concrete; $6.7 \sqrt{f'_c} / f_{ct} \geq 1.0$ for lightweight concrete with splitting tensile strength f_{ct} specified).

Table 4.1—Development length requirements in ACI 318 that may be used instead of Eq. (4-2)*

	No. 6 (No. 19) and smaller bars and deformed wires	No. 7 (No. 22) and larger bars
Clear spacing of bars being developed or spliced not less than d_b , clear cover not less than d_b , and stirrups or ties throughout l_d not less than the code minimum	$\frac{l_d}{d_b} = \frac{f_y \alpha \beta \lambda}{25 \sqrt{f'_c}}$	$\frac{l_d}{d_b} = \frac{f_y \alpha \beta \lambda}{20 \sqrt{f'_c}}$
or		
Clear spacing of bars being developed or spliced not less than $2d_b$ and clear cover not less than d_b	$\left[\frac{l_d}{d_b} = \frac{12 f_y \alpha \beta \lambda}{25 \sqrt{f'_c}} \right]$	$\left[\frac{l_d}{d_b} = \frac{3 f_y \alpha \beta \lambda}{5 \sqrt{f'_c}} \right]$
Other cases	$\frac{l_d}{d_b} = \frac{3 f_y \alpha \beta \lambda}{50 \sqrt{f'_c}}$ $\left[\frac{l_d}{d_b} = \frac{18 f_y \alpha \beta \lambda}{25 \sqrt{f'_c}} \right]$	$\frac{l_d}{d_b} = \frac{3 f_y \alpha \beta \lambda}{40 \sqrt{f'_c}}$ $\left[\frac{l_d}{d_b} = \frac{9 f_y \alpha \beta \lambda}{10 \sqrt{f'_c}} \right]$

*SI equations in brackets.

Based on limited comparisons for bars with very short development or splice lengths, l_d is also multiplied by a factor for bar size g .

g = reinforcement size factor (0.8 for No. 6 [No. 19] and smaller bars; 1.0 for No. 7 [No. 22] and larger bars).

As will be discussed in Section 4.5.2, the data does not support the use of $g = 0.8$, and Committee 408 does not recommend its use in design.

In lieu of Eq. (4-2), ACI 318 allows the use of a simplified table defining l_d/d_b as a function of bar size and confinement provided by transverse reinforcement and concrete cover (Table 4.1). The center column in Table 4.1 is for No. 6 (No. 19) and smaller bars, corresponding to $g = 0.8$, while the right-hand column is for No. 7 (No. 22) and larger bars, corresponding to $g = 1.0$.

The simplifications shown in Table 4.1 involve the selection of combinations of minimum transverse reinforcement, concrete cover (described in the left-hand column), or both, that allow the term $(c + K_{tr})/d_b$ in Eq. (4-2) to be replaced by either 1.0 or 1.5. Replacement by 1.0 ("Other cases" in Table 4.1) is consistent with Eq. (4-2), if the structure meets the other requirements of ACI 318 for cover and bar spacing, as is replacement by 1.5 when the bars have a clear spacing of not less than $2d_b$ and a cover of not less than d_b . For bars with a clear spacing of less than $2d_b$, however, stirrups or ties that meet the code minimum do not always provide a K_{tr} value that is high enough so that $(c + K_{tr})/d_b$ is at least 1.5 (Nilson, Darwin, and Dolan 2004). The reason is that code minimum transverse reinforcement is typically based on requirements for shear or bar size and spacing criteria to provide confinement for longitudinal column reinforcement. These criteria do not take into account the number of bars being developed or spliced, n , as reflected in the term $K_{tr} = A_{tr}/1500sn$. As a result, the expressions in Table 4.1 may provide a value of l_d that is less than the value calculated using Eq. (4-2).

ACI 318 allows l_d to be reduced by the ratio $(A_s \text{ required})/(A_s \text{ provided})$ when the reinforcement in a flexural member exceeds that required by analysis, except in cases where anchorage or development for the yield strength is specifically required or the reinforcement is designed for certain seismic applications. The basis for allowing a reduction in l_d when using a greater quantity of reinforcement than required is that an increase in steel area will reduce the stress in the steel to a value below f_y at the load corresponding to the nominal strength of the section. A lower value of f_s (refer to Eq. (4-1)) leads to a lower development length, l_d . In all cases, the minimum development length is 12 in. (300 mm).

Lapped splices are classified as Class A or Class B. Class A splices are those in which the ratio $(A_s \text{ provided})/(A_s \text{ required})$ is equal to or greater than 2, and 50% or less of the steel is spliced within the lap length. All other splices are designated as Class B. Splice lengths of $1.0l_d$ and $1.3l_d$ are used for Class A and Class B splices, respectively. Splice lengths may not be reduced by the ratio of $(A_s \text{ provided})/(A_s \text{ required})$ and must be at least 12 in. (300 mm). The extra length required for Class B splices is not based on strength criteria but rather is used as an incentive for designers to stagger splice locations. As will be discussed in Section 4.5, however, the 1.3 factor for Class B splices provides strength that helps make up for some unconservative aspects of the ACI 318 bond provisions. The lack of a f -factor in the development of Eq. (4-2) is also discussed in Section 4.5.

4.2—ACI 408.3

Based on the work by Darwin et al. (1996a,b) (Eq. (3-7) and (3-8)), Innovation Task Group 2 (ITG 2) of the ACI TAC Technology Transfer Committee developed design provisions (ACI T2-98) for spliced and developed high relative rib area bars, defined as bars with $0.10 \leq R_r \leq 0.14$. The provisions were subsequently adopted as ACI 408.3.

The provisions in ACI 408.3 were obtained by incorporating a strength-reduction factor f into Eq. (3-8) [because Eq. (3-8) is based on average strength] by multiplying the right side of the equation by f , replacing f_s by f_y , and then solving the expression for the ratio of development length l_d to bar diameter d_b

$$\frac{l_d}{d_b} = \frac{\frac{f_y}{\phi f_c'^{1/4}} - 2130 \left(0.1 \frac{c_{\max}}{c_{\min}} + 0.9 \right)}{80.2 \left(\frac{c + K_{tr}}{d_b} \right)} = \quad (4-4)$$

$$\frac{\frac{f_y}{f_c'^{1/4}} - \phi 2130 \left(0.1 \frac{c_{\max}}{c_{\min}} + 0.9 \right)}{\phi 80.2 \left(\frac{c + K_{tr}}{d_b} \right)}$$

where $K_{tr} = 35.3 t_r t_d A_{tr} / sn$, $c = c_{\min} [0.1(c_{\max}/c_{\min}) + 0.9] \leq 1.25c_{\min}$, and c_{\max} and c_{\min} are defined following Eq. (2-1).

Using a reliability-based factor f of 0.9 (Darwin et al. 1998), Eq. (4-4) becomes

$$\frac{l_d}{d_b} = \frac{\frac{f_y}{0.9f_c'^{1/4}} - 2130\left(0.1\frac{c_{\max}}{c_{\min}} + 0.90\right)}{80.2\left(\frac{c + K_{tr}}{d_b}\right)} \quad (4-5a)$$

$$\frac{l_d}{d_b} = \frac{\frac{f_y}{f_c'^{1/4}} - 1900\left(0.1\frac{c_{\max}}{c_{\min}} + 0.90\right)}{72\left(\frac{c + K_{tr}}{d_b}\right)} \quad (4-5b)$$

A comparison between development lengths obtained with Eq. (4-4) and (4-5) shows that, for Grade 60 (414 MPa) bars, l_d increases by about 16% due to the incorporation of $f = 0.9$ rather than 11%, the value that would be expected if l_d were proportional to bar stress (refer to Section 2.1.2). The application of f -factor for bond is discussed at greater length in Sections 4.3 and 4.5.

ITG 2 modified Eq. (4-5) to

$$\frac{l_d}{d_b} = \frac{(f_y/f_c'^{1/4} - 1900\omega)\alpha\beta\lambda}{72\left(\frac{c\omega + K_{tr}}{d_b}\right)} \quad (4-6)$$

where c is redefined as $c_{\min} + 0.5d_b$ (4-7)

$$\omega = 0.1\frac{c_{\max}}{c_{\min}} + 0.9 \leq 1.25 \quad (4-8)$$

$$K_{tr} = C_R(0.72d_b + 0.28)\frac{A_{tr}}{sn} \quad (4-9)$$

$$C_R = 44 + 330(R_r - 0.10) \quad (4-10)$$

c_{\max} and c_{\min} are defined following Eq. (2-1), and $(c\omega + K_{tr})/d_b \leq 4.0$.

ACI 408.3 limits $f_c'^{1/4} \leq 11.0$, and $f_y \leq 80$ ksi. A value of 1.0 may be used for the variable ω in place of the value calculated in Eq. (4-8).

The value of l_d is multiplied by the same factors a and l as used in ACI 318 (Section 4.1). The factor for excess reinforcement is also the same as used in ACI 318. The coating factor b is 1.2 for all epoxy-coated bars and 1.0 for uncoated reinforcement; $l_d \geq 12$ in. (300 mm), and $\geq 16d_b$.

Lapped splice criteria are similar to those in ACI 318, except that when the splice length is confined with transverse reinforcement at two or more locations with a spacing not greater than 10 in. (250 mm), providing a value of K_{tr}/d_b of at least 0.5, the provisions for a Class A splice govern. The provisions for high R_r reinforcement may only be applied to No. 11 (No. 36) and smaller bars.

4.3—Recommendations by ACI Committee 408

The splice and development length criteria recommended by this committee are based on the work by Zuo and Darwin (1998, 2000), as extended in Section 3.5. They apply to both conventional and high relative rib area reinforcement. The design expressions given in this section are based on Eq. (3-15) and (3-16).

Converting empirical, best-fit equations to design expressions involves the incorporation of strength-reduction f -factors to ensure a realistically low probability of failure. As demonstrated by Darwin et al. (1998), the f -factor for bond depends upon the f -factor used for tension, as well as the load factors used in design. ACI 318-02 contains two separate sets of load factors and f -factors, necessitating the use of two different f -factors for bond. Based on a Monte Carlo analysis (described in Section 4.5.3)

$f = 0.82$ is obtained for a dead load factor of 1.2, live load factor of 1.6, and $f_{\text{tension}} = 0.9$ (corresponding to Chapter 9 of ACI 318-02); and

$f = 0.92$ is obtained for a dead load factor of 1.4, live load factor of 1.7, and $f_{\text{tension}} = 0.9$ (corresponding to Appendix C of ACI 318-02 and Chapter 9 of ACI 318-99), and a dead load factor = 1.2, live load factor = 1.6, and $f_{\text{tension}} = 0.8$ (corresponding to Appendix C of ACI 318-99).

The derivation that follows, based on the use of $f = 0.92$ (corresponding to ACI 318-99 and Appendix C of 318-02), is presented first. Expressions based on $f = 0.82$ (Chapter 9 of 318-02) are presented in Section 4.3.2.

4.3.1 l_d for ACI 318-99 and Appendix C of ACI 318-02—Solving Eq. (3-16) for l_d/d_b , substituting f_y for f_s , and incorporating f and the factors for bar location, epoxy coating, and lightweight aggregate concrete gives

$$\frac{l_d}{d_b} = \frac{\left(\frac{f_y}{\phi f_c'^{1/4}} - 2400\omega\right)\alpha\beta\lambda}{76.3\left(\frac{c\omega + K_{tr}}{d_b}\right)} = \quad (4-11a)$$

$$\frac{\left(\frac{f_y}{f_c'^{1/4}} - \phi 2400\omega\right)\alpha\beta\lambda}{\phi 76.3\left(\frac{c\omega + K_{tr}}{d_b}\right)}$$

For $f = 0.92$,

$$\frac{l_d}{d_b} = \frac{\left(\frac{f_y}{f_c'^{1/4}} - 2210\omega\right)\alpha\beta\lambda}{70.2\left(\frac{c\omega + K_{tr}}{d_b}\right)} \quad (4-11b)$$

where c and ω are defined in Eq. (4-7) and (4-8), respectively

$$K_{tr} = (0.5t_r t_d A_{tr} / sn) f_c'^{1/2} \quad (4-12)$$

$$t_r = 9.6R_r + 0.28 \leq 1.72 \quad (4-13)$$

$$t_d = 0.78d_b + 0.22 \quad (4-14)$$

and $(c\omega + K_{tr})/d_b \leq 4.0$.

For conventional reinforcement, $K_{tr} = (0.5t_d A_{tr} / sn) f_c'^{1/2}$, corresponding to an average R_r value of 0.0727.

Equation (4-11b) may be simplified in cases in which: 1) the clear spacing of the bars being developed or spliced is not less than d_b , the cover is not less than d_b , and the stirrups or ties throughout l_d provide a value $K_{tr}/d_b \geq 0.5$; or 2) the clear spacing of the bars being developed or spliced is not less than $2d_b$ and the cover is not less than d_b . In this case, $(c\omega + K_{tr})/d_b \geq 1.5$. Setting $\omega = 1.0$, Eq. (4-11b) becomes

$$\frac{l_d}{d_b} = \left(\frac{f_y}{105.3f_c'^{1/4}} - 20.99 \right) \alpha \beta \lambda \quad (4-15)$$

Rounding the values in Eq. (4-15) gives

$$\frac{l_d}{d_b} = \left(\frac{f_y}{105f_c'^{1/4}} - 21 \right) \alpha \beta \lambda \quad (4-16)$$

For cases not meeting the spacing, cover and confinement criteria, Eq. (4-11b) may be simplified to

$$\frac{l_d}{d_b} = \left(\frac{f_y}{70f_c'^{1/4}} - 31 \right) \alpha \beta \lambda \quad (4-17)$$

To match the rounded values in Eq. (4-16) and (4-17), Eq. (4-11b) becomes

$$\frac{l_b}{d_b} = \frac{\left(\frac{f_y}{f_c'^{1/4}} - 2200\omega \right) \alpha \beta \lambda}{70 \left(\frac{c\omega + K_{tr}}{d_b} \right)} \quad (4-18)$$

Equation (4-18) may be further simplified by setting $\omega = 1.0$ and dropping the 0.25 in. term in the definition of the effective value c_{si} [refer to Eq. (2-1)]. The values of α , β , and λ and the term for excess reinforcement are as defined in Section 4.2, except that $\beta = 1.5$ for epoxy-coated bars for concrete with $f_c' > 10,000$ psi (70 MPa), based on observations by Zuo and Darwin (1998). The values of l_d in Eq. (4-16) to (4-18) are used for both development and lapped splice lengths. In addition, $l_d \geq 12$ in. (300 mm), $\geq 16d_b$.

4.3.2 l_d based on Chapter 9 of ACI 318-02—Using $f = 0.82$ for bond, Eq. (4-16), (4-17), and (4-18) are as follows:

For cases in which the clear spacing of the bars being developed or spliced is not less than d_b , the cover is not less

than d_b , and the stirrups or ties throughout l_d provide a value of $K_{tr}/d_b \geq 0.5$; or the clear spacing of the bars being developed or spliced is not less than $2d_b$ and the cover is not less than d_b

$$\frac{l_d}{d_b} = \left(\frac{f_y}{93f_c'^{1/4}} - 21 \right) \alpha \beta \lambda \quad (4-19)$$

For cases not meeting the spacing, cover, and confinement criteria

$$\frac{l_d}{d_b} = \left(\frac{f_y}{62f_c'^{1/4}} - 31 \right) \alpha \beta \lambda \quad (4-20)$$

Alternatively, development length may be calculated using Eq. (4-11a) with $f = 0.82$.

$$\frac{l_d}{d_b} = \frac{\left(\frac{f_y}{f_c'^{1/4}} - 1970\omega \right) \alpha \beta \lambda}{62 \left(\frac{c\omega + K_{tr}}{d_b} \right)} \quad (4-21)$$

All other criteria presented in Section 4.3.1 remain unchanged.

4.4—CEB-FIP Model Code

The factors included in the 1990 CEB-FIP Model Code for calculating development and splice lengths of straight reinforcing bars are similar to those included in the ACI procedures discussed in Sections 4.1 through 4.3, with some additional considerations. The CEB-FIP provisions are presented here using notation that is compatible with that used in the earlier sections.

The CEB-FIP design expression for development length is

$$\frac{l_d}{d_b} = \quad (4-22)$$

$$\frac{1}{950} \left(1.15 - 0.15 \frac{c_{\min}}{d_b} \right) \left(1 - K \frac{\Sigma A_{tr} - \Sigma A_{tr, \min}}{A_b} \right) \frac{M f_y}{\left(\frac{f_c' - 400}{1450} \right)^{2/3}}$$

where the first two terms in parentheses are between 0.7 and 1.0; $K = 0.10$ for a bar confined at a corner bend of a stirrup or tie, $K = 0.05$ for a bar confined by a single leg of a stirrup or tie, and $= 0$ for a bar that is not confined; ΣA_{tr} = area of transverse reinforcement along l_d ; $\Sigma A_{tr, \min} = 0.25 A_b$ for beams and 0 for slabs; A_b = area of the largest bar being developed or spliced; and M = ratio of the average yield strength to the design yield strength of the developed bar (values close to 1.15 are typical in U.S. practice).

The term containing f_c' is based on a characteristic strength, which is 1160 psi (8.0 MPa) below the average (not

the specified) strength. For simplicity, the average strength is assumed (in this report) to be 760 psi (5.2 MPa) greater than the specified compressive strength f'_c , resulting in a characteristic strength of $f'_c - 400$ psi (2.75 MPa). The value of l_d may be multiplied by $0.7 \leq (1 - 0.00028p) \leq 1.0$, where p = the transverse pressure in psi at the ultimate limit state along l_d , perpendicular to the splitting plane. For p in MPa, the term is $(1 - 0.04p)$.

The effect of bar location is included by dividing l_d by 0.7 for bars that are both more than 10 in. (250 mm) from the bottom and less than 12 in. (300 mm) from the top of a concrete layer during placement.

As for the other design methods, the development length may be reduced by the ratio (A_s required)/(A_s provided).

l_d is increased for lapped splices by multiplying by a factor $a_b = 1.2$ when $\leq 20\%$ of the bars are spliced at one location. a_b increases to 1.4 for 25%, 1.6 for 33%, 1.8 for 50%, and 2.0 for $\geq 50\%$ of the bars spliced at one location.

The minimum development length in tension is

$$l_{d,\min} = \max \left[\frac{0.3}{950} \frac{Mf_y}{\left(\frac{f'_c - 400}{1450} \right)^{2/3}}, 10d_b, 4 \text{ in.} \right] \quad (4-23)$$

The minimum splice length is

$$l_{s,\min} = \max \left[\frac{0.3\alpha_b}{950} \frac{Mf_y}{\left(\frac{f'_c - 400}{1450} \right)^{2/3}}, 15d_b, 8 \text{ in.} \right] \quad (4-24)$$

4.5—Structural reliability and comparison of design expressions

The principles of structural reliability help ensure that structures possess an acceptably small probability of failure. In this section, ACI Committee 408 Database 10-2001 is used to compare the accuracy and relative safety of the four design procedures. Because high relative rib area bars are not in general production, most comparisons are based on conventional reinforcement, although tests of high relative rib area bars not confined by transverse reinforcement are used in the analysis because they exhibit the same bond strength as conventional bars. Only tests with development or splice lengths of at least 12 in. (300 mm) and $l_d/d_b \geq 16$ are included to ensure that the comparisons only involve realistic development and splice lengths. The database used for the comparisons consists of 157 tests in which the developed or spliced bars are not confined by transverse reinforcement and 163 tests in which they are.

4.5.1 Comparison with data—Comparisons of the design expressions (the predictions) with the test data are summarized in Fig. 4.1 and 4.2 and Table 4.2. Figure 4.1 and 4.2 show the distribution in test-prediction ratios for ACI 318 (Eq. (4-2)), ACI 408.3 (Eq. (4-6)), ACI 408R (Eq. (4-18)) and CEB-FIP [Eq. (4-22)]. Table 4.2 gives the maximum, minimum, and average test-prediction ratios, along with the

Table 4.2—Test-prediction ratios for design provisions

Bars not confined by transverse reinforcement					
	ACI 318 (Eq. (4-2))	ACI 408.3 (Eq. (4-6))	ACI 408R (Eq. (4-18))	ACI 408R (Eq. (4-21))	CEB-FIP (Eq. (4-22))
For all f'_c (157 tests)					
Maximum	2.369	1.500	1.404	1.575	2.011
Minimum	0.624	0.768	0.749	0.843	0.322
Average	1.229	1.135	1.092	1.227	1.095
Standard deviation	0.281	0.138	0.125	0.140	0.325
Coefficient of variation	0.228	0.121	0.114	0.114	0.296
For $f'_c \leq 10,000$ psi (69 MPa) (114 tests)					
Maximum	1.908	1.472	1.401	1.574	2.011
Minimum	0.756	0.768	0.749	0.843	0.791
Average	1.229	1.128	1.089	1.224	1.230
Standard deviation	0.229	0.118	0.108	0.121	0.232
Coefficient of variation	0.186	0.104	0.099	0.099	0.188
Bars confined by transverse reinforcement					
	ACI 318 (Eq. (4-2))	ACI 408.3 (Eq. (4-6))	ACI 408R (Eq. (4-18))	ACI 408R (Eq. (4-21))	CEB-FIP (Eq. (4-22))
For all f'_c (163 tests)					
Maximum	2.192	1.668	1.525	1.715	2.482
Minimum	0.704	0.850	0.802	0.903	0.457
Average	1.232	1.185	1.132	1.273	1.392
Standard deviation	0.299	0.172	0.163	0.183	0.372
Coefficient of variation	0.242	0.145	0.144	0.144	0.267
For $f'_c \leq 10,000$ psi (69 MPa) (128 tests)					
Maximum	2.192	1.524	1.525	1.715	2.482
Minimum	0.704	0.850	0.845	0.951	0.894
Average	1.237	1.176	1.150	1.294	1.503
Standard deviation	0.311	0.162	0.155	0.175	0.306
Coefficient of variation	0.251	0.137	0.135	0.135	0.204

standard deviation and coefficient of variation, for the expressions shown in Fig. 4.1 and 4.2 plus the second ACI 408R equation, Eq. (4-21). The table presents the results for both the full range of compressive strengths and for specimens with compressive strengths below 10,000 psi (69 MPa).

The comparisons demonstrate that the test-prediction ratios for ACI 318 and CEB-FIP exhibit more scatter than those for ACI 408.3 and 408R. The greater scatter is especially apparent for CEB-FIP, which exhibits a range in test-prediction ratios from 0.32 to 2.48. As shown in Table 4.2, many of the lower test-prediction ratios result from the inaccuracy of the CEB-FIP expression for bond in high-strength concrete. When test results for $f'_c > 10,000$ psi (69 MPa) are removed, the minimum test-prediction ratio for Eq. (4-22) increases to 0.79, in line with the values produced by the other expressions.

Overall, the ACI 318 and CEB-FIP provisions provide higher average test-prediction ratios and higher coefficients of variation than do those of ACI 408.3 and ACI 408R. The result is that, on the average, ACI 318 and the CEB-FIP Model Code require longer development and splice lengths

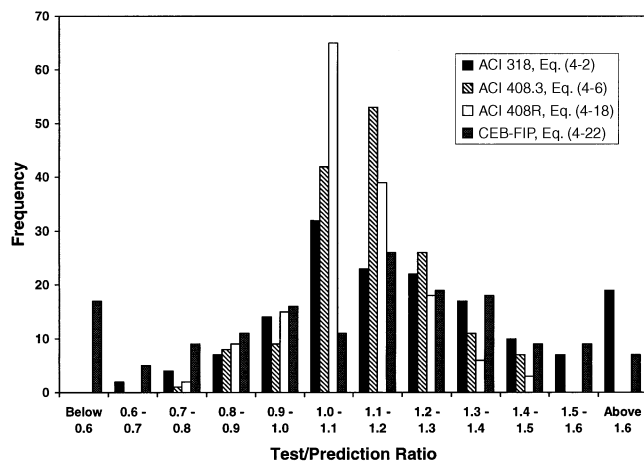


Fig. 4.1—Test-prediction ratios for design provisions for bars not confined by transverse reinforcement.

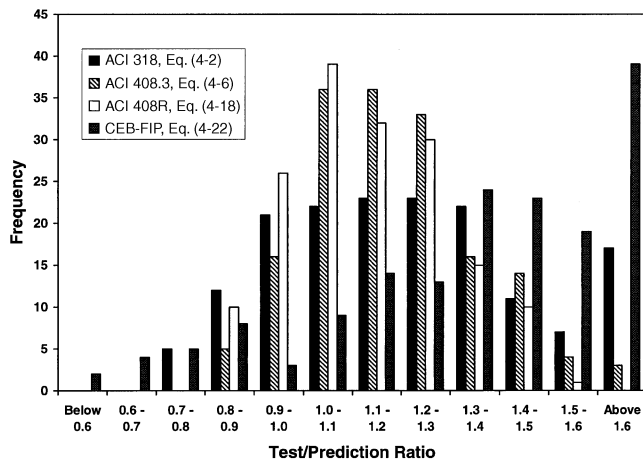


Fig. 4.2—Test-prediction ratios for design provisions for bars confined by transverse reinforcement.

than ACI 408.3 or ACI 408R, while simultaneously having a greater probability of low strength.

Equation (4-21), the ACI 408R equation for use with the load factors and strength reduction factors in Chapter 9 of ACI 318-02, provides average test-prediction ratios that are approximately the same or slightly higher than those provided by ACI 318. The range in test-prediction ratios obtained with Eq. (4-21), however, is considerably narrower. The test-prediction ratios obtained with ACI 318 have both higher maximums (2.37 and 2.19 for bars not confined and confined by transverse reinforcement, respectively) than Eq. (4-21) (1.58 and 1.72, respectively) and lower minimums (0.62 and 0.70 for bars not confined and confined by transverse reinforcement, respectively) than Eq. (4-21) (0.84 and 0.90, respectively).

Fortunately, the higher probability of low bond strength provided by ACI 318 and the CEB-FIP Model Code has not translated into structural failures because of the safety margin provided by load factors and by the ϕ -factors for bending and axial load, as well as other design provisions, such as those that limit the location of splices. The overall effect is that ACI 318 and the CEB-FIP Model Code provide

lower levels of reliability in bond, when compared to those in bending and axial load, than would be achieved if the development length provisions had been formulated based on a desired level of reliability, as done with the ACI 408.3 and ACI 408R design procedures.

4.5.2 γ -factor in ACI 318*—As described in Section 4.1, the development length provisions in ACI 318 include a factor for bar size g with $g = 0.8$ for No. 6 (No. 19) and smaller bars and 1.0 for No. 7 (No. 22) and larger bars. The commentary in ACI 318 justifies the use of $g = 0.8$ based on a “comparison with past provisions and a check of a database of experimental results maintained by ACI Committee 408” which “indicated that for No. 6 [No. 19] deformed bars and smaller, as well as deformed wire, development length could be reduced 20% using $g = 0.8$.” At the time these comparisons were made, the ACI 408 database only included tests of small bars with short development and splice lengths, most of which were less than 12 in. (300 mm).

As discussed in Section 2.2, expressions such as Eq. (4-2), which are based on a proportional relationship between bond force and bonded length, conservatively predict the bond strength of bars with low development and splice lengths. Equation (4-2) becomes progressively less conservative, however, as more realistic splice lengths are used.

In the years since the original comparison was made, the number of tests in the ACI 408 database for No. 6 (No. 19) and smaller bars with development and splice lengths in excess of 12 in. (300 mm) has increased to 63—22 for bars without confining transverse reinforcement, and 41 for bars with confining transverse reinforcement. Figure 4.3 and 4.4 compare test-prediction ratios for No. 6 (No. 19) and smaller bars for the ACI 318 provisions using $g = 0.8$ and 1.0 for bars without and with confining transverse reinforcement, respectively. The Class B splice factor of 1.3 is not used in the comparisons. For $g = 0.8$, seven tests, or 32% of the bars without confining transverse reinforcement, have test-prediction ratios of less than 1.0 (Fig. 4.3). For bars with confining transverse reinforcement, 23 tests, or 56% of the data, have test-prediction ratios of less than 1.0 (Fig. 4.4). Changing g to 1.0 substantially decreases the number of low test-prediction ratios to 1, or 4.5%, for bars without confining transverse reinforcement and to 4, or 10%, for bars with confining transverse reinforcement. Thus, based on bars with realistic splice and development lengths, it is the position of ACI Committee 408 that there is no justification for using g less than 1.0.

4.5.3 Reliability—ACI 318 and ACI 408R—This section summarizes the development of strength-reduction factors ϕ for bond for use with the provisions in ACI 318 (Eq. (4-2)) and for deriving the ACI 408R expressions (Eq. (4-18) and (4-21)) based on Eq. (3-16). The analyses follow the procedures described by Ellingwood et al. (1980), Mirza and MacGregor (1986), Lundberg (1993), and Darwin et al. (1998). Separate Monte Carlo simulations are carried out for bars without and with confining transverse reinforcement.

*Section 4.5.2 draws heavily on the discussion by Darwin and Zuo (2002) of the changes proposed for ACI 318-02.

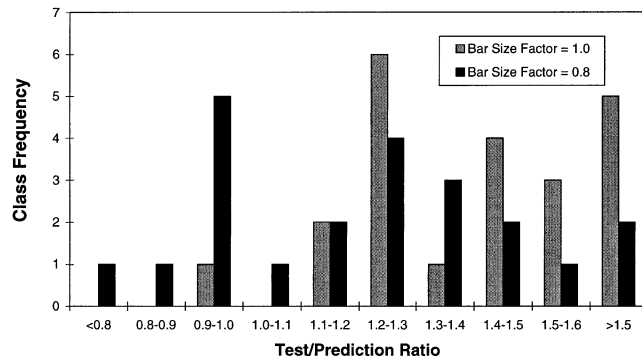


Fig. 4.3—Test-prediction ratios for spliced and developed No. 6 (No. 19) and smaller bars without confining transverse reinforcement for ACI 318; bar size factors $\gamma = 0.8$ and 1.0.

The analyses use dead load, live load, and tension f -factor combinations of:

- (a) 1.4, 1.7, and 0.9 (ACI 318-99, Chapter 9, and ACI 318-02, Appendix C);
- (b) 1.2, 1.6, and 0.8 (ACI 318-99, Appendix C) and
- (c) 1.2, 1.6, and 0.9 (ACI 318-02, Chapter 9).

A reliability index $b = 3.5$ is used, providing a probability of failure in bond equal to about 1/5 of the probability of failure in bending ($b = 3.0$). Comparisons are made for bottom-cast bars with development and splice lengths ≥ 12 in. (300 mm) and $16d_b$. Live-to-dead load ratios of 0.5, 1.0, and 1.5 are used. All analyses use a bar size factor $g = 1.0$ for small as well as large bars for the reasons discussed in Section 4.5.2.

For each combination of variables, two f -factors are calculated: one, a basic bond f -factor, f_b , represents the capacity-reduction factor that would be obtained based strictly on development and splice strength as a structural property. An effective f -factor, f_d , is then calculated by dividing f_b by the f -factor used for bars in tension f_{tension} . The higher effective f -factor for bond and development f_d recognizes that maximum bond force is independent of the flexural capacity and that the area of the bars has been increased (and the bar stress decreased) based on the f_{tension} .

The results of the analyses are summarized for Eq. (4-2) and Eq. (3-16) in Table 4.3 and 4.4, respectively. As shown in Table 4.3, the results justify the application of a f -factor $f_d \approx 0.85$ to the development and splice length criteria in ACI 318-99 and Appendix C of ACI 318-02. f_d drops to values of about 0.75 for Chapter 9 of ACI 318-02.

Darwin and Zuo (2002) observed that the provisions of ACI 318-99 provide a reliability index $b = 2.8$ to 3.0 for bond, somewhat lower than the desired reliability index for flexure. b drops to 2.4 to 2.6 for Chapter 9 of ACI 318-02. The conclusion is that, under the provisions of ACI 318-02, there is a greater probability of a bond failure than a flexural failure. This situation is mitigated to a large extent for Class B splices because of the 1.3 factor. The 1.3 factor is, however, not applied for developed bars and Class A splices.

The f -factors used with Eq. (3-16) to produce the two ACI 408R expressions, Eq. (4-18) and (4-21), are presented

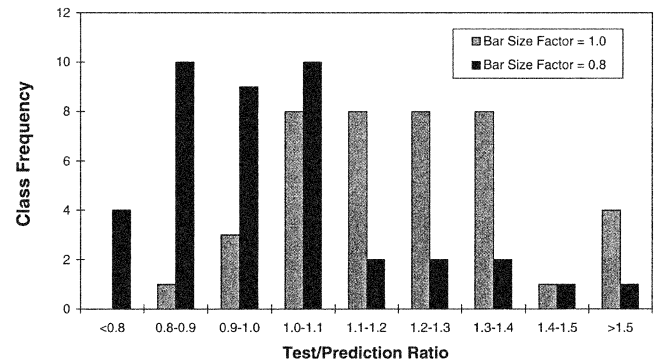


Fig. 4.4—Test-prediction ratios for spliced and developed No. 6 (No. 19) and smaller bars with confining transverse reinforcement for ACI 318; bar size factors $\gamma = 0.8$ and 1.0.

Table 4.3—Strength-reduction (f) factors for bond using ACI 318-99 and ACI 318-02; $b = 3.5$

\bar{r}	1.23			1.23		
V_r	0.23			0.24		
	Without confining transverse reinforcement			With confining transverse reinforcement		
	Dead load factor = 1.4; live load factor = 1.7; $f_{\text{tension}} = 0.9$					
$(Q_L/Q_D)_n$	0.50	1.00	1.50	0.50	1.00	1.50
\bar{q}	0.67	0.65	0.63	0.67	0.65	0.63
V_{f_q}	0.10	0.13	0.15	0.10	0.13	0.15
f_b	0.76	0.76	0.75	0.73	0.73	0.72
f_d	0.84	0.84	0.83	0.81	0.81	0.80
	Dead load factor = 1.2; live load factor = 1.6; $f_{\text{tension}} = 0.8$					
$(Q_L/Q_D)_n$	0.50	1.00	1.50	0.50	1.00	1.50
\bar{q}	0.76	0.72	0.69	0.76	0.72	0.69
V_{f_q}	0.10	0.13	0.15	0.10	0.13	0.15
f_b	0.68	0.68	0.68	0.65	0.66	0.65
f_d	0.84	0.86	0.85	0.81	0.82	0.82
	Dead load factor = 1.2; live load factor = 1.6; $f_{\text{tension}} = 0.9$					
$(Q_L/Q_D)_n$	0.50	1.00	1.50	0.50	1.00	1.50
\bar{q}	0.76	0.72	0.69	0.76	0.72	0.69
V_{f_q}	0.10	0.13	0.15	0.10	0.13	0.15
f_b	0.68	0.68	0.68	0.65	0.66	0.65
f_d	0.75	0.76	0.76	0.72	0.73	0.73

Notes:

\bar{r} = mean test-prediction ratio comparing Eq. (4-2) with results from Database 10-2001.

V_r = coefficient of variation of resistance random variable r .

$(Q_L/Q_D)_n$ = nominal ratio of live load to dead load.

\bar{q} = mean value of random loading variable.

V_{f_q} = coefficient of variation of loading random variable q .

$f_b = \frac{\bar{r}}{\bar{q}} e - (V_r^2 + V_{f_q}^2)^{1/2} \beta$.

$f_d = f_b / f_{\text{tension}}$.

in Table 4.4. The table includes separate results for high relative rib area bars (average $R_r = 0.1275$) confined by transverse reinforcement and for bars with conventional deformation patterns. As discussed in Section 4.3, values of $f_d = 0.92$ and 0.82 are selected for application with ACI 318-99 and Appendix C of ACI 318-02 (Eq. (4-18)) and Chapter 9 of ACI 318-02 (Eq. (4-21)), respectively.

The lower values of f_d for use with Chapter 9 of ACI 318-02, 0.75 for ACI 318 and 0.82 for ACI 408, reflect the

Table 4.4—Strength-reduction (f) factors for bond using Eq. (3-16) to develop Eq. (4-18) and (4-21); $b = 3.5$

\bar{r}	1.00			1.00					
V_r	0.11			0.12					
	Without confining transverse reinforcement			With confining transverse reinforcement					
				$R_r = 0.727$			$R_r = 0.1275$		
	Dead load factor = 1.4; live load factor = 1.7; $f_{\text{tension}} = 0.9$								
$(Q_L/Q_D)_n$	0.50	1.00	1.50	0.50	1.00	1.50	0.50	1.00	1.50
\bar{q}	0.67	0.65	0.63	0.67	0.65	0.63	0.67	0.65	0.63
V_{f_q}	0.10	0.13	0.15	0.10	0.13	0.15	0.10	0.13	0.15
f_b	0.87	0.85	0.82	0.86	0.83	0.81	0.85	0.83	0.80
f_d	0.97	0.94	0.91	0.95	0.93	0.90	0.95	0.92	0.89
Dead load factor = 1.2; live load factor = 1.6; $f_{\text{tension}} = 0.8$									
$(Q_L/Q_D)_n$	0.50	1.00	1.50	0.50	1.00	1.50	0.50	1.00	1.50
\bar{q}	0.76	0.72	0.69	0.76	0.72	0.69	0.76	0.72	0.69
V_{f_q}	0.10	0.13	0.15	0.10	0.13	0.15	0.10	0.13	0.15
f_b	0.78	0.77	0.75	0.76	0.75	0.74	0.76	0.75	0.73
f_d	0.97	0.96	0.93	0.95	0.94	0.92	0.95	0.94	0.92
Dead load factor = 1.2; live load factor = 1.6; $f_{\text{tension}} = 0.9$									
$(Q_L/Q_D)_n$	0.50	1.00	1.50	0.50	1.00	1.50	0.50	1.00	1.50
\bar{q}	0.76	0.72	0.69	0.76	0.72	0.69	0.76	0.72	0.69
V_{f_q}	0.10	0.13	0.15	0.10	0.13	0.15	0.10	0.13	0.15
f_b	0.78	0.77	0.75	0.76	0.75	0.74	0.76	0.75	0.73
f_d	0.86	0.85	0.83	0.84	0.84	0.82	0.84	0.83	0.82

Notes:

 \bar{r} = mean test-prediction ratio comparing Eq. (4-2) with results from Database 10-2001. V_r = coefficient of variation of resistance random variable r . $(Q_L/Q_D)_n$ = nominal ratio of live load to dead load. \bar{q} = mean value of random loading variable. V_{fq} = coefficient of variation of loading random variable q .

$$f_b = \frac{\bar{r}}{\bar{q}} e - (V_r^2 + V_{fq}^2)^{1/2} \beta.$$

$$f_d = f_b / f_{\text{tension}}.$$

combined effects of the higher value of f_{tension} and the lower load factors.

4.5.4 Comparisons of development and splice lengths *ACI 318, ACI 408.3, and ACI 408*—Development and splice lengths based on the design provisions of ACI 318 (Eq. (4-2)), ACI 408.3 (Eq. (4-6)), and ACI 408R (Eq. (4-18)) and (4-21)) are expressed in terms of l_d/d_b in **Table 4.5** for concrete strengths of 3000 to 8000, 10,000, 12,000, and 15,000 psi (21 to 55, 69, 83, and 103 MPa) and Grade 60 (414 MPa) reinforcing bars. The comparisons are for conventional reinforcing bars, and although ACI 408.3 is limited (by its provisions) to high relative rib area bars ($R_r \geq 0.10$), it is applied in this case to conventional reinforcement (average $R_r = 0.0727$). For simplicity, the comparisons are made for No. 8 (No. 25) bars ($g = 1.0$ for ACI 318 and $t_d = 1.0$ for ACI 408.3 and ACI 408) and $w = 1.0$ for ACI 408.3 and ACI 408. Three cases are covered:

1. Minimum confinement, $(c + K_{tr})/d_b = 1.0$;
2. $c/d_b = 1.0$ and $A_{tr}/s_n = 0.0125$, which corresponds to $(c + K_{tr})/d_b = 1.5$ for ACI 318, values less than 1.5 for ACI 408.3, and values less than or greater than 1.5 for ACI 408, depending on f'_c ; and
3. $(c + K_{tr})/d_b$ = maximum allowed by the provisions, = 2.5 for ACI 318 and = 4 for ACI 408.3 and ACI 408.

The comparisons of development and Class A splice lengths in **Table 4.5** show that the values obtained with ACI 408.3 and ACI 408R are greater than those required by ACI 318 when $(c + K_{tr})/d_b = 1.0$ for the range of concrete strengths evaluated. In this case, the development lengths required by ACI 408.3 exceed those required by ACI 318 by values that range from 5% for $f'_c = 3000$ psi (21 MPa) to 27% for $f'_c = 10,000$ psi (69 MPa), dropping to 9% for $f'_c = 15,000$ psi (103 MPa). The values of l_d provided by the ACI 408R design procedures for use with ACI 318-99 and Appendix C of ACI 318-02 (Eq. (4-18)) range from 3% greater than required by ACI 318 for $f'_c = 3000$ psi (21 MPa) to 21% greater at 10,000 psi (69 MPa), dropping to 2% greater at $f'_c = 15,000$ psi (103 MPa). The development and Class A splice lengths based on the ACI 408R design procedures for Chapter 9 of ACI 318-02 (Eq. (4-21)) range from 20% greater at 3000 psi (21 MPa) to 44% greater at 10,000 psi (69 MPa), dropping to 24% greater at 15,000 psi (103 MPa). The longer development lengths required by ACI 408.3 and ACI 408R provide a higher margin of safety compared with those calculated using ACI 318 and are a principal reason for the lower number of low test-prediction ratios obtained with these provisions (**Section 4.5.1**). For cases in which $1.0 < w \leq 1.25$, the development lengths l_d based on ACI 408.3 and

Table 4.5—Comparison of development and splice lengths for ACI 318, ACI 408.3, and ACI 408R; l_d/d_b for No. 8 (No. 25) Grade 60 (414 MPa) reinforcing bars; $w = 1$

f'_c , psi	Development and Class A splice length, in.				Class B splice length, in.			
	ACI 318 Eq. (4-2)	ACI 408.3* Eq. (4-6)	ACI 408R Eq. (4-18)	ACI 408R Eq. (4-21)	ACI 318 Eq. (4-2)	ACI 408.3* Eq. (4-6)	ACI 408R Eq. (4-18)	ACI 408R Eq. (4-21)
$(c + K_{tr})/d_b = 1$								
3000	82.2	86.2	84.4	99.0	106.8	86.2	84.4	99.0
4000	71.2	78.4	76.4	89.9	92.5	78.4	76.4	89.9
5000	63.6	72.7	70.5	83.3	82.7	72.7	70.5	83.3
6000	58.1	68.3	66.0	78.2	75.5	68.3	66.0	78.2
7000	53.8	64.7	62.3	74.0	69.9	64.7	62.3	74.0
8000	50.3	61.7	59.2	70.6	65.4	61.7	59.2	70.6
10,000	45.0	56.9	54.3	65.0	58.5	56.9	54.3	65.0
12,000	45.0	53.2	50.5	60.7	58.5	53.2	50.5	60.7
15,000	45.0	48.9	46.0	55.7	58.5	48.9	46.0	55.7
$c/d_b = 1$ and $A_{tr}/s_n = 0.0125$ —corresponds to $(c + K_{tr})/d_b = 1.5$ for ACI 318								
3000	54.8	60.0	62.9	73.7	71.2	60.0	62.9	73.7
4000	47.4	54.5	54.7	64.4	61.7	54.5	54.7	64.4
5000	42.4	50.6	48.9	57.8	55.2	50.6	48.9	57.8
6000	38.7	47.5	44.4	52.7	50.3	47.5	44.4	52.7
7000	35.9	45.0	40.9	48.6	46.6	45.0	40.9	48.6
8000	33.5	42.9	38.0	45.3	43.6	42.9	38.0	45.3
10,000	30.0	39.6	33.4	40.0	39.0	39.6	33.4	40.0
12,000	30.0	37.0	30.0	36.0	39.0	37.0	30.0	36.0
15,000	30.0	34.0	26.1	31.5	39.0	34.0	26.1	31.5
$(c + K_{tr})/d_b = \text{maximum}, = 2.5$ for ACI 318, $= 4$ for ACI 408.3 and ACI 408R								
3000	32.9	21.6	21.1	24.7	42.7	21.6	21.1	24.7
4000	28.5	19.6	19.1	22.5	37.0	19.6	19.1	22.5
5000	25.5	18.2	17.6	20.8	33.1	18.2	17.6	20.8
6000	23.2	17.1	16.5	19.5	30.2	17.1	16.5	19.5
7000	21.5	16.2	16.0	18.5	28.0	16.2	16.0	18.5
8000	20.1	16.0	16.0	17.6	26.2	16.0	16.0	17.6
10,000	18.0	16.0	16.0	16.3	23.4	16.0	16.0	16.3
12,000	18.0	16.0	16.0	16.0	23.4	16.0	16.0	16.0
15,000	18.0	16.0	16.0	16.0	23.4	16.0	16.0	16.0

*Applied to conventional reinforcing bars.

Note: 1 psi = 6.895×10^{-3} MPa; 1 in. = 25.4 mm.

ACI 408R could be reduced by as much as 35% from the values shown in Table 4.5.

For $c/d_b = 1$ and $A_{tr}/s_n = 0.0125$, ACI 408.3 and ACI 408R again require longer development lengths than ACI 318 by values that range up to 32% for ACI 408.3 and up to 15% and 36%, respectively, for ACI 408R Eq. (4-18) and (4-21). In this case, the ratios are greater than for $(c + K_{tr})/d_b = 1.0$ until f'_c exceeds 10,000 psi (69 MPa), because ACI 318 gives greater credit to transverse reinforcement (a higher value of K_{tr}) than do the ACI 408.3 and ACI 408R expressions at lower values of f'_c . This is another reason that ACI 318 may overpredict bond strength, as illustrated in [Section 4.5.1](#).

Because K_{tr} for ACI 408R is a function of f'_c , it exceeds K_{tr} for ACI 318 for $f'_c > 6400$ psi (44 MPa). The values of l_d for ACI 318 and ACI 408R Eq. (4-18) are equal at $f'_c = 12,000$ psi (83 MPa), with the value for Eq. (4-18) equal to 87% of that for ACI 318 at $f'_c = 15,000$ psi (103 MPa).

For cases in which $(c + K_{tr})/d_b$ equals the maximum allowed by each of the provisions ($= 2.5$ for ACI 318, $= 4$ for ACI 408.3 and ACI 408R), the values of l_d for the ACI 408.3 and ACI 408R provisions are consistently below the value for ACI 318 by from 11 to 36%. As f'_c increases, l_d for ACI 408.3 and ACI 408R is constrained by the minimum l_d/d_b ratio $= 16$. This occurs at 8000, 7000, and 12,000 psi (55, 48, and 83 MPa) for ACI 408.3 and ACI 408R Eq. (4-18) and (4-21), respectively.

The Class B splice lengths based on the ACI 408.3 and ACI 408R design procedures are, in most cases, below those required by ACI 318 because the 1.3 factor is not required. The ACI 408.3 provisions (Eq. (4-6)) provide splice lengths that range between 50 and 102% of those required by ACI 318. The ACI 408R procedures (Eq. (4-18)) provide splice lengths that range between 49 and 93% of those required by ACI 318, while those calculated using Eq. (4-21) range from 58 to 111% of the splice lengths required by ACI 318. The

lowest relative values are, of course, obtained when $(c + K_{tr})/d_b$ is equal to the maximum allowed.

An additional relative decrease in both development and splice length occurs for the ACI 408.3 and ACI 408R design procedures once $f'_c > 10,000$ psi (69 MPa) because of the limitation of $\sqrt{f'_c}$ to 100 psi (8.3 MPa) within the provisions of ACI 318. As demonstrated in Fig. 3.1 and 3.2, such a limitation is appropriate, since Eq. (4-2) is based on Eq. (3-4), which shows a decreasing test-prediction ratio with increasing compressive strength.

Overall, the development and Class A splice lengths required by the ACI 408.3 and ACI 408R design procedures are greater than those required by ACI 318 for conditions of low cover and confinement and lower concrete strengths. The values of l_d obtained with the ACI 408.3 and ACI 408R design procedures decrease with respect to those obtained with ACI 318 as cover, confinement, and compressive strength increase and when $w > 1.0$. The ACI 408.3 and ACI 408R design procedures include reliability-based ϕ -factors that are embedded in the expressions.

The shorter Class B splice lengths required under the ACI 408.3 and ACI 408R design procedures result from the fact that a 1.3 factor is not used, because the values of l_d are based principally on splice tests in which 100% of the bars are spliced, and thus, do not require an increase for the conditions applying to Class B splices. Although the ACI 318 Class B splice factor is not based on strength, it is clear from the analyses in this section that it does provide improved reliability and should not be set to 1.0 if the other development and splice provisions in ACI 318 remain unchanged.

CHAPTER 5—DATABASE

Databases maintained by ACI Committee 408 have played an important role in the development of design expressions adopted in ACI 318. The databases, however, have often been maintained on an ad hoc basis, and it has only been since 1997 that a formal database has been in existence. This chapter describes the procedures used to determine bar stresses at the time of failure in development and splice tests and provides a general description of the database used for the analyses presented in Chapters 3 and 4. As will be described in Section 5.2, the database is available in a form that can be readily used by researchers.

5.1—Bar stresses

The force in a developed or spliced bar at bond failure is a structural property of the same type as flexural or shear strength. Because most development and splice tests involve bending, determination of the force in the bar at failure involves a calculation that depends on both the bending moment corresponding with failure and the properties of the nonlinear, inelastic materials involved. Historically, three approaches have been used to calculate the force in reinforcement at bond failure: the working stress method, the strength method, and the moment-curvature method. In the working stress method, the stress in the concrete and steel can be determined based on static equilibrium and compatibility of strain using a transformed section in which the steel

area is replaced by an equivalent area of concrete based on the ratio of the moduli of elasticity. In the strength method, an average concrete compressive stress of 0.85 is assumed to be uniformly distributed over a stress block, the depth of which is equal to a portion of the depth to the neutral axis. The bar stress at failure can be calculated based on this assumption and equilibrium. In the moment-curvature method, stress-strain relationships are assumed for the concrete and the reinforcing steel. In all three methods, strains in the materials are assumed to vary linearly over the depth of the member.

Zuo and Darwin (1998) compared the three methods and concluded that the moment-curvature method provided the most realistic results. They observed that in cases where the bar stress is below the yield strength of the steel, the working stress method overestimates bar stresses for high-strength concrete and underestimates bar stresses for normal-strength concrete, compared to the moment-curvature method, especially for f'_c less than 3000 psi (21 MPa). The strength method, however, underestimates bar stresses in almost all cases.

For members in which the calculated bar stress exceeds the yield strength of the steel, the working stress method consistently overestimates bar stresses for high-strength concrete ($f'_c \geq 10,000$ psi [70 MPa]) and in slightly more than half the cases for beams made with normal-strength concrete compared to the moment-curvature method. In contrast, the strength method underestimates the bar stresses for high-strength concrete and in about 40% of the tests for beams made with normal-strength concrete. The evaluation included a total of 439 development or splice test specimens.

Based on this analysis, the bar stresses at failure in the ACI Committee 408 database are based on moment-curvature calculations. In about 3% of the tests, the bending capacity at failure in a splice or development test exceeds the value calculated based on the moment-curvature analysis. In these cases, the stress assigned to the steel at failure is based on the working stress method if the calculated stress is below the yield stress of the steel and the strength method if it is equal to or greater than the yield strength of the steel.

For calculations with the database, the expression in Section 8.5 of ACI 318 for normalweight concrete is used to determine the modulus of elasticity of concrete (all tests in the current database involve normalweight concrete).

$$E_c = 57,000 \sqrt{f'_c} \quad (5-1)$$

A modulus of elasticity E_s of 29,000 ksi (200,000 MPa) is used for steel bars. Concrete is treated as a material with no tensile strength and the area of the steel A_s is taken as the area of the bars assuming that they are continuous rather than spliced.

A parabolic equation (Hognestad 1951) is used for the relationship between concrete stress f_c and strain ϵ_c

$$f_c = f'_c \left[\frac{2\epsilon_c}{\epsilon_o} - \left(\frac{\epsilon_c}{\epsilon_o} \right)^2 \right] \quad (5-2)$$

where ϵ_o is the concrete strain at maximum concrete stress. The value of ϵ_o is a function of f'_c and is obtained from the experimental curves shown by Nilson (1997) for f'_c from 3000 to 12,000 psi (20.7 to 82.7 MPa); ϵ_o is nearly a linear function of f'_c for high-strength concrete ($f'_c \geq 8000$ psi [55.2 MPa]). Based on this observation, values of ϵ_o for $f'_c > 12,000$ psi (82.7 MPa) are obtained by extrapolation of the best-fit line for f'_c of 8000, 10,000, and 12,000 psi (55.2, 69.0, and 82.7 MPa). For concrete with compressive strength less than 3000 psi (20.7 MPa), the values of ϵ_o are determined using (Bashur and Darwin 1976, 1978).

$$\epsilon_o = \frac{f'_c}{363,000 + 400f'_c} \quad (5-3)$$

For values of f'_c greater than 3000 psi (20.7 MPa), the values of ϵ_o are given in Table 5.1. Intermediate values are obtained by interpolation.

Representative stress-strain curves for reinforcing steel (Nilson, Darwin, and Dolan 2004) are used to establish the stress-strain curves for moment curvature calculations. The steel strain at the initiation of strain hardening ϵ_{sh} is equal to 0.0086 for Grade 60 (414 MPa) steel and 0.0035 for Grade 75 (517 MPa) and above. The value of ϵ_{sh} varies linearly between the two grades. There is no yield plateau in the stress-strain curve for $f_y \geq 101.5$ ksi (700 MPa). The modulus of elasticity for strain hardening E_h is 614 ksi (4244 MPa), ($0.021 E_s$) for $f_y = 60$ ksi (414 MPa), 713 ksi (4916 MPa) ($0.025 E_s$) for $f_y = 75$ ksi (517 MPa), and 1212 ksi (8357 MPa) ($0.042 E_s$) for $f_y \geq 90$ ksi (620 MPa). The values of E_h for f_y between 60 and 75 ksi (412 and 517 MPa) and between 75 and 90 ksi (517 and 620 MPa) are obtained using linear interpolation. The idealized stress-strain curves used are shown in Fig. 5.1.

5.2—Database

At this writing, the ACI Committee 408 database includes the results of 635 development and splice tests of uncoated reinforcing bars. The data are currently limited to normal-weight concrete specimens for which compressive strength was obtained using cylinders that were tested in accordance with ASTM C 39. Tests for which compressive strength was measured solely on the basis of cubes are not included because of the highly variable relationship between cube and cylinder strength. Tests in the database are categorized based on bar placement, with individual databases maintained for bottom-cast (478 tests), top-cast (111 tests), and side-cast bars (46 tests).

The database is maintained by Subcommittee D of ACI Committee 408 and available in Microsoft® Excel™ from ACI headquarters or Committee 408. The reference list for the database is maintained in Microsoft® Word™.

Because the database is actively maintained and updated regularly, the database used for comparisons should be identified based on the month and year. Database 10-2001 was used in the analyses described in Chapters 3 and 4. The studies used to establish Database 10-2001 are listed in

Table 5.1—Values of concrete strain at maximum concrete stress ϵ_o for values of compressive strength $f'_c \geq 3000$ psi (20.7 MPa)

f'_c		ϵ_o
psi	MPa	$\mu\epsilon$
3000	20.7	1919
4000	27.8	2065
5000	34.5	2200
6000	41.4	2330
7000	48.3	2440
8000	55.2	2550
9000	62.1	2650
10,000	69.0	2750
11,000	75.9	2850
12,000	82.8	2950
13,000	89.7	3050
14,000	96.6	3015
15,000	103.4	3025
16,000	110.3	3035

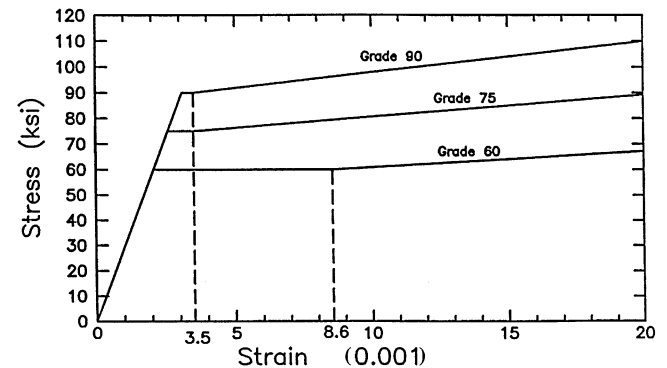


Fig. 5.1—Idealized stress-strain curves for reinforcing bars used to determine stress in development and splice tests (Zuo and Darwin 1998). (Note: 1 psi = 0.00689 MPa)

Table 5.2. As the database is upgraded, earlier versions of the database are maintained.

CHAPTER 6—TEST PROTOCOL

A single test procedure has not been established for determining the bond strength between reinforcing steel and concrete. As discussed in Section 1.2, however, a limited number of test specimen types are used in most studies. To be of the greatest use in understanding the bond behavior of reinforced concrete members, the results of the tests should be reported with at least a minimum level of detail. This chapter presents recommended testing and reporting criteria to allow for the equitable comparison and clear exchange of bond test data.

6.1—Reported properties of reinforcement

The properties of the reinforcing steel are required for basic identification and, in most cases, are needed to fully characterize the steel used in the tests. The following information should be provided for each heat or production run of reinforcing steel: the standard (ASTM, DIN, ISO, and so on) under which the bars were manufactured, the nominal diameter,

Table 5.2—References in Database 10-2001 for development and splice tests of reinforcing bars in tension*

Azizinamini et al. (1993)
Azizinamini, Chisala, and Ghosh (1995)
Azizinamini et al. (1999)
Chinn, Ferguson, and Thompson (1955)
Chamberlin (1956)
Chamberlin (1958)
Choi et al. (1990)
Choi et al. (1991)
Darwin et al. (1996a)
DeVries, Moehle, and Hester (1991)
Ferguson and Breen (1965)
Ferguson and Briceno (1969)
Ferguson and Krishnaswamy (1971)
Ferguson and Thompson (1962)
Ferguson and Thompson (1965)
Hamad and Jirsa (1990)
Hamad and Itani (1998)
Hasan, Cleary, and Ramirez (1996)
Hester et al. (1991)
Hester et al. (1993)
Kadoriku (1994)
Mathey and Watstein (1961)
Rezansoff, Konkankar, and Fu (1991)
Rezansoff, Akanni, and Sparling (1993)
Thompson et al. (1975)
Treece and Jirsa (1989)
Zekany, Neumann, Jirsa, and Breen (1981)
Zuo and Darwin (1998)
Zuo and Darwin (2000)

*Bars cast in normalweight concrete. Compressive strength based on cylinders. Includes bottom-, side-, and top-cast bars.

bar designation, yield strength, tensile strength, proof strength (if applicable), elongation at failure, Poisson's ratio (if nonferrous), weight (mass) per unit length, rib spacing and rib height (according to the standard under which the bar was manufactured as well as the average value), relative rib area (refer to [Section 6.6](#)), rib angle *b* (the included angle between the rib and the bar axis), rib-face angle *a*, and type of coating and coating thickness (if applicable).

6.2—Concrete properties

The properties of concrete play a critical role in the bond between reinforcement and concrete. Therefore, certain key properties must be known to properly characterize or model the concrete. The following information should be provided: the source of the concrete, the mixture proportions (including identification of the components: cement type, mineral admixtures, chemical admixtures, fine and coarse aggregates, and their properties, such as specific gravity (saturated surface dry) and absorption of aggregates, specific gravity and percent solids of chemical admixtures), the concrete compressive strength as obtained from a standard concrete cylinder (cylinder should be cured side-by-side with and in the same manner as the bond test specimens), the

size of the compressive strength specimens, the type and thickness of the cylinder caps, if used, and the age of testing. In addition, if possible, the flexural strength and fracture energy of the concrete should be recorded along with the specimen and test method used to establish each of these properties.

6.3—Specimen properties

A description of the test specimen should include: exterior dimensions, location of reinforcement (including the effective depth), the bottom or top cover, the side cover, the clear spacing between bars, the length of the specimen, the length of the developed or spliced bars, the number of developed or spliced bars, the quantity and nature of the transverse reinforcement used in the region of the developed or spliced bars, the average spacing of transverse reinforcement, the yield and tensile strengths of the transverse reinforcement, and the load (tensile or bending) on the specimen at the time of failure, including the specimen self-weight and the weight of the test system.

Specimen dimensions should be measured after casting. Cover and bar spacing should be measured before casting. If possible, cover should also be measured after casting, testing, or both. The most reliable values for cover and bar spacing should be reported.

6.4—Details of test

Based on what was considered to be the current understanding of bond behavior, investigators have often left out important aspects of the test in their description of the research. As the degree of understanding improves or changes with time, more details are often needed to fully understand earlier test results. With this in mind, the following information should be recorded for each test: a description of the test system; the weight of the loading system; the rate of loading, the time of test, or both; the presence or absence of strain gages on the developed or spliced reinforcing bars, the full load-deflection curves for the tests, and details of system calibration (calibration should be referenced to an accepted standard).

6.5—Analysis method

Results should be presented in terms of the average bar force at the time of failure. For flexural specimens, the calculated bar force should be determined based on moment-curvature calculations, such as described in [Section 5.1](#), using the nominal area of the continuous steel.

Realistic stress-strain curves for the concrete and reinforcing steel should be used in the moment-curvature calculation. The relations used should be reported. For cases in which the analysis indicates that bond failure occurred at a load that exceeds the flexural capacity of the member, average bar force should be determined using a stress block (strength) approach based on the net area of the reinforcement and the strength of the concrete (this will provide a value for the bar force at failure). The basis for the calculations should be included in the report.

6.6—Relative rib area

The relative rib area R_r is the ratio of the projected rib area normal to the bar axis to the product of the nominal bar perimeter and the average center-to-center rib spacing (refer also to Fig. 1.3, Section 2.2.2, and Eq. (2-6)).

Following the procedure described in ACI 408.3, R_r may be calculated as

$$R_r = \frac{h_r}{s_r} \left(1 - \frac{\Sigma \text{gaps}}{p} \right) \quad (6-1)$$

where h_r = average height of deformations (measured according to Section 6.6.1); s_r = average spacing of deformations; Σgaps = sum of the gaps between ends of transverse deformations, plus the width of any continuous longitudinal lines used to represent the grade of the bar multiplied by the ratio of the height of the line to h_r ; and p = nominal perimeter of bar. When transverse deformations tie into longitudinal ribs, the gap may be measured across the longitudinal rib at the midheight of the transverse deformation.

In European standards, R_r is calculated (for non-twisted bars) as

$$R_r = \frac{\Sigma A_r \sin \beta}{s_r p} \quad (6-2)$$

where ΣA_r = total area of ribs around bar perimeter measured on the longitudinal section of *each rib* using the trapezoidal method for approximating the area under a curve, and β = angle between transverse rib and longitudinal axis of the bar.

Methods that are more accurate than Eq. (6-1) or (6-2) may also be used (Tholen and Darwin 1996).

6.6.1 Measuring deformation height—The average height of deformations or ribs, h_r , should be based on measurements made on not less than two typical deformations on each side of the test bar. Determinations should be based on five measurements per deformation, one at the center of the overall length, two at the ends of the overall length, and two located halfway between the center and the ends. The measurements at the ends of the overall length are averaged to obtain a single value, and that value is combined with the other three measurements to obtain the average rib height h_r . Deformation measurements should be made using a depth gage with a knife-edge support that spans not more than two adjacent ribs. A knife edge is required to allow measurements to be made at the ends of the overall length of deformations, usually adjacent to a longitudinal rib. The calculation of h_r is based on a knife edge that spans only two ribs because measurements made with a longer knife edge result in higher average rib heights and, thus, an overestimate of the relative rib area of some bars.

CHAPTER 7—REFERENCES

7.1—Referenced standards and reports

The standards and reports listed below were the latest editions at the time this document was prepared. Because these documents are revised frequently, the reader is advised

to contact the proper sponsoring group if it is desired to refer to the latest version.

AASHTO

Standard Specifications for Highway Bridges

American Concrete Institute

309R	Guide for Consolidation of Concrete
318	Building Code Requirements for Structural Concrete
408.3	Splice and Development Length of High Relative Rib Area Reinforcing Bars in Tension
544.1R	State-of-the-Art Report on Fiber Reinforced Concrete

ASTM International

A 615/A 615M	Standard Specification for Deformed and Plain Billet-Steel Bars for Concrete Reinforcement
A 706/A 706M	Standard Specification for Low-Alloy Steel Deformed and Plain Bars for Concrete Reinforcement
A 767/A 767M	Standard Specification for Zinc-Coated (Galvanized) Steel Bars for Concrete Reinforcement
A 775	Standard Specification for Epoxy-Coated Steel Reinforcing Bar
A 934	Standard Specification for Epoxy-Coated Prefabricated Steel Reinforcing Bars
A 944	Standard Test Method for Comparing Bond Strength of Steel Reinforcing Bars to Concrete Using Beam-End Specimens
A 955/A 955M	Standard Specification for Deformed and Plain Stainless Steel Bars for Concrete Reinforcement
A 996/A 996M	Standard Specification for Rail-Steel and Axle-Steel Deformed Bars for Concrete Reinforcement
C 39	Standard Test Method for Compressive Strength of Cylindrical Concrete Specimens

These publications may be obtained from these organizations:

American Association of State Highway and
Transportation Officials
P.O. Box 96716
Washington, DC 20090

American Concrete Institute
P.O. Box 9094
Farmington Hills, MI 48333-9094

ASTM International
100 Barr Harbor Dr.
West Conshohocken, PA 19428

7.2—Cited references

- Abrams, D. A., 1913, "Tests of Bond between Concrete and Steel," *Bulletin* No. 71, Engineering Experiment Station, University of Illinois, Urbana, Ill., 105 pp.
- ACI Committee 318, 1947, "Building Code Requirements for Reinforced Concrete (ACI 318-47)," American Concrete Institute, Farmington Hills, Mich., 64 pp.
- ACI Committee 318, 1951, "Building Code Requirements for Reinforced Concrete (ACI 318-51)," American Concrete Institute, Farmington Hills, Mich., 63 pp.
- ACI Committee 318, 1963, "Building Code Requirements for Reinforced Concrete (ACI 318-63)," American Concrete Institute, Farmington Hills, Mich., 144 pp.
- ACI Committee 318, 1971, "Building Code Requirements for Reinforced Concrete (ACI 318-71)," American Concrete Institute, Farmington Hills, Mich., 78 pp.
- ACI Committee 318, 1995, "Building Code Requirements for Reinforced Concrete (ACI 318-95) and Commentary (318R-95)," American Concrete Institute, Farmington Hills, Mich., 369 pp.
- ACI Committee 318, 1999, "Building Code Requirements for Structural Concrete (318-99) and Commentary (318R-99)," American Concrete Institute, Farmington Hills, Mich., 391 pp.
- ACI Committee 408, 1966, "Bond Stress—The State of the Art," *ACI JOURNAL, Proceedings* V. 63, No. 11, Nov., pp. 1161-1188.
- ACI Committee 408, 1970, "Opportunities in Bond Research," *ACI JOURNAL, Proceedings* V. 67, No. 11, Nov., pp. 857-867.
- ACI Committee 408, 1979, "Suggested Development, Splice, and Standard Hook Provisions for Deformed Bars in Tension (ACI 408.1R-79)," *Concrete International*, V. 1, No. 7, July, pp. 44-46.
- ACI Committee 408, 1992, "State-of-the-Art Report: Bond under Cyclic Loads (ACI 408.2R-92 (Reapproved 1999))," American Concrete Institute, Farmington Hills, Mich., 32 pp.
- ACI Committee 544, 1999, "Fiber Reinforced Concrete (ACI 544.1R-96)," American Concrete Institute, Farmington Hills, Mich., 66 pp.
- ACI Innovation Task Group 2, 1998, "Splice and Development Length of High Relative Rib Area Reinforcing Bars in Tension (ACI ITG-2-98)," American Concrete Institute, Farmington Hills, Mich., 5 pp.
- Ahmad, S. H., and Shah, S. P., 1985, "Standard Properties of High Strength Concrete and Its Implications for Precast Prestressed Concrete," *PCI Journal*, V. 30, No. 6, Nov.-Dec., pp. 92-119.
- Altowaiji, W. A. K.; Darwin, D.; and Donahey, R. C., 1984, "Preliminary Study of the Effect of Revibration on Concrete-Steel Bond Strength," *SL Report* No. 84-2, University of Kansas Center for Research, Lawrence, Kans., Nov., 29 pp.
- Altowaiji, W. A. K.; Darwin, D.; and Donahey, R. C., 1986, "Bond of Reinforcement to Revibrated Concrete," *ACI JOURNAL, Proceedings* V. 83, No. 6, Nov.-Dec., pp. 1035-1042.
- ASTM A 305T, 1947, "Tentative Specifications for Minimum Requirements for Deformations of Deformed Steel Bars for Concrete Reinforcement, A 305-47T," ASTM International, West Conshohocken, Pa.
- ASTM A 305, 1949, "Specifications for Minimum Requirements for Deformations of Deformed Steel Bars for Concrete Reinforcement, A 305-49," ASTM International, West Conshohocken, Pa.
- ASTM C 234-91a, 1991, "Standard Test Method for Comparing Concretes on the Basis of the Bond Developed with Reinforcing Steel, C 234-91a," ASTM International, West Conshohocken, Pa., withdrawn Feb. 2000.
- Aziznamini, A.; Chisala, M.; and Ghosh, S. K., 1995, "Tension Development Length of Reinforcing Bars Embedded in High-Strength Concrete," *Engineering Structures*, V. 17, No. 7, pp. 512-522.
- Aziznamini, A.; Pavel, R.; Hatfield, E.; and Ghosh, S. K., 1999, "Behavior of Spliced Reinforcing Bars Embedded in High Strength Concrete," *ACI Structural Journal*, V. 96, No. 5, Sept.-Oct., pp. 826-835.
- Aziznamini, A.; Stark, M.; Roller, J. J.; and Ghosh, S. K., 1993, "Bond Performance of Reinforcing Bars Embedded in High-Strength Concrete," *ACI Structural Journal*, V. 90, No. 5, Sept.-Oct., pp. 554-561.
- Baldwin, J. W., 1965, "Bond of Reinforcement in Lightweight Aggregate Concrete," *Preliminary Report*, University of Missouri, Mar., 10 pp.
- Barham, S., and Darwin, D., 1999, "Effects of Aggregate Type, Water-to-Cementitious Material Ratio, and Age on Mechanical and Fracture Properties of Concrete," *SM Report* No. 56, University of Kansas Center for Research, Lawrence, Kans., 95 pp.
- Bashur, F. K., and Darwin, D., 1976, "Nonlinear Model for Reinforced Concrete Slabs," *CRINC Report* SL-76-03, University of Kansas Center for Research, Lawrence, Kans., Dec., 128 pp.
- Bashur, F. K., and Darwin, D., 1978, "Nonlinear Model for Reinforced Concrete Slabs," *Journal of the Structural Division*, ASCE, V. 104, No. ST1, Jan., pp. 157-170.
- Berge, O., 1981, "Reinforced Structures in Lightweight Aggregate Concrete," *Publication* 81.3, Chalmers University of Technology, Goteborg.
- Brettmann, B. B.; Darwin, D.; and Donahey, R. C., 1984, "Effect of Superplasticizers on Concrete-Steel Bond Strength," *SL Report* No. 84-1, University of Kansas Center for Research, Lawrence, Kans., Apr., 32 pp.
- Brettmann, B. B.; Darwin, D.; and Donahey, R. C., 1986, "Bond of Reinforcement to Superplasticized Concrete," *ACI JOURNAL, Proceedings* V. 83, No. 1, Jan.-Feb., pp. 98-107.
- Brown, C. J.; Darwin, D.; and McCabe, S. L., 1993, "Finite Element Fracture Analysis of Steel-Concrete Bond," *SM Report* No. 36, University of Kansas Center for Research, Lawrence, Kans., Nov., 100 pp.
- Cairns, J., and Abdullah, R., 1994, "Fundamental Tests on the Effect of an Epoxy Coating on Bond Strength," *ACI Materials Journal*, V. 91, No. 4, July-Aug., pp. 331-338.
- Cairns, J., and Jones, K., 1995, "Influence of Rib Geometry on Strength of Lapped Joints: An Experimental and Analytical Study," *Magazine of Concrete Research*, V. 47, No. 172, Sept., pp. 253-262.

CEB-FIP, 1990, "Model Code for Concrete Structures," Comité Euro-International du Béton, c/o Thomas Telford, London.

CEB-FIP, 1999, "Lightweight Aggregate Concrete, Codes and Standards," State-of-Art Report prepared by Task Group 8.1, Fédération Internationale du Béton, Lausanne, Switzerland.

Chamberlin, S. J., 1952, "Spacing of Spliced Bars in Tension Pull-Out Specimens," *ACI JOURNAL, Proceedings* V. 49, No. 3, Nov., pp. 261-274.

Chamberlin, S. J., 1956, "Spacing of Reinforcement in Beams," *ACI JOURNAL, Proceedings* V. 53, No. 1, July, pp. 113-134.

Chamberlin, S. J., 1958, "Spacing of Spliced Bars in Beams," *ACI JOURNAL, Proceedings* V. 54, No. 8, Feb., pp. 689-698.

Chana, P. S., 1990, "A Test Method To Establish Realistic Bond Stresses," *Magazine of Concrete Research*, V. 42, No. 151, pp. 83-90.

Chinn, J.; Ferguson, P. M.; and Thompson, J. N., 1955, "Lapped Splices in Reinforced Concrete Beams," *ACI JOURNAL, Proceedings* V. 52, No. 2, Oct., pp. 201-213.

Choi, O. C.; Hadje-Ghaffari, H.; Darwin, D.; and McCabe, S. L., 1990, "Bond of Epoxy-Coated Reinforcement to Concrete: Bar Parameters," *SM Report* No. 25, University of Kansas Center for Research, Lawrence, Kans., July, 217 pp.

Choi, O. C.; Hadje-Ghaffari, H.; Darwin, D.; and McCabe, S. L., 1991, "Bond of Epoxy-Coated Reinforcement: Bar Parameters," *ACI Materials Journal*, V. 88, No. 2, Mar.-Apr., pp. 207-217.

Clark, A. P., 1946, "Comparative Bond Efficiency of Deformed Concrete Reinforcing Bars," *ACI JOURNAL, Proceedings* V. 43, No. 4, Dec., pp. 381-400.

Clark, A. P., 1950, "Bond of Concrete Reinforcing Bars," *ACI JOURNAL, Proceedings* V. 46, No. 3, Nov., pp. 161-184.

Clarke, J. L., and Birjandi, F. K., 1993, "Bond Strength Tests For Ribbed Bars in Lightweight Aggregate Concrete," *Magazine of Concrete Research*, V. 45, No. 163, pp. 79-87.

Cleary, D. B., and Ramirez, J. A., 1993, "Epoxy-Coated Reinforcement under Repeated Loading," *ACI Structural Journal*, V. 90, No. 4, July-Aug., pp. 451-458.

Collier, S. T., 1947, "Bond Characteristics of Commercial and Prepared Reinforcing Bars," *ACI JOURNAL, Proceedings* V. 43, No. 10, June, pp. 1125-1133.

CSA Standard A23.3-94, 1994, "Design of Concrete Structures," Canadian Standards Association, Ontario, Canada.

CUR, 1963, Commissie voor Uitvoering van Research Ingesteld door de Betonvereniging, "Onderzoek naar de samenwerking van geprofileerd staal met beton," *Report* No. 23, The Netherlands (Translation No. 112, 1964, Cement and Concrete Association, London, "An Investigation of the Bond of Deformed Steel Bars with Concrete"), 28 pp.

Dakhil, F. H.; Cady, P. D.; and Carrier, R. E., 1975, "Cracking of Fresh Concrete as Related to Reinforcement," *ACI JOURNAL, Proceedings* V. 72, No. 8, Aug., pp. 421-428.

Darwin, D., 1987, "Effects of Construction Practice on Concrete-Steel Bond," *Lewis H. Tuthill International*

Symposium on Concrete and Concrete Construction, SP-104, G. T. Halvorsen, ed., American Concrete Institute, Farmington Hills, Mich., pp. 27-56.

Darwin, D.; Barham, S.; Kozul, R.; and Luan, S., 2001, "Fracture Energy of High-Strength Concrete," *ACI Materials Journal*, V. 98, No. 5, Sept.-Oct., pp. 410-417.

Darwin, D., and Graham, E. K., 1993a, "Effect of Deformation Height and Spacing on Bond Strength of Reinforcing Bars," *ACI Structural Journal*, V. 90, No. 6, Nov.-Dec., pp. 646-657.

Darwin, D., and Graham, E. K., 1993b, "Effect of Deformation Height and Spacing on Bond Strength of Reinforcing Bars," *SL Report* 93-1, University of Kansas Center for Research, Lawrence, Kans., Jan., 68 pp.

Darwin, D.; Idun, E. K.; Zuo, J.; and Tholen, M. L., 1998, "Reliability-Based Strength Reduction Factor for Bond," *ACI Structural Journal*, V. 95, No. 4, July-Aug., pp. 434-443.

Darwin, D.; McCabe, S. L.; Brown, C. J.; and Tholen, M. L., 1994, "Fracture Analysis of Steel-Concrete Bond," *Fracture and Damage in Quasibrittle Structures: Experiment, Modelling, and Computer Analysis*, Z. P. Bazant, Z. Bittnar, M. Jirasek, and J. Mazars, eds., E&FN Spon, London, pp. 549-556.

Darwin, D.; McCabe, S. L.; Idun, E. K.; and Schoenekase, S. P., 1992, "Development Length Criteria: Bars Not Confined by Transverse Reinforcement," *ACI Structural Journal*, V. 89, No. 6, Nov.-Dec., pp. 709-720.

Darwin, D.; Tholen, M. L.; Idun, E. K.; and Zuo, J., 1996a, "Splice Strength of High Relative Rib Area Reinforcing Bars," *ACI Structural Journal*, V. 93, No. 1, Jan.-Feb., pp. 95-107.

Darwin, D.; Zuo, J.; Tholen, M. L.; and Idun, E. K., 1996b, "Development Length Criteria for Conventional and High Relative Rib Area Reinforcing Bars," *ACI Structural Journal*, V. 93, No. 3, May-June, pp. 347-359.

Darwin, D., and Zuo, J., 2002, Discussion of proposed changes to ACI 318 in "ACI 318-02 Discussion and Closure," *Concrete International*, V. 24, No. 1, Jan., pp. 91, 93, 97-101.

Davies, R., Jr., 1981, "Bond Strength of Mild Steel in Polypropylene Fiber Reinforced Concrete (PFRC)," master's thesis, Marquette University, Milwaukee, Wis., Aug.

Davis, R. E.; Brown, E. H.; and Kelly, J. W., 1938, "Some Factors Influencing the Bond Between Concrete and Reinforcing Steel," *Proceedings of the Forty-First Annual Meeting of the American Society for Testing and Materials*, V. 38, Part II, Philadelphia, Pa., pp. 394-406.

DeVries, R. A.; Moehle, J. P.; and Hester, W., 1991, "Lap Splice of Plain and Epoxy-Coated Reinforcements: An Experimental Study Considering Concrete Strength, Casting Position, and Anti-Bleeding Additives," *Report* No. UCB/SEMM-91/02 Structural Engineering Mechanics and Materials, University of California, Berkeley, Calif., Jan., 86 pp.

DIN 488, 1984, 1986, *Reinforcing Steel*, Parts 1-7, Deutsches Institut für Normung, Berlin.

Donahey, R. C., and Darwin, D., 1983, "Effects of Construction Procedures on Bond in Bridge Decks," *SM Report* No. 7, University of Kansas Center for Research, Lawrence, Kans., Jan., 125 pp.

Donahey, R. C., and Darwin, D., 1985, "Bond of Top-Cast Bars in Bridge Decks," *ACI JOURNAL, Proceedings* V. 82, No. 1, Jan.-Feb., pp. 57-66.

Eligehausen, R., 1979, "Bond in Tensile Lapped Splices of Ribbed Bars with Straight Anchorages," *Publication* 301, German Institute for Reinforced Concrete, Berlin, 118 pp. (in German)

Eligehausen, R.; Popov, E. P.; and Bertero, V. V., 1983, "Local Bond Stress-Slip Relationships of Deformed Bars under Generalized Excitations," *Report* No. UCB/EERC-82/23, Earthquake Engineering Research Center, University of California at Berkeley, Calif., 169 pp.

Ellingwood, B.; Galambos, T. V.; MacGregor, J. G.; and Cornell, C. A., 1980, "Development of a Probability Based Criterion for American National Standard A58," *NBS Special Publication* 577, U.S. Dept. of Commerce, Washington, D.C., June, 222 pp.

Esfahani, M. R., and Vijaya Rangan, B., 1996, "Studies on Bond between Concrete and Reinforcing Bars," School of Civil Engineering, Curtin University of Technology, Perth, Western Australia, 315 pp.

Esfahani, M. R., and Vijaya Rangan, B. V., 1998a, "Local Bond Strength of Reinforcing Bars in Normal Strength and High-Strength Concrete (HSC)," *ACI Structural Journal*, V. 95, No. 2, Mar.-Apr., pp. 96-106.

Esfahani, M. R., and Vijaya Rangan, B. V., 1998b, "Bond between Normal Strength and High-Strength Concrete (HSC) and Reinforcing Bars in Splices in Beams," *ACI Structural Journal*, V. 95, No. 3, May-June, pp. 272-280.

Ezeldin, A. S., and Balaguru, P. N., 1989, "Bond Behavior of Normal and High-Strength Fiber Concrete," *ACI Materials Journal*, V. 86, No. 5, Sept.-Oct., pp. 515-524.

Ferguson, P. M., 1977, "Small Bar Spacing or Cover—A Bond Problem for the Designer," *ACI JOURNAL, Proceedings* V. 74, No. 9, Sept., pp. 435-439.

Ferguson, P. M., and Breen, J. E., 1965, "Lapped Splices for High-Strength Reinforcing Bars," *ACI JOURNAL, Proceedings* V. 62, No. 9, Sept., pp. 1063-1078.

Ferguson, P. M., and Briceno, A., 1969, "Tensile Lap Splices—Part 1: Retaining Wall Type, Varying Moment Zone," *Research Report* No. 113-2, Center for Highway Research, The University of Texas at Austin, July.

Ferguson, P. M., and Krishnaswamy, C. N., 1971, "Tensile Lap Splices—Part 2: Design Recommendation for Retaining Wall Splices and Large Bar Splices," *Research Report* No. 113-2, Center for Highway Research, The University of Texas at Austin, Tex., Apr., 60 pp.

Ferguson, P. M., and Thompson, J. N., 1962, "Development Length for Large High Strength Reinforcing Bars in Bond," *ACI JOURNAL, Proceedings* V. 59, No. 7, July, pp. 887-922.

Ferguson, P. M., and Thompson, J. N., 1965, "Development Length for Large High Strength Reinforcing Bars," *ACI JOURNAL, Proceedings* V. 62, No. 1, Jan., pp. 71-94.

Furr, H. L., and Fouad, F. H., 1981, "Bridge Slab Concrete Placed Adjacent to Moving Live Load," *Research Report* No. 226-IF, Texas Dept. of Highways and Public Transportation, Jan., pp. 131.

Gjorv, O. E.; Monteiro, P. J. M.; and Mehta, P. K., 1990, "Effect of Condensed Silica Fume on the Steel-Concrete Bond," *ACI Materials Journal*, V. 87, No. 6, Nov.-Dec., pp. 573-580.

Goto, Y., 1971, "Cracks Formed in Concrete Around Deformed Tension Bars," *ACI JOURNAL, Proceedings* V. 68, No. 4, Apr., pp. 244-251.

Hadje-Ghaffari, H.; Darwin, D.; and McCabe, S. L., 1991, "Effects of Epoxy-Coating on the Bond of Reinforcing Steel to Concrete," *SM Report* No. 28, University of Kansas Center for Research, Inc., Lawrence, Kans., July, 288 pp.

Hadje-Ghaffari, H.; Choi, O. C.; Darwin, D.; and McCabe, S. L., 1992, "Bond of Epoxy-Coated Reinforcement to Concrete: Cover, Casting Position, Slump, and Consolidation," *SL Report* 92-3, University of Kansas Center for Research, Inc., Lawrence, Kans., June, 42 pp.

Hadje-Ghaffari, H.; Choi, O. C.; Darwin, D.; and McCabe, S. L., 1994, "Bond of Epoxy-Coated Reinforcement: Cover, Casting Position, Slump, and Consolidation," *ACI Structural Journal*, V. 91, No. 1, Jan.-Feb., pp. 59-68.

Hamad, B. S., and Itani, M. S., 1998, "Bond Strength of Reinforcement in High-Performance Concrete: The Role of Silica Fume, Casing Position, and Superplasticizer Dosage," *ACI Materials Journal*, V. 95, No. 5, Sept.-Oct., pp. 499-511.

Hamad, B. S., and Jirsa, J. O., 1990, "Influence of Epoxy Coating on Stress Transfer from Steel to Concrete," *Proceedings*, First Materials Engineering Congress, ASCE, New York, V. 2, pp. 125-134.

Hamad, B. S., and Jirsa, J. O., 1993, "Strength of Epoxy-Coated Reinforcing Bar Splices Confined with Transverse Reinforcement," *ACI Structural Journal*, V. 90, No. 1, Jan.-Feb., pp. 77-88.

Hamad, B. S., and Mansour, M. Y., 1996, "Bond Strength of Noncontact Tension Lap Splices," *ACI Structural Journal*, V. 93, No. 3, May-June, pp. 316-326.

Hamza, A. M., and Naaman, A. E., 1996, "Bond Characteristics of Deformed Reinforcing Steel Bars Embedded in SIFCON," *ACI Materials Journal*, V. 93, No. 6, Nov.-Dec., pp. 578-588.

Harajli, M. H.; Hout, M.; and Jalkh, W., 1995, "Local Bond Stress-Slip Behavior of Reinforcing Bars Embedded in Plain and Fiber Concrete," *ACI Materials Journal*, V. 92, No. 4, July-Aug., pp. 343-354.

Harajli, M. H., and Salloukh, K. A., 1997, "Effect of Fibers on Development/Splice Strength of Reinforcing Bars in Tension," *ACI Materials Journal*, V. 94, No. 4, July-Aug., pp. 317-324.

Harsh, S., and Darwin, D., 1984, "Effects of Traffic-Induced Vibrations on Bridge Deck Repairs," *SM Report* No. 9, University of Kansas Center for Research, Lawrence, Kans., Jan., 60 pp.

Harsh, S., and Darwin, D., 1986, "Traffic-Induced Vibrations and Bridge Deck Repairs," *Concrete International*, V. 8, No. 5, May, pp. 36-42.

Hasan, H. O.; Cleary, D. B.; and Ramirez, J. A., 1996, "Performance of Concrete Bridge Decks and Slabs Reinforced with Epoxy-Coated Steel under Repeated Loading," *ACI Structural Journal*, V. 93, No. 4, July-Aug., pp. 397-403.

- Hester, C. J.; Salamizavaregh, S.; Darwin, D.; and McCabe, S. L., 1991, "Bond of Epoxy-Coated Reinforcement to Concrete: Splices," *SL Report* 91- 1, University of Kansas Center for Research, Lawrence, Kans., May, 66 pp.
- Hester, C. J.; Salamizavaregh, S.; Darwin, D.; and McCabe, S. L., 1993, "Bond of Epoxy-Coated Reinforcement: Splices," *ACI Structural Journal*, V. 90, No. 1, Jan.-Feb., pp. 89-102.
- Hognestad, E., 1951, "A Study of Combined Bending and Axial Load in Reinforced Concrete Members," *Bulletin Series* No. 399, University of Illinois Engineering Experiment Station, Urbana, Ill.
- Hota, S., and Naaman, A. E., 1997, "Bond Stress-Slip Response of Reinforcing Bars Embedded in FRC Matrices Under Monotonic and Cyclic Loading," *ACI Structural Journal*, V. 94, No. 5, Sept.-Oct., pp. 525-537.
- Hulshizer, A. J., and Desai, A. J., 1984, "Shock Vibration Effects on Freshly Placed Concrete," *Journal of Construction Engineering and Management*, V. 110, No. 2, June, pp. 266-285.
- Hwang, S.-J.; Lee, Y.-Y.; and Lee, C.-S., 1994, Effect of Silica Fume on the Splice Strength of Deformed Bars of High-Performance Concrete," *ACI Structural Journal*, V. 91, No. 3, May-June, pp. 294-302.
- Hyatt, T., 1877, *An Account of Some Experiments with Portland-Cement-Concrete Combined with Iron, as a Building Material*, Chiswick Press, London, 47 pp.
- Idun, E. K., and Darwin, D., 1999, "Bond of Epoxy-Coated Reinforcement: Coefficient of Friction and Rib Face Angle," *ACI Structural Journal*, V. 96, No. 4, July-Aug., pp. 609-615.
- Jeanty, P. R.; Mitchell, D.; and Mirza, M. S., 1988, "Investigation of 'Top Bar' Effects in Beams," *ACI Structural Journal*, V. 85, No. 3., May-June, pp. 251-257.
- Jirsa, J. O., and Breen, J. E., 1981, "Influence of Casting Position and Shear on Development and Splice Length—Design Recommendation," *Research Report* No. 242-3F, Center for Transportation Research, The University of Texas at Austin, Tex.
- Johnston, D. W., and Zia, P., 1982, "Bond Characteristics of Epoxy Coated Reinforcing Bars," *Report* No. FHWA-NC-82-002, Federal Highway Administration, Washington, D.C., 163 pp.
- Kadoriku, J., 1994, "Study on Behavior of Lap Splices in High-Strength Reinforced Concrete Members," doctorate thesis, Kobe University, Mar., Japan, 201 pp.
- Kemp, E. L.; Brezny, F. S.; and Unterspan, J. A., 1968, "Effect of Rust and Scale on the Bond Characteristics of Deformed Reinforcing Bars," *ACI JOURNAL, Proceedings* V. 65, No. 9, Sept., pp. 743-756.
- Kozul, R., and Darwin, D., 1997, "Effects of Aggregate Type, Size, and Content on Concrete Strength and Fracture Energy," *SM Report* No. 43, University of Kansas Center for Research, Inc., Lawrence, Kans.
- Larnach, W. J., 1952, "Changes in Bond Strength Caused by Revibration of Concrete and the Vibration of Reinforcement," *Magazine of Concrete Research*, London, No. 10, July, pp. 17-21.
- Losberg, A., and Olsson, P.-A., 1979, "Bond Failure of Deformed Reinforcing Bars Based on the Longitudinal Splitting Effect of the Bars," *ACI JOURNAL, Proceedings* V. 76, No. 1, Jan., pp. 5-18.
- Luke, J. J.; Hamad, B. S.; Jirsa, J. O.; and Breen, J. E., 1981, "The Influence of Casting Position on Development and Splice Length of Reinforcing Bars," *Research Report* No. 242-1, Center for Transportation Research, Bureau of Engineering Research, University of Texas at Austin, Tex., June, 153 pp.
- Lundberg, J. E., 1993, "The Reliability of Composite Columns and Beam Columns," *Structural Engineering Report* No. 93-2, University of Minnesota, Minneapolis, Minn., June, 233 pp.
- Lutz, L. A., and Gergely, P., 1967, "Mechanics of Bond and Slip of Deformed Bars in Concrete," *ACI JOURNAL, Proceedings* V. 64, No. 11, Nov., pp. 711-721.
- Lutz, L. A.; Gergely, P.; and Winter, G., 1966, "The Mechanics of Bond and Slip of Deformed Reinforcing Bars in Concrete," *Report* No. 324, Department of Structural Engineering, Cornell University, Ithaca, N.Y., Nov., pp. 711-721.
- Lyse, I., 1934, "Lightweight Slag Concrete," *ACI JOURNAL, Proceedings* V. 31, No. 1, pp. 1-20.
- MacGregor, J. G., 1997, *Reinforced Concrete, Mechanics & Design*, Prentice Hall, 3rd Edition, Upper Saddle River, N.J., 939 pp.
- Maeda, M.; Otani, S.; and Aoyama, H., 1991, "Bond Splitting Strength in Reinforced Concrete Members," *Transactions of the Japan Concrete Institute*, V. 13, pp. 581-588.
- Martin, H., 1982, "Bond Performance of Ribbed Bars," *Bond in Concrete—Proceedings of the International Conference on Bond in Concrete*, Paisley, Applied Science Publishers, London, pp. 289-299.
- Mathey, R., and Watstein, D., 1961, "Investigation of Bond in Beam and Pull-Out Specimens with High-Yield-Strength Deformed Bars," *ACI JOURNAL, Proceedings* V. 58, No. 9, Mar., pp. 1071-1090.
- Mathey, R., and Clifton, J. R., 1976, "Bond of Coated Reinforcing Bars in Concrete," *Journal of the Structural Division*, ASCE, V. 102, No. 1, Jan., pp. 215-229.
- Menzel, C. A., 1952, "Effect of Settlement of Concrete on Results of Pullout Tests," *Research Department Bulletin* 41, Research and Development Laboratories of the Portland Cement Association, Nov., 49 pp.
- Menzel, C. A., and Woods, W. M., 1952, "An Investigation of Bond, Anchorage and Related Factors in Reinforced Concrete Beams," *Research Department Bulletin* 42, Portland Cement Association, Nov., 114 pp.
- Mirza, S. A., and MacGregor, J. G., 1986, "Strength Variability of Bond of Reinforcing Bars in Concrete Beams," *Civil Engineering Report Series* No. CE-86-1, Lakehead University, Thunder Bay, Ontario, Jan., 35 pp.
- Mor, A., 1992, "Steel-Concrete Bond in High-Strength Lightweight Concrete," *ACI Materials Journal*, V. 89, No. 1, Jan.-Feb., pp. 76-82.
- Musser, P. L.; Carrasquillo, R. L.; Jirsa, J. O.; and Klingner, R. E., 1985, "Anchorage and Development of Reinforcement in Concrete Made Using Superplasticizers,"

Research Report 383-1, Center for Transportation Research, Bureau of Engineering Research, University of Texas at Austin, Tex., Sept., 189 pp.

Nilson, A. H., 1997, *Design of Concrete Structures*, 12th Edition, with contributions by D. Darwin, McGraw-Hill, New York, 780 pp.

Nilson, A. H.; Darwin, D.; and Dolan, C. W., 2004, *Design of Concrete Structures*, 13th Edition, McGraw-Hill, New York, 779 pp.

Niwa, J., and Tangtermsirikul, 1997, "Fracture Properties of High-Strength and Self-Compacting High Performance Concretes," *Transactions of the Japan Concrete Institute*, V. 19, pp. 73-80.

Olsen, N. H., 1990a, "Strength of Lapped Splices in High-Strength Concrete," *High-Strength Concrete*, Proceedings of the Second International Symposium, SP-121, W. T. Hester, ed., American Concrete Institute, Farmington Hills, Mich., pp. 179-193.

Olsen, N. H., 1990b, "Strength of Overlapped Deformed Tensile Reinforcement Splices in High-Strength Concrete," *Report Series R*, No. 234, Department of Structural Engineering, Technical University of Denmark, 160 pp.

Orangun, C. O.; Jirsa, J. O.; and Breen, J. E., 1975, "The Strength of Anchored Bars: A Reevaluation of Test Data on Development Length and Splices," *Research Report No. 154-3F*, Center for Highway Research, The University of Texas at Austin, Tex., Jan., 78 pp.

Orangun, C. O.; Jirsa, J. O.; and Breen, J. E., 1977, "Reevaluation of Test Data on Development Length and Splices," *ACI JOURNAL, Proceedings* V. 74, No. 3, Mar., pp. 114-122.

Petersen, P. H., 1948, "Properties of Some Lightweight Aggregate Concretes with and without an Air-Entraining Admixture," *Building Materials and Structures Report BMS112*, U.S. Department of Commerce, National Bureau of Standards, Aug., 7 pp.

Rehm, G., 1961, "Über die Grundlagen des Verbundes Zwischen Stahl und Beton," *Deutscher Ausschuss für Stahlbeton*, No. 1381, 59 pp. (C & CA Library Translation No. 134, 1968, "The Basic Principle of the Bond between Steel and Concrete.")

Rehm, G., and Eligehausen R., 1979, "Bond of Ribbed Bars Under High Cycle Repeated Loads," *ACI JOURNAL, Proceedings* V. 76, No. 2, Feb., pp. 297-309.

Rezansoff, T.; Akanni, A.; and Sparling, B., 1993, "Tensile Lap Splices under Static Loading: A Review of the Proposed ACI 318 Code Provisions," *ACI Structural Journal*, V. 90, No. 4, July-Aug., pp. 374-384.

Rezansoff, T.; Konkankar, U. S.; and Fu, Y. C., 1991, "Confinement Limits for Tension Lap Splices Under Static Loading," *Report No. S7N OW0*, University of Saskatchewan, Aug.

Robin, R. C.; Olsen, P. E.; and Kinnane, R. F., 1942, "Bond Strength of Reinforcing Bars Embedded Horizontally in Concrete," *Journal of the Institute of Engineers*, London, V. 14, Sept., pp. 201-217.

Robins, P. J., and Standish, I. G., 1982, "Effect of Lateral Pressure on Bond of Reinforcing Bars in Concrete," *Bond in*

Concrete—Proceedings of the International Conference on Bond in Concrete, Paisley, Applied Science Publishers, London, pp. 262-272.

Sagan, V. E.; Gergely, P.; and White, R. N., 1991, "Behavior and Design of Noncontact Lap Splices Subjected to Repeated Inelastic Tensile Loading," *ACI Structural Journal*, V. 88, No. 4, July-Aug., pp. 420-431.

Sakurada, T.; Morohashi, N.; and Tanaka, R., 1993, "Effect of Transverse Reinforcement on Bond Splitting Strength of Lap Splices," *Transactions of the Japan Concrete Institute*, V. 15, pp. 573-580.

Shideler, J. J., 1957, "Lightweight-Aggregate Concrete for Structural Use," *ACI JOURNAL, Proceedings* V. 54, No. 4, Oct., pp. 299-328.

Skorobogatov, S. M., and Edwards, A. D., 1979, "The Influence of the Geometry of Deformed Steel Bars on Their Bond Strength in Concrete," *Proceedings*, The Institution of Civil Engineers, V. 67, Part 2, June, pp. 327-339.

Soretz, S., and Holzenbein, H., 1979, "Influence of Rib Dimensions of Reinforcing Bars on Bond and Bendability," *ACI JOURNAL, Proceedings* V. 76, No. 1, Jan., pp. 111-127.

Soroushian, P.; Mirza, F.; and Alhozaimy, A., 1994, "Bonding of Confined Steel Fiber Reinforced Concrete to Deformed Bars," *ACI Materials Journal*, V. 91, No. 2, Mar.-Apr., pp. 141-149.

Tan, C.; Darwin, D.; Tholen, M. L.; and Zuo, J., 1996, "Splice Strength of Epoxy-Coated High Relative Rib Area Bars," *SL Report 96-2*, University of Kansas Center for Research, Lawrence, Kans., May, 69 pp.

Tepfers, R., 1973, "A Theory of Bond Applied to Overlapping Tensile Reinforcement Splices for Deformed Bars," *Publication 73:2*, Division of Concrete Structures, Chalmers University of Technology, Goteborg, Sweden, 328 pp.

Tholen, M. L., and Darwin, D., 1996, "Effects of Deformation Properties on the Bond of Reinforcing Bars," *SM Report No. 42*, University of Kansas Center for Research, Inc., Lawrence, Kans.

Thompson, M. A.; Jirsa, J. O.; Breen, J. E.; and Meinheit, D. F., 1975, "The Behavior of Multiple Lap Splices in Wide Sections," *Research Report No. 154-1*, Center for Highway Research, University of Texas at Austin, Tex., Feb., 75 pp.

Treece, R. A., and Jirsa, J. O., 1989, "Bond Strength of Epoxy-Coated Reinforcing Bars," *ACI Materials Journal*, V. 86, No. 2, Mar.-Apr., pp. 167-174.

Tuthill, L. H., and Davis, H. E., 1938, "Overvibration and Revibration of Concrete," *ACI JOURNAL, Proceedings* V. 35, No. 4, Sept., pp. 41-47.

Tuthill, L. H., 1977, "Revibration Reexamined," *Concrete Construction*, V. 22, No. 10, Oct., pp. 537-539.

Untrauer, R. E., 1965, Discussion of "Development Length for Large High Strength Reinforcing Bars," *ACI Journal, Proceedings* V. 62, No. 9, Sept., pp. 1153-1154.

Untrauer, R. E., and Warren, G. E., 1977, "Stress Development of Tension Steel in Beams," *ACI JOURNAL, Proceedings* V. 74, No. 8, Aug., pp. 368-372.

Vollick, C. A., 1958, "Effects of Revibrating Concrete," *ACI Journal, Proceedings* V. 54, No. 9, Mar., pp. 721-732.

Wafa, F. F., and Ashour, S. A., 1992, "Mechanical Properties of High-Strength Fiber Reinforced Concrete," *ACI Materials Journal*, V. 89, No. 5, Sept.-Oct., pp. 449-455.

Walker, W. T., 1951, "Laboratory Tests of Spaced and Tied Reinforcing Bars," *ACI JOURNAL, Proceedings* V. 47, No. 5, Jan., pp. 365-372.

Welch, G. B., and Patten, B. J. F., 1965, "Bond Strength of Reinforcement Affected by Concrete Sedimentation," *ACI JOURNAL, Proceedings* V. 62, No. 2, Feb., pp. 251-263.

Zekany, A. J.; Neumann, S.; Jirsa, J. O.; and Breen, J. E., 1981, "The Influence of Shear on Lapped Splices in Reinforced Concrete," *Research Report* 242-2, Center for Transportation Research, Bureau of Engineering Research, University of Texas at Austin, Tex., July, 88 pp.

Zilveti, A.; Sooi, T. K.; Klingner, R. E.; Carrasquillo, R. L.; and Jirsa, J. O., 1985, "Effect of Superplasticizers on the Bond Behavior of Reinforcing Steel in Concrete Members," *Research Report* 383-2F, Center for Transportation Research, Bureau of Engineering Research, University of Texas at Austin, Tex., Nov., 104 pp.

Zsutty, T., 1985, "Empirical Study of Bar Development Behavior," *Journal of Structural Engineering*, ASCE, V. 111, No. 1, Jan., pp. 205-219.

Zuo, J., and Darwin, D., 1998, "Bond Strength of High Relative Rib Area Reinforcing Bars," *SM Report* No. 46, University of Kansas Center for Research, Lawrence, Kans., 350 pp.

Zuo, J., and Darwin, D., 2000, "Splice Strength of Conventional and High Relative Rib Area Bars in Normal and High-Strength Concrete," *ACI Structural Journal*, V. 97, No. 4, July-Aug., pp. 630-641.

APPENDIX A—SI EQUATIONS

The equations presented in this appendix are (primarily soft) SI conversions of equations in the report that contain terms that depend on the units of measure.

$$u = 20 \frac{\sqrt{f'_c}}{d_b} \leq 5.52 \text{ MPa} \quad (1-5)$$

$$l_d = 0.019 A_b \frac{f_y}{\sqrt{f'_c}} \quad (1-6)$$

$$t_d = 0.03 d_b + 0.22 \quad (2-5)$$

$$\frac{u_c}{\sqrt{f'_c}} = 0.101 + 0.268 \frac{c_{\min}}{d_b} + 4.4 \frac{d_b}{l_d} \quad (3-1)$$

$$\frac{u_c}{\sqrt{f'_c}} = 0.10 + 0.25 \frac{c_{\min}}{d_b} + 4.15 \frac{d_b}{l_d} \quad (3-2)$$

$$\frac{u_b}{\sqrt{f'_c}} = \frac{u_c + u_s}{\sqrt{f'_c}} = \quad (3-3)$$

$$0.10 + 0.25 \frac{c_{\min}}{d_b} + \frac{4.15 d_b}{l_d} + \frac{A_{tr} f_{yt}}{41.5 s n d_b}$$

$$\frac{T_b}{\sqrt{f'_c}} = \frac{T_c + T_s}{\sqrt{f'_c}} = \frac{A_b f_s}{\sqrt{f'_c}} = \quad (3-4)$$

$$0.25 \pi l_d (c_{\min} + 0.4 d_b) + 16.6 A_b + \frac{\pi l_d A_{tr}}{41.5 s n} f_{yt}$$

$$\frac{1}{d_b} \left(c_{\min} + 0.4 d_b + \frac{A_{tr} f_{yt}}{10.34 s n} \right) \leq 2.5 \quad (3-5)$$

$$\frac{T_c}{\sqrt{f'_c}} = \frac{A_b f_s}{\sqrt{f'_c}} = \quad (3-6)$$

$$0.554 l_d (c_{\min} + 0.5 d_b) \left(0.08 \frac{c_{\max}}{c_{\min}} + 0.92 \right) + 24.9 A_b$$

$$\frac{T_c}{f'_c{}^{1/4}} = \frac{A_b f_s}{f'_c{}^{1/4}} = \quad (3-7)$$

$$[1.5 l_d (c_{\min} + 0.5 d_b) + 51 A_b] \left(0.1 \frac{c_{\max}}{c_{\min}} + 0.90 \right)$$

$$\frac{T_b}{f'_c{}^{1/4}} = \frac{T_c + T_s}{f'_c{}^{1/4}} = \frac{A_b f_s}{f'_c{}^{1/4}} = \quad (3-8)$$

$$[1.5 l_d (c_{\min} + 0.5 d_b) + 51 A_b] \left(0.1 \frac{c_{\max}}{c_{\min}} + 0.90 \right)$$

$$+ 53.3 t_r t_d \frac{N A_{tr}}{n} + 1019$$

where $t_d = 0.028 d_b + 0.28$.

$$\frac{T_c}{f'_c{}^{1/4}} = \frac{A_b f_s}{f'_c{}^{1/4}} = \quad (3-10)$$

$$[1.43 l_d (c_{\min} + 0.5 d_b) + 56.2 A_b] \left(0.1 \frac{c_{\max}}{c_{\min}} + 0.90 \right)$$

$$\frac{T_b}{f'_c{}^{1/4}} = \frac{T_c + T_s}{f'_c{}^{1/4}} = \frac{A_b f_s}{f'_c{}^{1/4}} = \quad (3-11)$$

$$[1.43 l_d (c_{\min} + 0.5 d_b) + 56.2 A_b] \left(0.1 \frac{c_{\max}}{c_{\min}} + 0.90 \right)$$

$$+ \left(9t_d \frac{NA_{tr}}{n} + 744 \right) f_c'^{1/2}$$

where $t_d = 0.03d_b + 0.22$.

$$\frac{1}{d_b} \left[(c_{\min} + 0.5d_b) \left(0.1 \frac{c_{\max}}{c_{\min}} + 0.90 \right) \right] \quad (3-12)$$

$$+ \left(\frac{6.26t_d A_{tr}}{sn} \right) f_c'^{1/2} \leq 4.0$$

$$\frac{T_c}{\sqrt{f_c'}} = \frac{A_b f_s}{\sqrt{f_c'}} = \quad (3-13)$$

$$2.7\pi l_d \frac{(c_{\min} + 0.5d_b) \left(1 + \frac{1}{M} \right)}{\left(\frac{c_{\min}}{d_b} + 3.6 \right) (1.85 + 0.024\sqrt{M})} \left(0.12 \frac{c_{\text{med}}}{c_{\min}} + 0.88 \right)$$

$$\frac{T_c}{\sqrt{f_c'}} = \frac{A_b f_s}{\sqrt{f_c'}} = \quad (3-14)$$

$$M = \cosh(0.0022l_d \sqrt{rf_c'/d_b})$$

$$4.73\pi l_d \frac{(c_{\min} + 0.5d_b) \left(1 + \frac{1}{M} \right)}{\left(\frac{c_{\min}}{d_b} + 5.5 \right) (1.85 + 0.024\sqrt{M})} \left(0.12 \frac{c_{\text{med}}}{c_{\min}} + 0.88 \right)$$

$$\frac{T_c}{f_c'^{1/4}} = \frac{A_b f_s}{f_c'^{1/4}} = \quad (3-15)$$

$$[1.43l_d(c_{\min} + 0.5d_b) + 57.4A_b] \left(0.1 \frac{c_{\max}}{c_{\min}} + 0.90 \right)$$

$$\frac{T_b}{f_c'^{1/4}} = \frac{T_c + T_s}{f_c'^{1/4}} = \frac{A_b f_s}{f_c'^{1/4}} = \quad (3-16)$$

$$[1.43l_d(c_{\min} + 0.5d_b) + 57.4A_b] \left(0.1 \frac{c_{\max}}{c_{\min}} + 0.90 \right)$$

$$+ \left(8.9t_d \frac{NA_{tr}}{n} + 558 \right) f_c'^{1/2}$$

$$\frac{l_d}{d_b} = \frac{\frac{f_s}{\sqrt{f_c'}} - 16.6}{\left(\frac{c + K_{tr}}{d_b} \right)} \quad (4-1)$$

$$\text{where } K_{tr} = \frac{A_{tr} f_{yt}}{10.34sn}.$$

$$\frac{l_d}{d_b} = 0.9 \frac{f_y}{\sqrt{f_c'} \left(\frac{c + K_{tr}}{d_b} \right)} \quad (4-2)$$

The value of $\sqrt{f_c'}$ is limited to a maximum value of 8.3 MPa.

$$\frac{l_d}{d_b} = \frac{\frac{f_y}{f_c'^{1/4}} - 51 \left(0.1 \frac{c_{\max}}{c_{\min}} + 0.90 \right)}{1.92 \left(\frac{c + K_{tr}}{d_b} \right)} = \quad (4-4)$$

$$\frac{\frac{f_y}{f_c'^{1/4}} - \phi 51 \left(0.1 \frac{c_{\max}}{c_{\min}} + 0.90 \right)}{\phi 1.92 \left(\frac{c + K_{tr}}{d_b} \right)}$$

where $K_{tr} = 35.3t_d A_{tr}/sn$.

$$\frac{l_d}{d_b} = \frac{\frac{f_y}{f_c'^{1/4}} - 51 \left(0.1 \frac{c_{\max}}{c_{\min}} + 0.90 \right)}{1.92 \left(\frac{c + K_{tr}}{d_b} \right)} \quad (4-5a)$$

$$\frac{l_d}{d_b} = \frac{\frac{f_y}{f_c'^{1/4}} - 45.5 \left(0.1 \frac{c_{\max}}{c_{\min}} + 0.90 \right)}{1.72 \left(\frac{c + K_{tr}}{d_b} \right)} \quad (4-5b)$$

$$\frac{l_d}{d_b} = \frac{(f_y/f_c'^{1/4} - 45.5\omega)\alpha\beta\lambda}{1.72 \left(\frac{c\omega + K_{tr}}{d_b} \right)} \quad (4-6)$$

$$K_{tr} = C_R(0.0283d_b + 0.28) \frac{A_{tr}}{sn} \quad (4-9)$$

ACI 408.3 limits $f_c'^{1/4} \cdot 3.2$, and $f_y \cdot 552$ MPa.

$$\frac{l_d}{d_b} = \frac{\left(\frac{f_y}{\phi f_c'^{1/4}} - 57.4\omega \right) \alpha\beta\lambda}{1.83 \left(\frac{c\omega + K_{tr}}{d_b} \right)} = \quad (4-11a)$$

$$\frac{\left(\frac{f_y}{f_c'^{1/4}} - \phi 57.4\omega \right) \alpha\beta\lambda}{\phi 1.83 \left(\frac{c\omega + K_{tr}}{d_b} \right)}$$

$$\frac{l_d}{d_b} = \frac{\left(\frac{f_y}{f_c'^{1/4}} - 52.9\omega\right)\alpha\beta\lambda}{1.68\left(\frac{c\omega + K_{tr}}{d_b}\right)} \quad (4-11b)$$

$$K_{tr} = (6.26t_r t_d A_{tr}/sn)f_c'^{1/2} \quad (4-12)$$

$$t_d = 0.03d_b + 0.22 \quad (4-14)$$

$$\frac{l_d}{d_b} = \left(\frac{f_y}{1.48f_c'^{1/4}} - 31\right)\alpha\beta\lambda \quad (4-20)$$

$$\frac{l_d}{d_b} = \frac{\left(\frac{f_y}{f_c'^{1/4}} - 47.1\omega\right)\alpha\beta\lambda}{1.48\left(\frac{c\omega + K_{tr}}{d_b}\right)} \quad (4-21)$$

For conventional reinforcement, $K_{tr} = (6t_d A_{tr}/sn)f_c'^{1/2}$.

$$\frac{l_d}{d_b} = \frac{1}{6.55} \left(1.15 - 0.15 \frac{c_{\min}}{d_b}\right) \left(1 - K \frac{\Sigma A_{tr} - \Sigma A_{tr, \min}}{A_b}\right) \quad (4-22)$$

$$\frac{l_d}{d_b} = \left(\frac{f_y}{2.51f_c'^{1/4}} - 20.99\right)\alpha\beta\lambda \quad (4-15)$$

$$\frac{l_d}{d_b} = \left(\frac{f_y}{2.5f_c'^{1/4}} - 21\right)\alpha\beta\lambda \quad (4-16)$$

$$\frac{l_d}{d_b} = \left(\frac{f_y}{1.67f_c'^{1/4}} - 31\right)\alpha\beta\lambda \quad (4-17)$$

$$\frac{l_b}{d_b} = \frac{\left(\frac{f_y}{f_c'^{1/4}} - 52.6\omega\right)\alpha\beta\lambda}{1.67\left(\frac{c\omega + K_{tr}}{d_b}\right)} \quad (4-18)$$

$$\frac{l_d}{d_b} = \left(\frac{f_y}{2.2f_c'^{1/4}} - 21\right)\alpha\beta\lambda \quad (4-19)$$

$$\frac{Mf_y}{\left(\frac{f_c' - 2.75}{10}\right)^{2/3}}$$

$$l_{d, \min} = \max \left[\frac{0.3}{6.55} \frac{Mf_y}{\left(\frac{f_c' - 2.75}{10}\right)^{2/3}}, 10d_b, 100 \text{ mm} \right] \quad (4-23)$$

$$l_{s, \min} = \max \left[\frac{0.3\alpha_b}{6.55} \frac{Mf_y}{\left(\frac{f_c' - 2.75}{10}\right)^{2/3}}, 15d_b, 200 \text{ mm} \right] \quad (4-24)$$

$$E_c = 4734 \sqrt{f_c'} \quad (5-1)$$

$$\epsilon_o = \frac{f_c'}{2500 + 400f_c'} \quad (5-3)$$